Applied Research and Innovation Branch

INVESTIGATION OF SEISMIC PERFORMANCE AND DESIGN OF TYPICAL CURVED AND SKEWED BRIDGES IN COLORADO

Suren Chen
Hussam Mahmoud
Thomas Wilson
Robert Johnson
Guangyang Houuthors

Report No. CDOT-2018-08
January 2018

The contents of this report reflect the views of the author(s), who is(are) responsible for the facts and accuracy of the data presented herein. The contents do not necessarily reflect the official views of the Colorado Department of Transportation or the Federal Highway Administration. This report does not constitute a standard, specification, or regulation.

Technical Report Documentation Page

1. Report No.	2. Government Accession No.	3. Recipient's Catalog No.
CDOT-2018-08		

4. Title and Subtitle	5. Report Date
INVESTIGATION OF SEISMIC PERFORMANCE AND DESIGN OF TYPICAL CURVED AND SKEWED BRIDGES IN COLORADO	1/15/2018
	6. Performing Organization Code

7. Author(s)	8. Performing Organization Report No.
Suren Chen, Hussam Mahmoud, Thomas Wilson, Robert Johnson, Guangyang Hou	CDOT-2018-08

9. Performing Organization Name and Address	10. Work Unit No. (TRAIS)
Colorado State University Fort Collins, CO	11. Contract or Grant No.

12. Sponsoring Agency Name and Address	13. Type of Report and Period Covered
Colorado Department of Transportation - Research 4201 E. Arkansas Ave. Denver, CO 80222	Final: 2/15/12 to 10/1/15
	14. Sponsoring Agency Code 087-00

15. Supplementary Notes
Prepared in cooperation with the US Department of Transportation, Federal Highway Administration

16. Abstract
This report summarizes the analytical studies on the seismic performance of typical Colorado concrete bridges, particularly those with curved and skewed configurations. A set of bridge models with different geometric configurations derived from a prototype bridge selected in Denver area were studied. Some discussions about the connection modeling are carried out in terms of the interior bent support. For the displacement-based and force-based designs, due to the lack of design details that may be adopted for different Colorado bridges, some specific recommendations cannot be made at this point without detailed analyses of all possible detailing options. Therefore, some general observations of these two design concepts are summarized in the end of the report. In the appendices, the design examples of 2-span and 3-span bridges are listed to help the engineers to conduct bridge seismic analysis in Colorado.

The SAP2000 modeling example and four design examples are included in the appendices of this report.

Implementation

17. Keywords	18. Distribution Statement
Denver Area, Colorado, 2-span, 3-span, SAP2000, connection detail, bent support	This document is available on CDOT's website http://www.coloradodot.info/programs/research/pdfs

19. Security Classif. (of this report)	20. Security Classif. (of this page)	21. No. of Pages	22. Price
Unclassified	Unclassified	187	

INVESTIGATION OF SEISMIC PERFORMANCE AND DESIGN OF TYPICAL CURVED AND SKEWED BRIDGES IN COLORADO

by

Suren Chen
Hussam Mahmoud
Thomas Wilson
Robert Johnson
Guangyang Hou

Sponsored by the
Colorado Department of Transportation

Colorado Department of Transportation
Applied Research & Innovation Branch
4201 E. Arkansas Ave.
Denver, CO 80222

Acknowledgement

The authors wish to thank the CDOT Applied Research and Innovation Branch for funding this study. The authors like to acknowledge the project panel for providing valuable technical discussion and guidance throughout the project period. The time, participation and feedback provided by the project panel members: Richard Osman, Derrell Manceaux, Trever Wang, Mac Hasan, Steve Yip, David Thomas and Su Cheng, is greatly appreciated.

Executive Summary

This report presents the results of a study conducted on the seismic behavior of select RC bridges in Colorado with a focus on curved and skewed configurations. Numerical models of bridges with different geometric configurations were derived from a typical prototype bridge in Colorado. Detailed nonlinear time-history analyses with SAP2000 are conducted on these bridge models with a seismic site hazard for Denver, Colorado.

In the first part of the report, detailed background information is provided that relates to earthquake engineering and the Colorado hazard. A review of the seismic hazard is presented with documentation on the AASHTO LRFD Design Specification and AASHTO Guide Specifications, including different types of computational modeling, structural analysis and ground motion-scaling methodologies. Secondly, a 2 and 3-span RC bridges were selected for use in the seismic investigation with the intention of being representative of the general Colorado bridge inventory. The 3-span bridge was independently modified to explore the effects of skew and curvature under seismic loads, in addition to loading constraints and support alternatives. Modal and non-linear time-history analyses were performed on 9 different bridge models in SAP2000 using two sets of two seismic hazard levels from the AASHTO codes. An evaluation of major structural components using SAP2000 and a section analysis is included, in addition to an extensive study on the impact and behavior of skew and curvature. The effects of support condition, earthquake input direction and soil stiffness are also included. The discussions are also made in terms of different modeling options of interior bent connections for the specific designs of the prototype bridge based on comparative study results. Due to the lack of site-specific design detail alternatives of major connections, the general discussion about the difference between displace-based and force-based approaches is made.

Lastly, design examples for creating the numerical models constructed in SAP2000 are also provided with detailed steps on model construction, seismic analyses and post-processing of results as appendices of the report. This is supplemented with comprehensive details on seismic design procedures for SDC A and SDC B using the AASHTO LRFD Bridge Design Specifications and AASHTO Guide Specifications for LRFD Bridge Design, Zones 1 & 2.

Table of Contents (Organization)

1. Background Information

1.1. Introduction

Earthquakes are a present-day hazard to the expanding infrastructure in the United States and are currently responsible for approximately $5.3 billion in annual economic losses (FEMA 366, 2008). An earthquake can cause damage to, and in cases collapse of buildings, railways, and bridges. In the case of a severely damaged or collapsed bridge the consequences can be substantial in terms of financial losses from cost of repair or replacement and socioeconomic losses through the value of lost time to the public by a longer travel time. Bridges are typically designed for life loss prevention under large seismic demand, which requires a design that prevents structural collapse under large cyclic demands. The response of bridges subjected to earthquake ground motion, however is difficult to predict and often requires rigorous analyses.

All states, independent of the seismic hazard, are required to conduct seismic design following the American Association of State Highway and Transportation Officials (AASHTO) LRFD Bridge Design Specifications (called "LRFD Specifications" hereafter) or the AASHTO Guide Specifications for LRFD Seismic Bridge Design (called "Guide Specifications" or "GS" hereafter). Each code presents a methodology of design against earthquakes following force-based methods or displacement-based design practices. In this study, both specifications will be reviewed in the following sections.

Structural codes typically classify bridges into seismic Zones or Categories based on site-specific ground acceleration and site classification. Mountainous states in the central U.S. are typically classified as low seismic regions and incorporate little to no seismic design or analyses into their bridge practices. Colorado, as reviewed in the following section, is classified as a low seismic state. According to seismologists, however, Colorado may be exposed to a higher

seismic risk than currently considered by structural codes. In this report, the following chapters document studies primarily based on nonlinear time-history analyses to investigate the dynamic response of representative Colorado bridges and provide insight on the effects of geometric and structural configurations. Prior to conducting the time-history simulations, a review of Colorado seismic hazard is provided; followed by classification of the bridges according to current bridge specifications and an overview of state-of-the-art modeling and analysis methods of bridges under earthquake excitations.

1.2. Colorado Seismic Hazard

Earthquakes pose an on-going threat to society and infrastructure in the United States and around the world. Improper design of infrastructure against seismic events can result in collapse or extensive damage to roads, bridges, buildings, and utility lines. The AASHTO codes utilize the United States Geological Survey (USGS) hazard maps (Fig. 1.1) that assign representative horizontal accelerations based on geography and tectonic activity across the United States. Based on the ground acceleration coefficient and the site classification for the location of interest, the level of seismic analysis required can be determined. Colorado is classified state wide as either Seismic Design Category A or B (Zones 1 & 2) and requires minimal to limited seismic analysis according to the AASHTO LRFD Specifications and Guide Specifications.

Figure 1.1 Seismic Hazard Maps for AASHTO Guide Specifications, Peak Ground Acceleration (PGA) (7% in 75-year) (2011)

The seismicity of Colorado is still uncertain according to seismologists and the state may be more active than currently presumed (Charlie et al. 2006; Sheehan et al. 2003). Generally, Colorado is thought to be a low seismic region; it has a low number of previously recorded seismic events in the area and is located a far distance from major inter-plate fault lines. Inter-plate faults are typically characterized by the junction and interaction of two tectonic plates. Present at these junctions are large tectonic forces that result in fracturing of the lithosphere-asthenosphere complex generating frequent and larger magnitude earthquakes. Therefore, the seismic activity present in Colorado is rather characterized by intra-plate tectonic interaction and the occurrence of intra-plate earthquakes is attributed to internal fractures of the lithosphere on the tectonic plate. The generation of earthquakes across the lithosphere may be attributed to anomalies in temperature, strength or by the nature of the geological site conditions. Colorado has 58 mountain peaks of elevation higher than 14,000 feet, apparent Neogene and active quaternary deformation, and the second to largest heat flow anomaly, which all point towards an active tectonic area (Charlie et al., 2002). In addition, there are ninety-two potentially active

quaternary faults documented. Of the ninety two faults, thirteen have a maximum credible earthquake (MCE) of higher than 6.25 M_L (Fig. 2.2) on the Richter Scale (Widmann et al. 1998). The maximum credible earthquake scale is based on a 2500-year return period, and is utilized to assess the highest magnitude earthquake that a fault line may produce. In light of the inherent impracticalities of design and construction of bridges using the MCE, the design based earthquake (DBE) is utilized for most designs of bridges and represents a 1000 year return period.

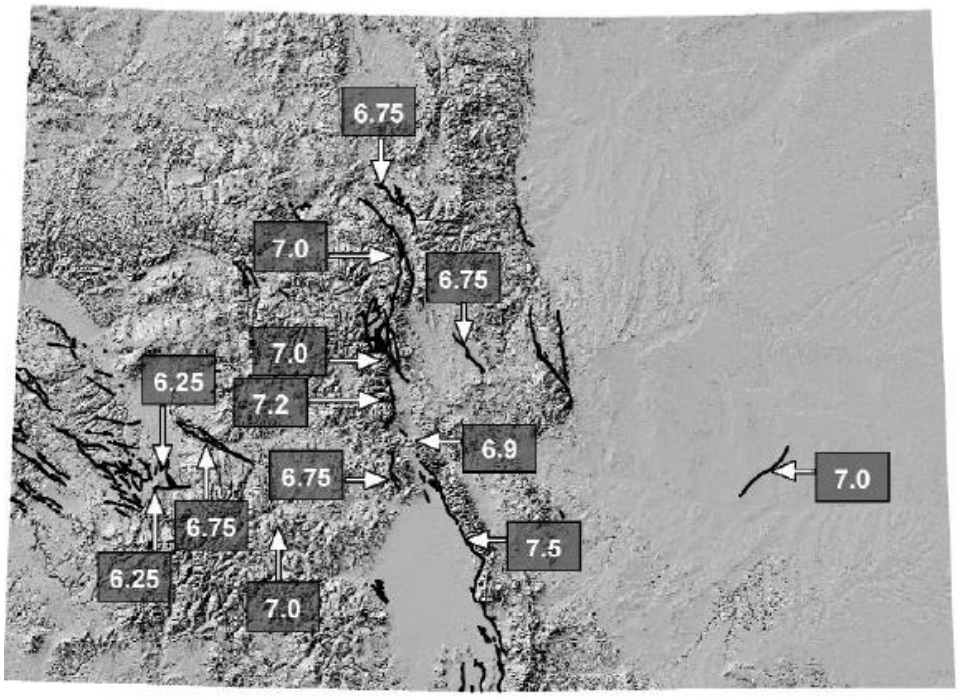

Figure 1.2 (Matthews, 2002) Quaternary Fault Lines with Assigned Maximum Credible Earthquake Magnitudes for the State of Colorado

The focal point of recorded seismic activity has been centered just west of the Rocky Mountain Front Range and in Southern Colorado near Trinidad. The largest earthquake to date was recorded on November 7, 1882 with magnitude of 6.6 ± 0.6 M_L on the Richter Scale (Spence et al. 1996; Kirkham & Rogers 2000). The ground motion was observed throughout

several neighboring states, as shown in Figure 1.3, and is estimated to have affected an area of 330,000 mi^2 (Spence 1999). The unified estimate on the Modified Mercalli Intensity (MMI) scale was assessed by seismologists at an intensity of VII (Kirkham 1986). In fact, Colorado is one of only fourteen states across the country to have documented an earthquake of magnitude 6.0 or greater (Stover & Coffman 1993).

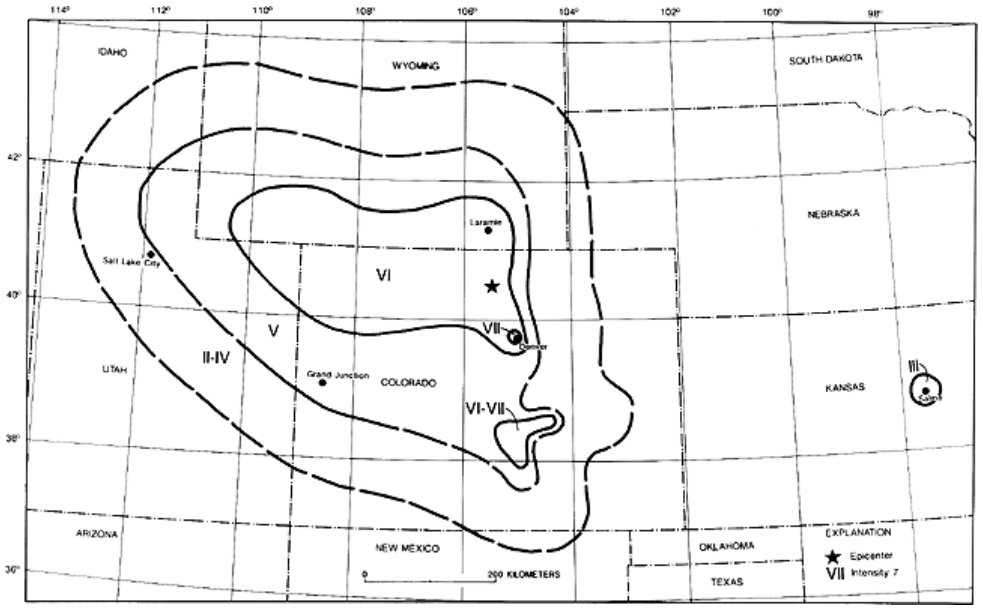

Figure 1.3 (Stover & Coffman, 1993) Isoseismal Map for November 7th, 1882 Earthquake in Colorado

A total of 570 earthquakes have also been recorded from 1870 to 2005 of Moment Magnitude (M_w) 2.0 or higher. Of these 570 earthquakes, 82 earthquakes have been recorded at a MMI scale of V or higher. Colorado's highest probability for a seismic event measure using the MCE scale, is estimated at magnitude 7.5 M_L on the Richter scale (Kirkham & Rogers, 1985). According to Charlie et al. (2006), data collected from independent earthquakes yields a mean recurrence interval of 420 years for an earthquake of magnitude 6.5 M_L or larger. Applying a Gutenberg-Richter magnitude-recurrence relation developed by Charlie et al. (2002) yields that a

magnitude 6.6 M_L or larger earthquake will have a corresponding return period of 500 years. Applying the same relationship, a 1000-year return period corresponds to a 7.0 M_L event, and a 2500-year return period corresponds to a 7.5 M_L event. In comparison, by current AASHTO design criteria, most of Colorado falls into a Seismic Design Category A for a 1000 year return period, which dictates that seismic design is not required. Comparing the estimated earthquake magnitudes by seismologists and AASHTO seismic hazard maps for comparable return periods, one can find that there appears to be a significantly larger estimated hazard by seismologists than what is estimated by the AASHTO bridge codes in Colorado.

1.3. AASHTO LRFD Specifications and Guide Specifications

Prior to the moment that the magnitude 6.6 M_w earthquake struck the San Fernando Valley in the state of California in 1971, guidelines on seismic design were fairly rudimentary. A fraction of the dead load from the structure was used to estimate the lateral seismic loads, based on which the members of the structural system were designed. Following the earthquake in 1971, a group of experts in the field of seismology and structural engineering wrote a document, which was published in 1981 by the Applied Technology Council (ATC), titled "Seismic Design Guidelines for Highway Bridges" (ATC-6 1981). ATC-6 was later adopted as a Guide Specification and a required Specification for seismic design in the AASHTO Standard Specification Division 1-A. Since then, further development and updates have followed in the AASHTO LRFD Bridge Design Specification (AASHTO 2007). In 2007, AASHTO introduced the LRFD Guide Specifications for Seismic Design of Highway Bridges in addition to updates to the existing specifications. Life safety performance dictated that a bridge would be designed such that it has low probability of collapse, although it may sustain significant amounts of damage such that partial or complete rehabilitation may be required following a high magnitude seismic event.

Supplementing this change was an increase in the return period of the design event from 475 years to 1000 years in both specifications, which was also motivated by the AASHTO's desire to stay current with the building design codes.

The AASHTO LRFD Bridge Design Specifications is based on traditional force-based seismic design and relies on the strength capacity of the specified structural members to perform in the inelastic range through an elastic analysis. To determine the level of analysis required, the AASHTO Bridge Specifications differentiates all bridge sites into four Seismic Zones (SZ) partitioned by acceleration coefficient ranges and site (soil) conditions. The acceleration coefficients are determined from the 1-second seismic hazard maps developed by the USGS. Based on the seismic zone and bridge importance classification, the minimum analysis requirements are determined. For SZ 1, applicable to most of Colorado, no seismic analysis is required. However a fraction of the vertical reaction is applied horizontally to determine the required connection strength and ensure that minimum requirements for deck unseating are met. In contrast, critical bridges in SZ 4 require time history analysis as the minimum analysis requirement. The general method for analyses requires developing a unique response spectrum using spectral maps and site-specific soil classifications. Following calculation of elastic forces using the response spectrum, a response modification factor (R-factor) (Fig. 1.4) was utilized to modify the seismic forces in recognition that it is uneconomical to design bridges to resist large earthquake forces elastically (AASHTO 2007). The structural components of the bridge are then designed based on the modified load, which varies for different substructure components and importance categories. By modifying the elastic forces with the Response Modification Factor, "R", it is recognized that yielding of the structure may occur.

Substructure	Importance Category		
	Critical	Essential	Other
Wall-type piers—larger dimension	1.5	1.5	2.0
Reinforced concrete pile bents			
• Vertical piles only	1.5	2.0	3.0
• With batter piles	1.5	1.5	2.0
Single columns	1.5	2.0	3.0
Steel or composite steel and concrete pile bents			
• Vertical pile only	1.5	3.5	5.0
• With batter piles	1.5	2.0	3.0
Multiple column bents	1.5	3.5	5.0

Connection	All Importance Categories
Superstructure to abutment	0.8
Expansion joints within a span of the superstructure	0.8
Columns, piers, or pile bents to cap beam or superstructure	1.0
Columns or piers to foundations	1.0

Figure 1.4 Response Modification Factors in AASHTO LRFD Bridge Design Specifications (2007) (Table 3.10.7.1-1 & 2)

The AASHTO Guide Specifications (GS) was developed under the guidance of the AASHTO T-3 Committee as part of a National Cooperative Highway Research Program (NCHRP) task. The method of identifying seismic hazard utilizes identical USGS ground motion hazard maps and life safety performance criteria as the existing specifications. The Guide Specification also determines the demand on the structure by placing it into Seismic Design Categories (SDC). The SDC is synonymous to the AASHTO LRFD Bridge Specifications Seismic Zones. The Guide Specifications, however, employs ductility-based design after the realization that this method of design is significantly less sensitive to sharp increases in the uncertain and variable seismic loading (Elnashai & Di Sarno, 2008). Ductility-based design evaluates the performance of a structural system based on the displacement capacity of the system and applies detailing requirements to provide ductility with inelastic deformation. The first steps required by the Guide Specifications (GS) are similar to the existing LRFD

Specifications; analysis requirements are determined through the use of hazard maps and site coefficients, and SDC classification. The extent of the analysis includes determination of connection requirements similar to the LRFD Specifications, a check against minimum criteria for unseating at supports, along with column detailing and foundation design. For SDC B, C and D, the GS incorporate more rigorous analysis and design methods. SDC B suggests an implicit displacement capacity check or pushover analysis. SDC C and D involve the engineer's choice of a design strategy referred to as the Earthquake Resisting System (ERS) and development of earthquake resisting elements (ERE). This is ensured by detailing specified components to yield using specified procedures in the code to "capacity protect" all other elements connecting the yielding component. The capacity protection method is employed where the individual component resistances should have the ability to avoid that connecting components reach their overstrength capacity (American Association of State and Highway Transportation Officials, 2011).

1.4. Review of Different Structural Modeling Methods

Once the method of analysis is established, a model that approximates the response of the bridge structure is often required. There are several model types that are applicable for providing a representation of the structural characteristics of bridges, although they have varying degrees of accuracy and time efficiency. These include single-degree-of-freedom (SDOF) systems, multiple-degree-of-freedom (MDOF) models, and detailed finite element (FE) models. SDOF models have the advantages of minimum computational demand and yielding a fair representation of the global behavior. SDOF models are limited primarily to standard structures and do not account for tridimensional effects and local behavior (Elnashai & Di Sarno, 2008). Stick models accounting for multiple degrees of freedom, are applicable to all regular structures,

and accommodate tridimensional effects. But similar to SDOF models, stick models only account for the global response. In a recent publication by Abdel-Mohti and Pekan (2008) on the comparison between detailed finite element models and beam stick models for skewed bridges in SAP2000, it was concluded that for bridge decks with skew angles larger than 30 degrees, detailed finite element models should be utilized in order to correctly represent higher mode effects. For practicing Engineers, the preferred methods are always the simplest models that provide adequate results. Therefore, to hit the optimal balance between more accurate results from complex models and the simplicity of the analytical procedure still remains a topic worthy discussion for engineering community.

In recent years, finite element models using SAP2000 have been extensively developed by many researchers in seismic engineering. Mwafy and Elnashai (2007) investigated the seismic integrity of multi-span curved bridges using SAP2000. Itani and Pekcan (2011) investigated the seismic performance of steel plate girder bridges with integral-abutments using SAP2000. Kappos et al. (2005) utilized the analysis program to show that modal-pushover analysis can be effectively employed for seismic assessment of bridges. SAP2000 is also currently used in several design offices of State Departments of Transportation (DOT) for seismic analysis around the country. For example, Washington DOT utilizes SAP2000 and the AASHTO Guide specifications as the basis for evaluation of bridge structures and have developed guidelines and design examples (Washington Department of Transportation 2011). In addition to Washington, SAP2000 is also used for seismic analysis by other State Departments of Transportations, such as Indiana, Nevada and California DOTs.

1.5. Review of Demand Analysis Methods

1.5.1. Introduction

There are several available methods for estimating the demand imposed by earthquakes on bridges. The conventional analysis methods adopted in research and structural codes are discussed in the following section. The methods covered include: response spectrum method and time history analysis.

1.5.2. Response Spectrum Method

The response spectrum analysis (RSA) method is an elastic seismic analysis approach, which usually can give reasonable response prediction for ordinary standard bridges under seismic excitation. Based on modal properties of the structure, a response spectrum method reduces the dynamic analysis to a series of static analyses to assess the peak response of a structure. As a type of popular and efficient approach adopted in structural codes such as the AASHTO LRFD, and Guide Specifications, the response spectrum method is often used when the basic equivalent static analysis (ESA) is not sufficient. The analytical method is governed by the following dynamic equations to ground motions:

$$M\,\ddot{x}(t) + C\dot{x}(t) + Kx(t) = m_x\ddot{x}_{gx}(t) + m_y\ddot{x}_{gy}(t) + m_z\ddot{x}_{gz}(t)$$

where K represents the stiffness matrix, M represents the diagonal mass matrix and C represents the proportional damping matrix; The variables of x(t) represent the motion with respect to the ground, $\ddot{x}_{gx,y,z}$ represents the components of uniform ground acceleration, and lastly $m_{x,y,z}$ represents the unit acceleration loads (CSI 2011). Response spectrum analysis evaluates the model at the maximum response to the dynamic equilibrium equation at the fundamental period of vibration. The input is a response spectrum curve of spectral acceleration versus structural period. This is developed using the guidelines provided in the structural codes. The computed dynamic response of the bridge represents a statistical calculation of the maximum magnitude for

that measure. Response-spectrum analysis is generally based upon superposition with modes computed using Ritz-vector analysis. With the modal analyses results, single-mode spectral method and multimode spectral method can be used. In the following, the multimode spectral method, which is popular in engineering practice, is briefly introduced. Typically, a multi-degree-of-freedom (MDOF) structural model is excited by a transient signal and decomposed analytically into a series of single degree of freedom (SDOF) systems. Modal dynamic response is firstly calculated for each mode, which is combined to yield the global response of the MDOF system using mode superposition concept. Such a method is typically limited to linear-elastic systems with very little nonlinearity due to mode-superposition nature. Although MDOF approach offers a convenient and valid tool to predict global response of most standard bridges with little nonlinearities, time-history analysis is usually recommended for non-ordinary bridges or scenarios with high nonlinearity.

1.5.3. Time-history Analysis

Due to the known limitations of the response spectrum method, nonlinear time history analysis (NLTHA) is usually recommended for non-ordinary bridges and/or when considerable nonlinearities are expected on bridge structures subjected to seismic. Although it usually requires advanced modeling skills and high computational cost, NLTHA is recognized as the most accurate and rigorous analysis method in both open-source and commercial finite element software (Burdetteet al. 2008; Mwafy & Elnashai, 2007). NLTHA is a step function analysis and evaluates the dynamic response of the bridge structure due to a specific earthquake loading at discrete time steps and iteration is often required. When nonlinear behaviors are developed in the

structure, the stiffness of the bridge needs to be recalculated due to degradation of strength as well as redistribution of forces (Aviram et. al. 2008).

The equations of motion defining this type of analysis are as follows:

$$M\ddot{x}(t) + C\ddot{x}(t) + Kx(t) = F(t)$$

where K, M, and C, represent the stiffness matrix, the mass matrix, and the damping matrix, respectively and x(t) and $F(t)$ represent the displacement increment at a specified time increment and the forcing function, respectively. The forcing function is typically represented by an earthquake record, scaled to the level of seismic hazard at the location of the bridge, which will be discussed in the following section.

In the present study with SAP2000, direct integration utilizing the Hilber-Hughes-Taylor method is selected as the method of calculating the equations of motion for each time step (Hilber et al. 1979). Direct integration offers the advantages of displaying full damping properties of coupled modes, and more efficient integration of wave and impact propagation of higher modes. The Hilber-Hughes-Taylor method is optimal for nonlinear analysis where the reduction in stiffness may lead to excitation of higher modes in later time steps (CSI 2011).

1.6. Ground Motion Scaling

In nonlinear time-history analysis, the numerical models are subjected to an array of ground motion records. Code requirements for ground motions call for utilization of a minimum of three time histories to represent the design earthquakes (two horizontal and one vertical motion). Prior to conducting the analysis, however, the ground motion records require scaling to match the seismic exposure of the area. There are several methods that can be used to scale ground motion

records. In addition, the earthquake records should be obtained from geological conditions representing similar shear wave velocity characteristics and have similar magnitudes and distances as to reduce the scaling factor.

The scaling of spectral accelerations at single spectral periods, has also been widely utilized in research fields (e.g. Kunnath et al. 2006; among others). Kurama and Farrow (2003) introduced a method of scaling based on the maximum incremental velocity. Baker and Cornell (2006), proposed that if earthquake records are selected with appropriate spectral shapes, the structural response reduction and amplifications are comparable to the variation in earthquake intensity. The most recent developments in ground motion scaling came from Kalkan and Chopra (2010) and Kalkan and Kwong (2010), who developed modal-pushover-based scaling approaches. Other methods of scaling have been shown to produce inaccuracy and large variances in response. For example, scaling based on the peak ground acceleration (PGA) has been shown to produce widely scattered results (Vidic et al. 1994, Shome& Cornell 1998). Kuruma and Farrow (2003) summarized that scalar intensity measures such as effective peak acceleration and effective peak velocity can be inaccurate and insufficient for analysis. A comprehensive evaluation of the scaling methods including those listed above can be found in a National Science Foundation (NSF) report authored by Donnell et al. (2011).

2. Bridge Plans and Specifications

2.1. Structural Components of the 2- Span Bridge

The 2-span bridge selected by CDOT as a representative bridge is constructed of eight parallel I-girders that support concrete deck with 8” thickness. The girders utilize the BT42 type detailing and are 5’-7” overall depth, and 2’- 3” base width. The superstructure is supported at either end by integral abutments, creating a rigid connection to the foundation. The substructure is composed of four circular pier-columns that are tied to the superstructure through an integrated bent cap. Each pier column is 3’ in diameter and is confined by transverse hoop reinforcement with 1’ spacing. The columns are supported by 3’-7” caissons that are embedded into the soil.

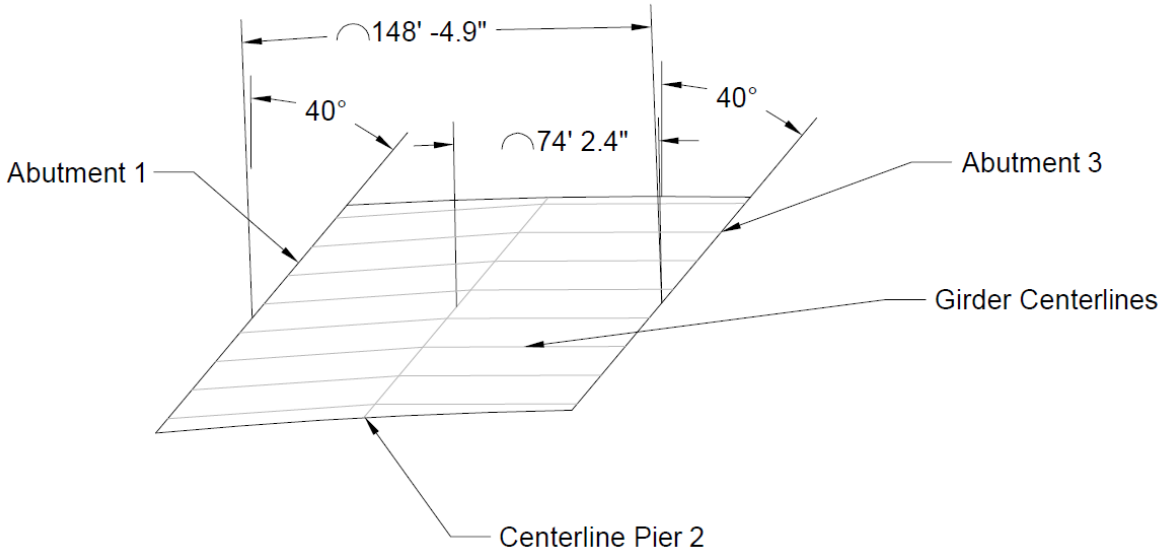

Figure 2.1 Plan View of 2-Span Bridge – Radius 4500 ft Skew 40^0

2.2. *Structural Components of the 3- Span Bridge*

A series of 3-span bridges analyzed are of varying geometric configurations but are all constructed with the same structural components as a straight prototype one. Due to the similarities of the structural components, one curved and skewed bridge (Radius 4500 ft. Skew 45^0) is selected to demonstrate the structural components. The bridge superstructure (Fig.2.2a) is composed of 8-in concrete slab deck supported by eight, 5'-8" deep, parallel pre-stressed concrete I-girders (Fig. 2.2c). The girders are reinforced longitudinally at the tops of the cross sections and are braced with stirrups at 18-in intervals. The junctions between adjacent girders, supported by the pier cap, are embedded in a concrete diaphragm creating an integral, fixed connection. Supporting the concrete diaphragms are rectangular pier caps of 5' depth, each supported by an interior and exterior columns with constant average depths (Fig. 2.2b). Each column contains standard longitudinal reinforcement, and transverse confinement at spacing of 2'-9". The abutments and piers are parallel and skewed at the same angle to the transverse axis. The integral abutment is adopted for these bridges. So it encases the contiguous I-girders, and is also tied by reinforcement to the adjacent deck.

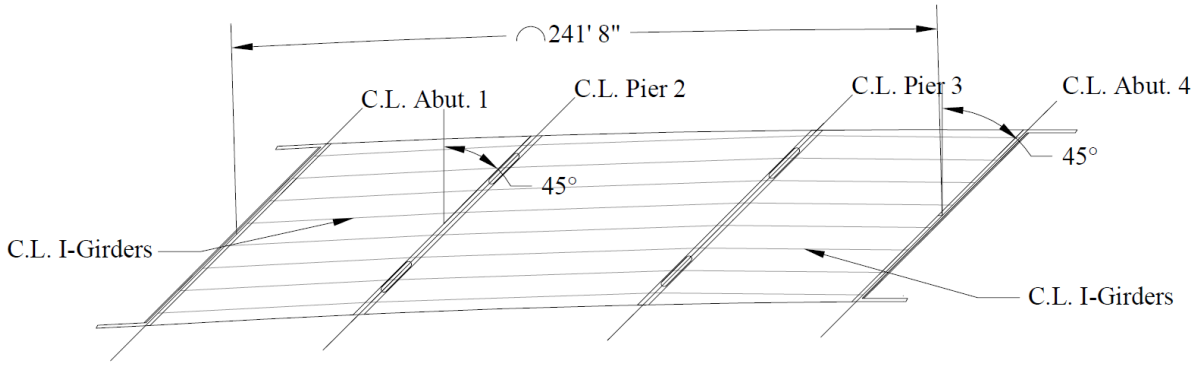

(a) Plan View

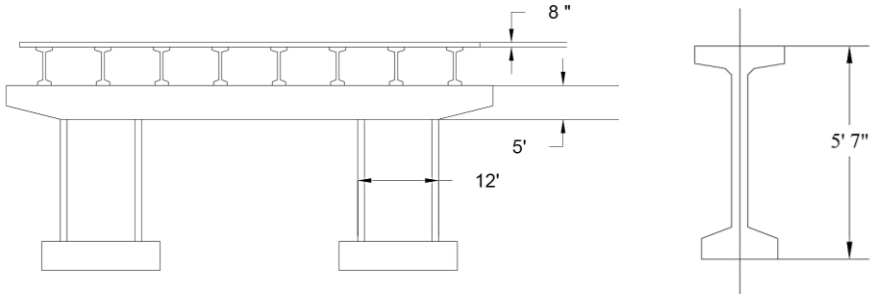

(b) (c)

Elevation View

Figure 2.2 (a) Plan View of Bridge – Radius 4500 ft. Skew 45^0 (b) Pier X-Section and (c) I-Girder X-section

2.3. Configuration of 3-Span Bridges

2.3.1. Part I - Baseline bridge model configuration (Radius: 4500 ft; Skew: 30)

Part one of the analysis examines a baseline bridge model with a single degree of skew and radii of curvature in great detail, and identifies critical areas of interest that will be the focus points later in the geometric variation portion of the study. In addition, it also examines the impact of typical design decisions such as the abutment support condition, and the directional components of the loading (Table 2.1). The baseline bridge model includes a radius of curvature of 4500 feet, a skew angle of 30 degrees, and a super elevation of 4 degrees. A plan view and an elevation view of the baseline bridge configuration used for comparative purposes is shown in Figure 2.3a and 2.3b, respectively,

Table 2.1 Bridge Components for Baseline Comparison

Scenario	Skew (degrees)	Curvature Radius (ft)	Component
1	30	4500	Baseline Model
2	30	4500	Reversed Directional Loading
3	30	4500	Bearing Support

2.3.2. Geometric Configurations of Bridges

Eight RC bridges of varying curvature and skew are constructed from the baseline model for comparison of geometric effects. Each bridge consists of three spans, with two identical side spans and a middle span kept at consistent lengths of 72'–6" and 96'-8", respectively. Characteristics that would otherwise affect the structural response such as the member material properties, deck width, mean pier height, and member cross-section are identical to the baseline bridge. Characteristics such as the skewed length of support piers and abutments are subject to changes in accordance to the variations of skew angles and curvature and other realistic design considerations. The superelevation of the bridges follows the typical values as defined in the AASHTO (2007) design guidelines. The geometries selected for the parametric study are summarized in Table 2.2.

Bridge #1 is a representation of a regular, straight bridge serving as a benchmark case for comparison purposes. Bridges #2 – 5 were constructed for evaluating independent effects of skew and curvature, as well as studying the effects of the parameter. Bridges #6 – 8 incorporate both skew and curvature, and Bridge #6 serves as the baseline model as described above.

Table 2.2 3-Span Bridge Configurations

Bridge #	Skew (degrees)	Curvature Radius (ft)	Super Elevation (degrees)
1*	0	0	0
2	30	0	0
3	45	0	0
4	0	4500	4
5	0	3000	6
6**	30	4500	4
7	45	4500	4
8	30	3000	6

Note: * Benchmark model and ** Baseline model

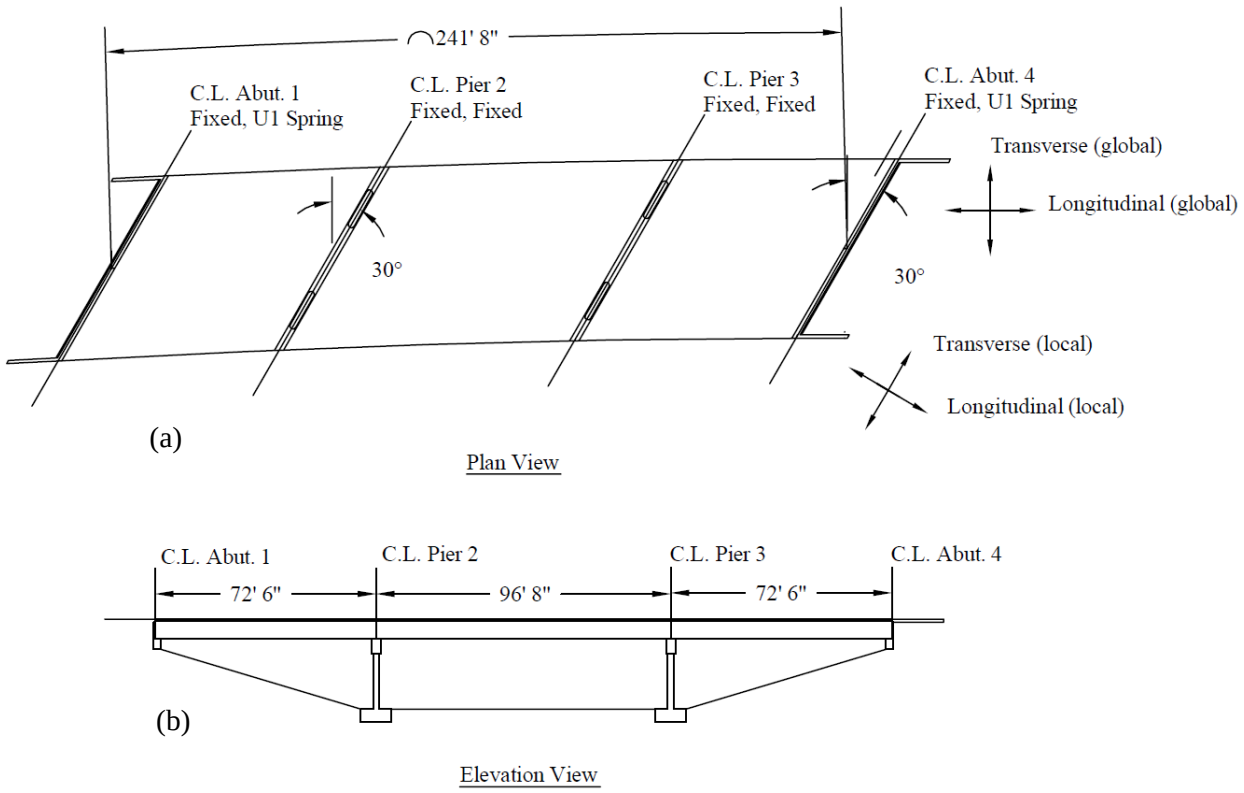

Figure 2.3 (a) Plan View (b) Elevation View of Bridge – Radius 4500 ft. Skew 30^0

3. Numerical Modeling Method

3.1. Development of the Finite Element Models

The structural performance of the bridges being studied is evaluated using 3-D finite element (FE) models (Fig. 3.1) constructed in SAP2000 (CSI 2011). The model was constructed following the practices developed by authors in previous research studies who have utilized SAP2000, guidelines utilized used for analysis of bridges in high seismic regions, and recommendations made by the software developer (Kappos et al. 2005, Mwafy and Elnashai 2007; Itani and Pekcan 2011; WSDOT 2011; CSI 2011).

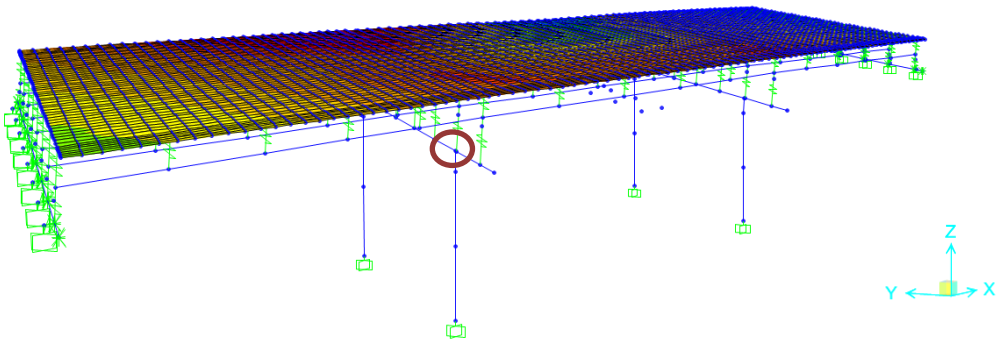

*Location 1 – Circled

Figure 3.1 SAP2000 Finite Element Model of the Bridge

3.2. SAP2000: Advantages for Structural Design and Analysis

As popular commercial FEM software primarily targeting at Civil Structures, SAP2000 has some advantages in terms of conducting structural design and analysis. For example, SAP2000 can provide an accurate representation of the global response of a bridge to dead loads, traffic

loads and seismic conditions. It can also calculate the axial, shear and bending demand on frame and shell elements, which can represent the deck, as well as major super and substructure components. SAP2000 also offers a range of flexibility for engineers to build the analytical model: the structural designer can choose to build a more simplified 2-D beam-stick type model or a more complex 3-D model depending on the needs. Furthermore, the designer can perform a variety of analyses, from a simple static linear dead load analysis, to a seismic pushover analysis, or a nonlinear time-history analysis, depending on the software version.

3.3. SAP2000: Disadvantages and Limitations

The limitations to SAP2000 are that the construction of detailed models, like the one shown in Figure 3.1, can be time consuming. However, if sets of guidelines or design examples are followed, and a step-by-step process that includes recommendations on construction and analysis techniques, the time spent could be considerably reduced. Another limitation to SAP2000 is that it does not handle connections and complex local nonlinear performance very well. Idealized elements such as rigid links are often used which approximates the behavior of the connection.

3.4. Details of the Finite Element Modeling Process

Details of the modeling process are discussed in this section. The model construction method is more detailed than required in most designs. However, such a model is required as an accurate depiction of the global and local behavior of the bridge is crucial to the research conducted in this study. The modeling methods described in the following sections were utilized in the development of both the 2-span and 3-span bridges; however the exact details are specific to the 3-span bridges. A more in depth review of the modeling can be found in Design Example No. 3 – SAP 2000.

A spine structure of the overall dimensions and 3-D layout of the bridge is first constructed in AutoCAD. Dimensions of the bridge and basic orientation of the superstructure and substructure are established using the centroids of each section to construct spine model. Once developed, the spine layout is exported as a DXF file and imported into SAP2000. After this step is completed, the finite element member properties are modeled as summarized in the following:

Major structural components

The bridge deck was modeled using shell elements that span intermediate nodes of the girder and are further meshed into quadrants. Due to minimal contribution to the structural response, reinforcing in the deck was neglected. The girders are modeled using linear beam elements and divided into 5 segments per span in accordance with AASHTO Guide Specifications (5.4.3) (AASHTO 2011). Prestressing components are modeled using lumped tendons at each girder, and the prestressing force (after losses) is applied as end-wise point loads. Beam elements are connected to shell elements through the adoption of fully constrained rigid links. The substructure is modeled using beam elements representing the columns and pier caps. The columns are fixed at the spread footing in six rotational and translational directions. The columns are connected directly to the pier cap and the lengths are adjusted by the use of end length offsets. In order to account for inelastic column behavior, plastic hinges were assigned at a specific distance from the top and bottom of the columns. The hinging mechanism follows the established details by Caltrans, and the locations are developed in accordance with WashDOT procedures (Caltrans 2004; WSDOT 2011).

The integral abutment is modeled using beam elements representative of the abutment cross section. The abutment-girder connection is modeled using a rigid link, characteristic of the

integral fixity between the abutment and girder (CSI 2011). The abutment is considered to have fixity from the surrounding soil and pile foundation in all degrees of freedom except the longitudinal direction. The backing soil behind the abutment is represented by the use of a tri-linear, longitudinal, compressive spring (Fig. 3.2) following the Caltrans design procedures for backing soil behind an integral abutment (Caltrans 2004).

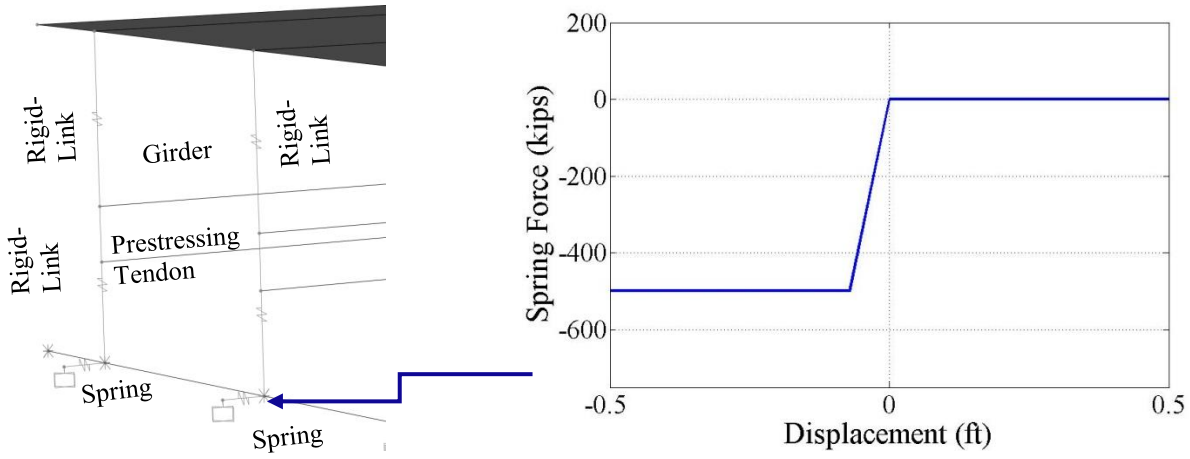

Figure 3.2 Abutment Spring and Force-Displacement Relationship

Connection modeling

Connection modeling is important for bridge seismic assessment since the way these connections are modeled not only affects the seismic performance due to the different FE modeling details required, but also due to the possible damage outcomes of the connections themselves. Similar to the prototype bridge evaluated in this study, many multi-span bridges are often constructed with simple-span girders made continuous for live load to increase efficiency and redundancy. CIP Diaphragms, often adopted for these bridges, are very important components that are used to connect adjacent girders and also pier caps. During seismic events, the continuity of superstructure of the simple-made-continuous bridges is usually maintained. This continuity is

usually preferred and can be implemented in the construction phase by developing appropriate details.

Comparatively, the connection between diaphragm and the interior pier cap for multi-span bridges is more complex to model for seismic analysis. According to the study by NCHRP (NCHRP 2004), there are three types of typical connections between the diaphragm and pier cap: (1) isolated connections. The continuous girders and diaphragm are placed on bearing pads without physical connections with the substructure. As a result, no moment, and sometimes no horizontal force as well, is transferred from the ground motion to the superstructure in the longitudinal or transverse directions. In practice, the connections between the girders and the pier caps are often molded as idealized pin or roller supports and there are also many variations of this type of design across the U.S. (2) Integral continuity with full rigid connection between the superstructure and pier cap, which is popular in California. (3) Similar to Type 1, however, the diaphragm is connected to the pier cap with limited shear and moment transferred during ground motion. Popular in states like Washington, this type of connection often requires the diaphragm to be partially casted before the composite deck is built. Studies on Type 3 connections are found limited and more studies along this direction were found needed as future topics (NCHRP 2004).

For the CIP Diaphragms of the prototype bridge as shown in Figure 3.3a, the two girders sit on thin bearing pads connected with CIP concrete diaphragms on an intermediate pier, including a steel anchor projected into the pier cap. This detail is similar to the old hinged design (not used on new bridges at WA any more) by WSDOT (Figure 3.3.b) except that the diaphragm of the prototype bridge shares the same width as the intermediate bent cap, thin bearing pads are used

and no recessed space to allow relative rotation. For low seismic zone like Colorado, some limited moment resistance capacity about the transverse axis exists for this specific design details. With respect to the longitudinal axis, two-column design makes the corresponding rotational stiffness significantly large so that the connection is acting rigidly about the longitudinal axis for piers with more than one column, as suggested by Priestley et al. (2007). In respect to the transverse axis, the specific detail of the connection as shown in Fig. 3.3a will allow very limited relative rotation first before the compressed thin bearing pad and the pier cap stops further relative rotation. So the actual performance of the connection is mostly likely in a semi-rigid and time-variant style when subjected to seismic, somewhere between an idealized pin support and an idealized fixed support. It is typically known that the rigid connection assumption usually gives more conservative results for the substructures. This is of course the case assuming low seismic demand where the connection rigidity is maintained during an earthquake event. For higher levels of excitations, however, plastic hinges could develop which could cause softening in the connection. Given the discussed considerations, the following study will focus on the assumption of an idealized rigid connection between the continuous girders and the intermediate pier cap. To provide more insights about the effect of different connection assumptions on bridge behavior, a comparative study of pinned and also roller connections are conducted and some discussions are made in Chapter 6.

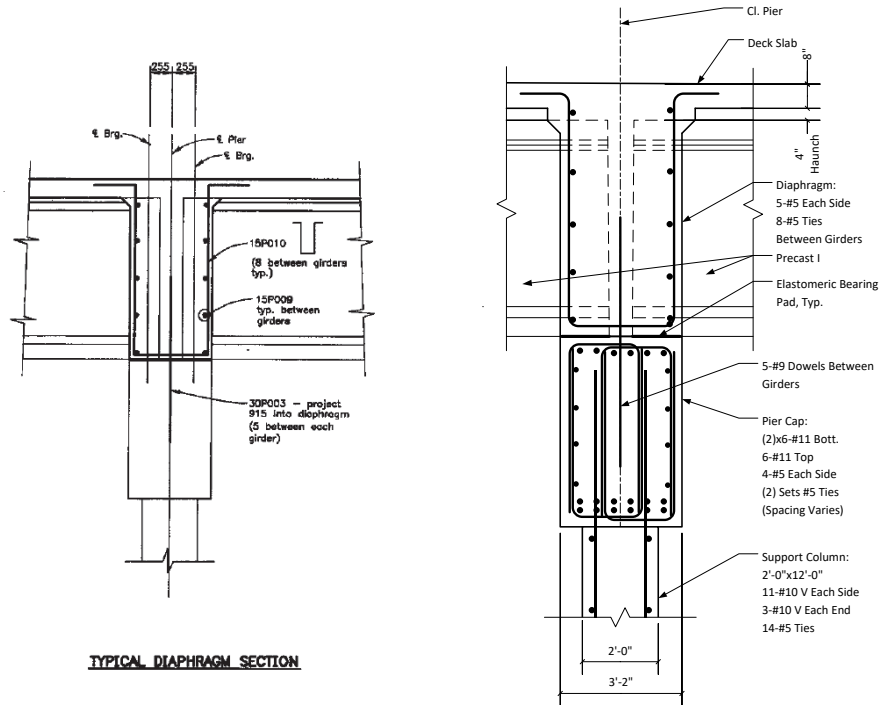

(a) CDOT prototype bridge

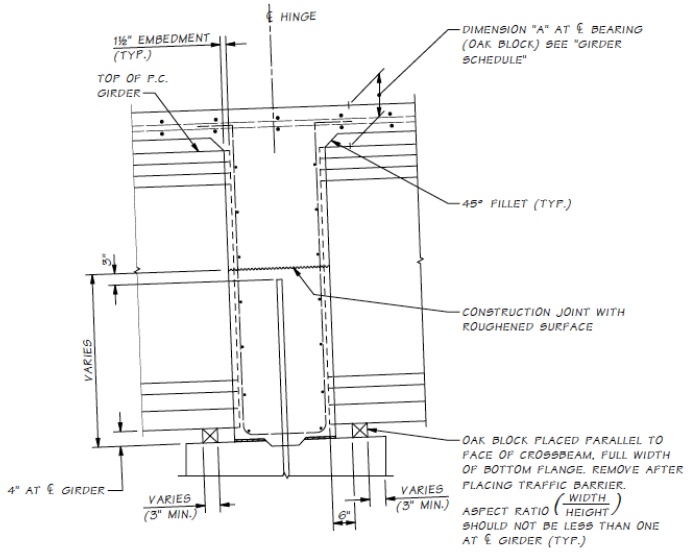

End Type C (Intermediate Hinge Diaphragm)
Figure 5.6.2-5

(b) WSDOT(WSDOT Design Manual 2015)

Figure 3.3 CIP Diaphragms details

3.5. *Alternative Modeling Capacity Software: KSU_RC*

SAP2000, as well as some other FEM software, can provide accurate capacity modeling, which can be incorporated into time-history analyses. In consideration of time and design-efficiency for the construction of detailed FEM models, a simplified program is available to estimate section capacities. KSU_RC is open source section analysis software that specializes in estimating moment-curvature and force-deflection of reinforced concrete members with monotonic and hysteresis response. It was developed by Asad Esmaeily at Kansas State University and is currently in an ongoing stage of development. Figure 3.4 show the basic interface and stress strain relationship, of a typical member developed through KSU_RC.

Link to KSU_RC: http://www.ce.ksu.edu/faculty/esmaeily/KSU_RC.htm

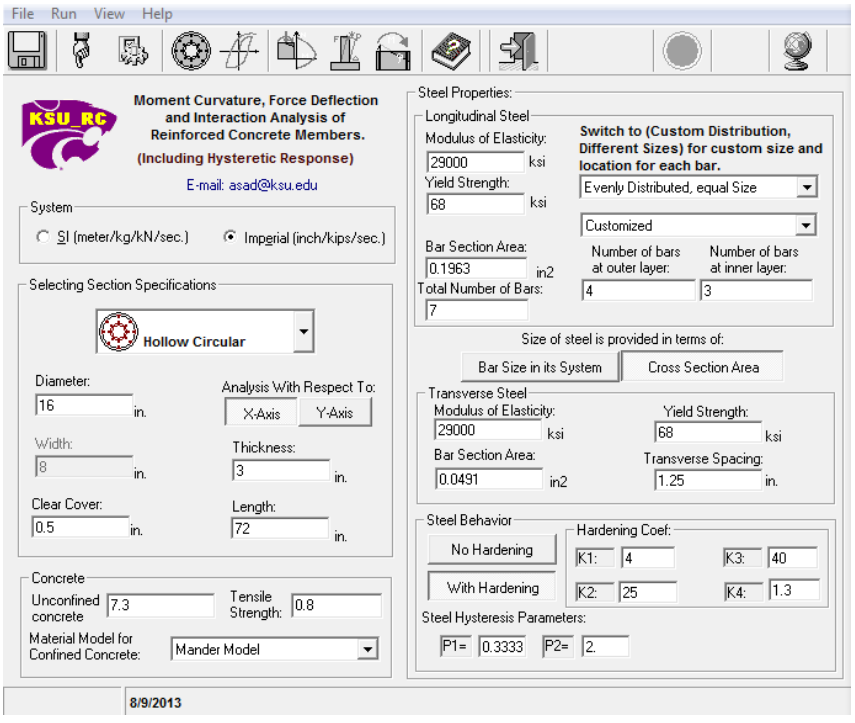

(a) KSU_RC Input Parameters Page

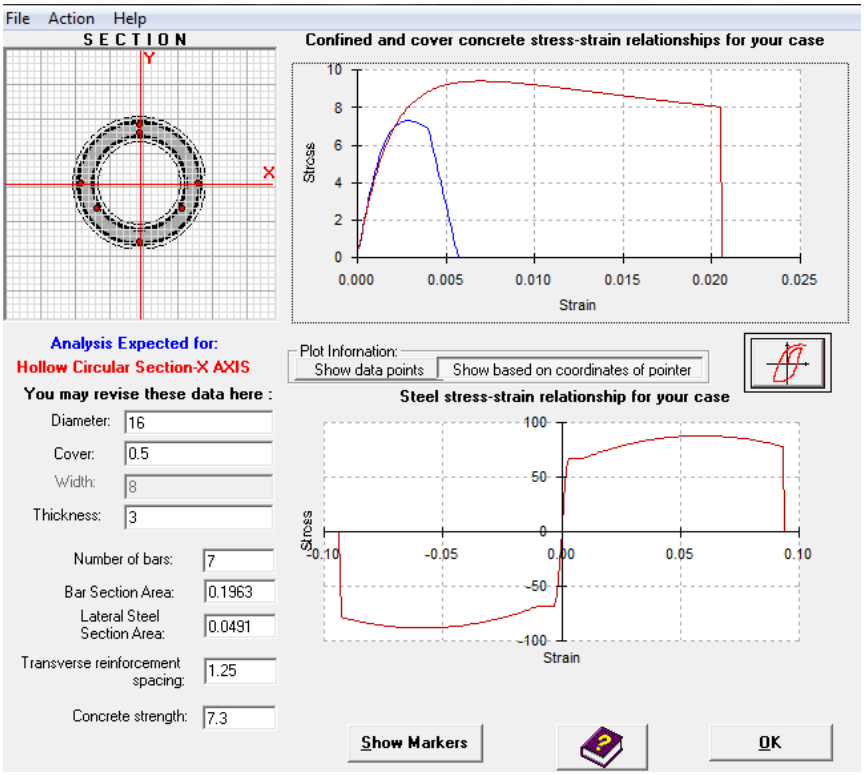

(b) Output Stress- Strain Diagram

Figure 3.4 KSU_RC interface

KSU_RC is easy to use with friendly interface and can provide an accurate, detailed estimate of the capacity of structural members. This can be used by a structural designer to check or analyze members against structural demand in an efficient manner. The disadvantage of the software is that the current version (ver. 1.0.11) has a limited number of typical sections and is limited to reinforced concrete members. However, if the demands are estimated through hand calculations using code-based procedures (e.g. AASHTO 2011), rather than FEM-based integrated software or through alternative software, capacities can be checked through this program.

4. Ground Motion Scaling and Analytical Method

4.1. Ground Motion Selection and Scaling

Ground motion scaling can be conducted through several different methods as reviewed in Section 1.7: Ground Motion Scaling. The approach taken to scale the ground motion used in the evaluation of the Colorado bridges uses response spectrum based scaling. This method is often employed in research and design and provides a simplified yet accurate representation of the ground motion hazard level of a state. The steps involved include selection of ground motion records, development of a design response spectrum and scaling of time histories using the difference in spectrums at the fundamental period of the bridge. The exact details of the method used are described in the following section.

Seven sets of earthquake records are first selected from the Pacific Earthquake Engineering Research (PEER) Center strong motion database (Table 4.1). To simulate typical earthquake motion for Colorado, Denver is chosen as a site location. A stiff soil profile for Denver is selected, and a design response spectrum is developed using the USGS database and AASHTO Guide Specifications (2011). Strong motion records were chosen based on a moment magnitude range between Mw 6.5 and 7.0, a stiff soil condition with shear wave velocity range of 650 - 1200 mi/h, and a 14 - 19 mi range for the Joyner-Boore distance of the fault to the site (Rjb). The characteristics of the selected ground motions are listed in Table 4.1. Figures 4.1and 4.2 show a representation of the fault normal response spectra for the selected records, and the design response spectrum developed for the site condition spectrum, respectively. The scaling factor is computed for the fault normal and parallel directions by matching the AASHTO design response spectrum (AASHTO 2011) to the average of the seven earthquake response spectrums at the fundamental period of the bridge structure.

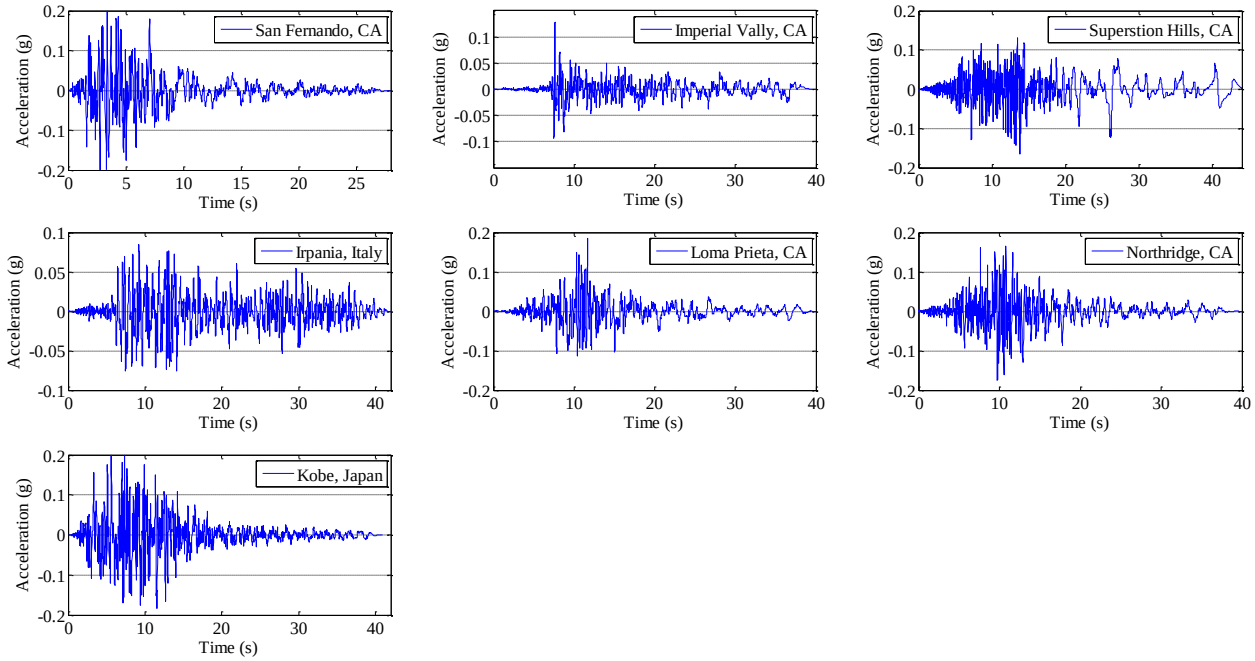

Figure 4.1 Earthquake Time-Histories Used in the Analysis

Table 4.1 Earthquake Characteristics

Record #	Event	Year	Station	Mag. (M_w)	Significant Duration (5-95%, s)	R_{jb} (mi)	Vs30 (mi/h)
1	San Fernando	1971	LA - Hollywood Stor FF	6.61	11.9	14.2	1038
2	Imperial Valley	1979	Calipatria Fire Station	6.53	25.1	14.4	675
3	Superstition Hills	1987	Wildlife Liquef. Array	6.54	29.1	14.9	681
4	Irpinia, Italy	1980	Mercato San. Severino	6.9	28.4	18.5	1148
5	Loma Prieta	1989	Agnews State Hospital	6.93	18.4	15.1	787
6	Northridge	1994	LA - Baldwin Hills	6.69	17.6	14.6	975
7	Kobe, Japan	1995	Kakogawa	6.9	17.6	14.0	1024

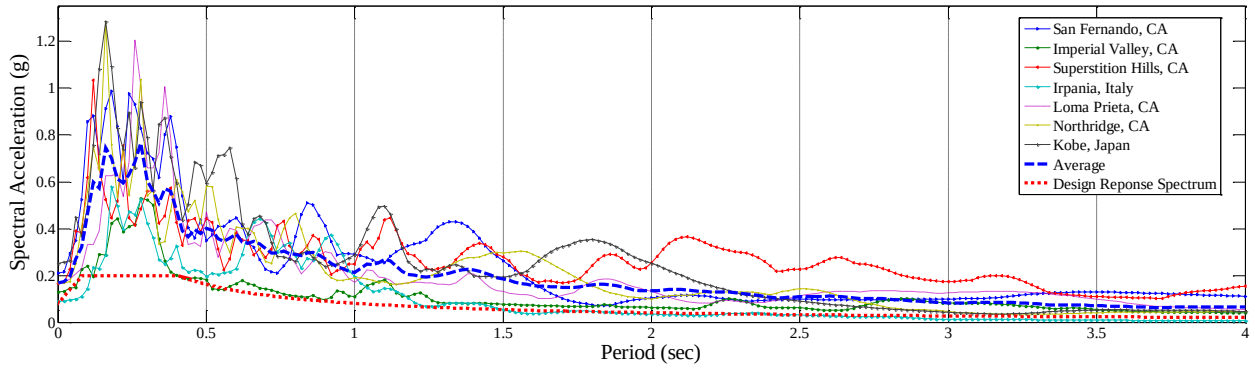

Figure 4.2 Earthquake and AASHTO Design Response Spectrum

4.2. *Applied Analysis Method: Nonlinear Time-history Analysis*

Nonlinear time-history dynamic analysis is selected as the primary method for evaluating the seismic performance of the Colorado bridges. As stated in Section 1.7, nonlinear time-history analysis is the most rigorous and accurate method of analyzing a structure since it provides realistic simulation of structural response through considering various nonlinearities or strength degradation of different members when subjected to earthquake ground motions. Less rigorous analysis methods that are commonly employed in the evaluation of the performance of structures are the response spectrum method using uniform load, single mode, or multi-mode analysis methods, which are essentially all linear analysis without considering nonlinearities. The inherent limitation of time-history analysis method lies on the fact that typically a set of representative ground motion records are employed that are targeted at representing the realistic ground motion that the bridge might observe. In cases where ground records in the area are lacking, existing ground motion from other areas or synthetic ground motion records need to be used. The method of time-step integration and damping was based on recommendations by existing research studies and also the software developer of SAP2000.

In the present study, time-history dynamic analysis is conducted with SAP2000 by adopting the direct integration method to consider both material and geometric nonlinearities. Fixed Rayleigh damping coefficients are used that represent 2% damping in the first and second modes. The method of time integration follows the Hilber-Hughes-Taylor method with alpha, beta and gamma values at 0, 0.25, and 0.5. The integration time step is kept constant at 0.01 sec and a standard iteration convergence tolerance of 0.0001 is used following a sensitivity study. Vertical ground motion is typically incorporated into the analysis of bridges in high seismic regions and bridges in close proximity to active faults (Button et al. 2002, Caltrans 2006). Given

the geographic nature of mountain states and seismic classification, the study considers effects of horizontal ground motions only. Two orthogonal components of the ground motion set were applied in each analysis. The fault normal component of the ground motion is applied to the global longitudinal direction, while 40 percent of the fault parallel component is applied in the global transverse direction. In a study conducted by Bisadi and Head (2011), it was found the adoption of 40% in perpendicular direction produced the lowest probability of underestimation of seismic demand. Although it is also common for a design engineer to utilize a 30% participation in the perpendicular direction, 40% participation in the perpendicular direction is adopted in the evaluation of the Colorado bridges for the sake of conservatism.

5. Numerical Analysis of Representative Bridges

5.1. Introduction

The seismic performance evaluation of the Colorado bridges was conducted in a series of stages. First, a modal analysis was conducted to identify the primary modes of vibration and the corresponding fundamental periods of vibrations. Next, a detailed time-history analysis was carried out on the 2-span bridge and the 3-span baseline bridges with configurations as discussed in section 4.2. Impacts of varying structural and geometric components on the seismic vulnerability of the bridge are included. Last, the effects of skew and curvature are evaluated through a comparison of several different 3-span bridge configurations, and a section analysis is performed for member capacity.

5.2. Modal Analysis Results

A modal analysis is conducted on each of the 2 and 3-span bridges configurations for participations in the first 25 modes. Ritz vectors are utilized for determining the mode shapes, and the target dynamic participation mass ratios are set at 99% in the local longitudinal and transverse directions. Scaled depictions of the resulting mode shapes and tabulated summaries of the periods of vibration for the first three modes are shown in Fig. 5.1 and Table 5.1, respectively.

The 2-Span bridge (#9 in Table 5.1) induces a longitudinal mode of vibration with a first mode period of 0.45 sec (Fig 5.1). The second and third modes of vibration have vertical and transverse mode shapes and have periods of 0.15 and 0.09 sec respectively.

Of the 3-Span bridges, the benchmark model (#1 in Table 5.1), which contains no skew or curvature, induces a longitudinal fundamental mode of vibration with a period of 0.21 sec (Fig.

5.1). Transverse and vertical modes follow with lesser periods and contain negligible rotational participation. The curved bridge configurations (#4 and #5) show comparable mode shapes and translational participation ratios to the benchmark bridge. The curved bridges differ from the benchmark bridge since torsional rotation was introduced into the mode shapes, as seen for example in the primary longitudinal mode that incurs twist about the vertical DOF. Higher contributions from rotational DOF are also observed in the mode shapes for transverse and vertical directions, as seen in Table #4. In skewed bridges (#2 and #3), participation in secondary translational directions of the first two modes is observed. This is reflected in the fundamental longitudinal modes shape, where torsional vibration occurs about the primary axis. In the skewed and curved bridges, independent geometric effects are superposed. The alternate translational participation associated with skew is observed in combination with increased rotational participation associated with curvature.

Table 5.1 Modal Participation Factors of Bridges

Bridge #	Skew (deg.)	Curv. Radius (m)	Mode	Period (Sec)	U_X (kip-s^2)	U_Y (kip-s^2)	U_Z (kip-s^2)	R_X (kip-ft-s^2)	R_Y (kip-ft-s^2)	R_Z (kip-ft-s^2)
1*	0	0	1	0.21	10	0	0	0	-10	0
			2	0.13	0	-8	0	22	0	0
			3	0.11	0	0	-8	0	1	2
2	30	0	1	0.19	10	-3	0	-18	6	0
			2	0.11	-4	-8	0	27	-25	0
			3	0.10	0	0	7	0	0	-35
3	45	0	1	0.19	9	-4	0	-20	1	69
			2	0.12	4	7	0	-15	72	-119
			3	0.10	0	0	-7	0	-128	55
4	0	4500	1	0.20	10	0	0	40	3030	-43315
			2	0.13	0	8	0	-2064	50	-1518
			3	0.10	0	0	7	33201	893	5
5	0	3000	1	0.21	10	0	0	89	3141	-29850
			2	0.13	0	-7	0	2556	-22	1288
			3	0.10	0	1	6	18499	667	-25
6**	30	4500	1	0.20	9	-3	0	1901	2829	-39736
			2	0.12	-4	-7	0	1852	-1207	17656
			3	0.10	0	0	-7	-29514	-749	-549
7	45	4500	1	0.19	9	-4	0	3712	2722	-37483

			2	0.12	-5	-6	0	1660	-1606	22543
			3	0.10	0	0	7	32996	945	297
8	30	3000	1	0.20	9	-4	0	2146	2905	-27126
			2	0.13	-4	-7	0	3280	-1363	14078
			3	0.11	0	0	7	21793	965	-392
9	40	4500	1	0.43	10	0	0	-32	2809	-19724
			2	0.15	0	-1	6	12021	398	-51
			3	0.09	0	8	1	49	127	-867

Note: * Benchmark model and ** Baseline model

5.3. Evaluation Criteria

The seven earthquake records previously described are applied to each of the bridge models through non-linear dynamic time-history analysis. The demand is compared to the component section capacity using demand-deformation relationships based on a fiber model for member sections (CSI 2011). Demand/capacity (D/C) ratios for the column section are calculated for column sections using axial force-uniaxial moment relationships, and further investigated using an axial force, biaxial moment surface interaction, shown in Fig. 5.1. Using strain relationships for axial forces and moments in any two orthogonal directions in the horizontal plane, 3-dimensional curves representing the capacity are developed and plotted together to generate a surface. The section capacity is also heavily dependent on the axial load; for higher axial loads both directional components positively increase moment for structures below the balance point on the moment interaction diagram as shown below.

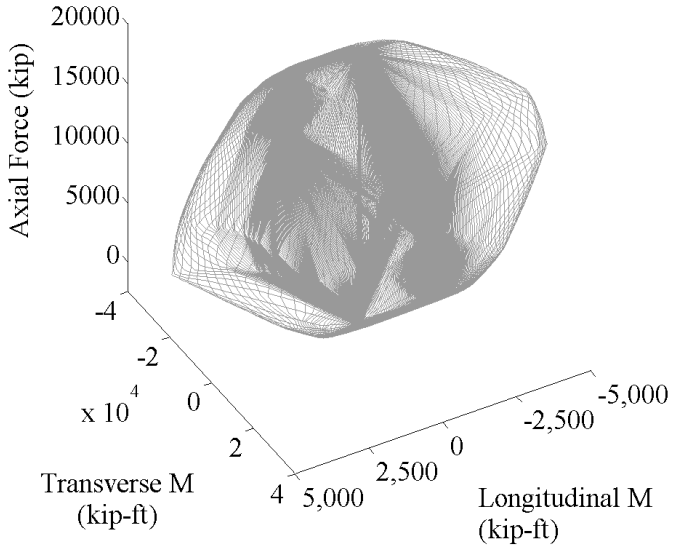

Figure 5.1 Axial Force, Biaxial Moment Interaction Surface for the Pier-column Section

5.4. *Time-history Analysis Results of the 2-span Baseline Model*

Time-history analysis is first performed on the 2-span bridge for the seven earthquake records previously described. Ground motion excitation at supports of the bridge induces, among other responses, planar torsion about the superstructure and large demands imposed on the pier-columns. The largest response across the earthquake records is induced by the Loma Prieta earthquake record, which causes both higher demands and deformations. Longitudinal drift in the pier-columns is the largest at the exterior column with respect to the center of curvature, followed by the interior column. The drift at these locations reaches a maximum of 0.213% in the longitudinal direction, and 0.03% in the transverse direction. At the abutments, the resistance of the soil ranges from 303.9 kips to 1605.1 kips. Significant demands are generated in the substructure of the bridge under ground motion excitation. The highest moment demand is generated under the Loma Prieta earthquake and about the interior column. The generated

demand and relative capacity are summarized in Table 5.1 below. The axial and shear demands in the longitudinal and transverse directions generated in the pier-column are 494.1, 74.3 and 164.4 kips respectively and do not exceed the capacity of the section. In terms of bending forces, the section resists the moments in the transverse direction of the column safely. In the longitudinal direction, the moment generated at the bases of the pier-columns induces plastic hinging behavior (Figure 5.2). The hinge capacity per FEMA-356 guidelines is estimated at 0.137 radians and is shown for positive rotations in Figure 5.2 (FEMA 2000). Plastic hinges are not observed at the top of the pier-columns, and the induced rotation at the base is reduced for columns further from the interior.

Table 5.2 Maximum Demand on Bridge Pier –at Interior Column for the 2-Span Bridge (Local Coordinates)

	Axial Force (kips)	Shear (long.) (kips)	Shear (trans.) (kips)	Uniaxial Moment (long.) (kip-ft)	Uniaxial Moment (trans.) (kip-ft)
Maximum Demand	494.1	74.3	164.4	1328	442.3
Demand/Capacity	0.64	0.29	0.65	1.08	0.36

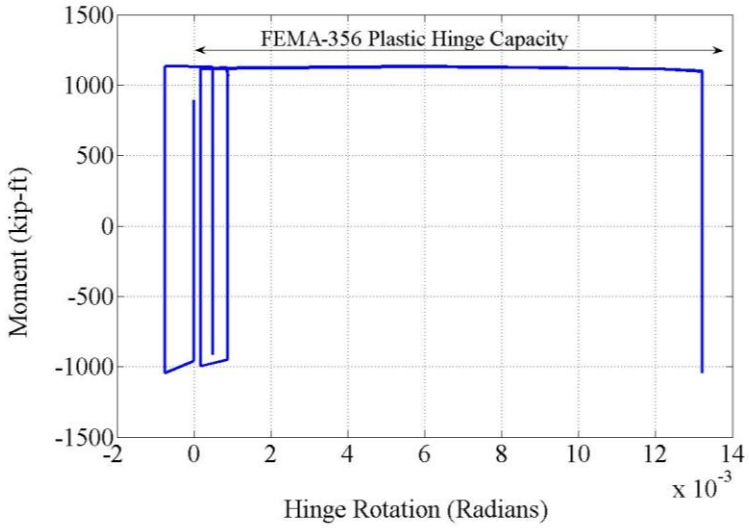

Figure 5.2 Plastic Hinge Rotation for Interior Column w/ FEMA-356 Ultimate Capacity

5.5. *Time-history Analysis Results of the 3-span Baseline Model*

Nonlinear time-history analysis is conducted on the 3-span baseline bridge model. The baseline bridge configuration (#6 in Table 2.2) consists of a 4500 ft radius of curvature and a 30-degree skew. Under seven sets of dynamic time-history earthquake loading, ground motion excitation of supports induces: longitudinal drift at the top of the piers (Fig. 5.3a); concentrated actions at the column bases (Table 5.2); and concentrated loads on the abutments in the transverse and longitudinal directions. Among the earthquake records, deformations are more notably observed when the bridge is excited by the San Fernando, Loma Prieta, or Kobe earthquake records. The San Fernando earthquake time-history induces the highest demands observed in the substructure, and is therefore used as a basis for evaluation of triaxial capacity against axial and bending forces.

The highest drift ratios in the pier-columns are observed at the tops of the interior column, and undergo peak excitations of 0.18% and 0.037% in the local longitudinal and transverse directions, respectively. Resistance of the soil across the back of the abutment ranges from no observed resistance to 1104.7 kips. The large variance is attributed to the level of deformation induced in the superstructure and the consequent impact on the soil. Under dead load, the bridge is pulled towards the center of mass, and away from the backing soil. If the excitation of the bridge does not cause a large enough deformation to close the gap and induce impact on the soil, no resistance is observed.

Coupling effects are observed between diagonally opposite pier-columns as an effect of the skewed substructure and abutments. Although the relative deformation is limited in the superstructure, significant actions are developed in the substructure (Table 5.2). Uniaxial analysis shows column shear and moment in the local longitudinal (weak) axis to be controlling

the design. The longitudinal shear generated in the columns reaches 92.3% of the nominal capacity, while the longitudinal moment reaches 69.2% of its capacity. In addition to the unidirectional analysis, the demand on the critical interior column for the San Fernando earthquake is plotted against the triaxial surface capacity (Figs. 5.3a-b). The section cut of the triaxial surface shows that the section capacity is exceeded by the demand in several instances of the earthquake excitation, and that subsequent damage may be expected.

Table 5.3 Maximum Demand on Bridge Pier –at Location 1 for the Baseline Bridge (Local Coordinates)

	Axial Force (kips)	Shear (long.) (kips)	Shear (trans.) (kips)	Uniaxial Moment (long.) (kip-ft)	Uniaxial Moment (trans.) (kip-ft)
Maximum Demand	870.6	440.0	158.8	1749	6852.5
Demand/Capacity	0.076	0.923	0.289	0.692	0.465

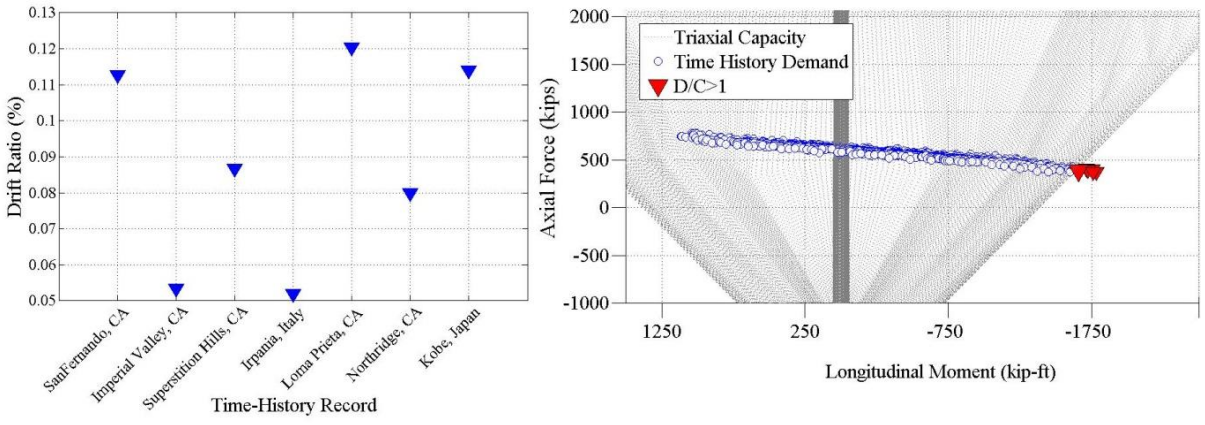

(a) (b)

Figure 5.3 (a) Triaxial Capacity Demand and (b) Drift Ratio - Loma Prieta Time-history

5.6. *Effect of Earthquake Input Direction*

In the analysis of the baseline model above, the earthquake input hereafter referred to as the Primarily Longitudinal Combination, is applied (100%) in the global longitudinal and partially (40%) in the global transverse direction. To study the effect of a different earthquake input direction, a new seismic input combination is defined. The new combination consists of a full (100%) load contribution to the global transverse direction and a partial (40%) contribution to the longitudinal direction. This input is referred to as the Primarily Transverse Combination, with which the structural model of the baseline bridge is reanalyzed.

In comparison to the analysis using the Primarily Longitudinal Combination, the drift ratios at the pier cap for the Primarily Transverse Combination are reduced in both the longitudinal and transverse directions (Figs. 5.4a and b). Comparatively, maximum D/C ratios developed in the pier-columns for the Primarily Transverse Combination are also on average 55.5% smaller. This is predominantly attributed to the asymmetrical strength and rigidity of the column sections in the global transverse direction, and the added resistance derived from the abutments in the transverse direction. The abutment reactions are also lower in all six degrees of freedom for the transverse combination in comparison to the longitudinal combination. The column critical locations do match for both combinations and those critical locations are the focus points for the analyses to follow.

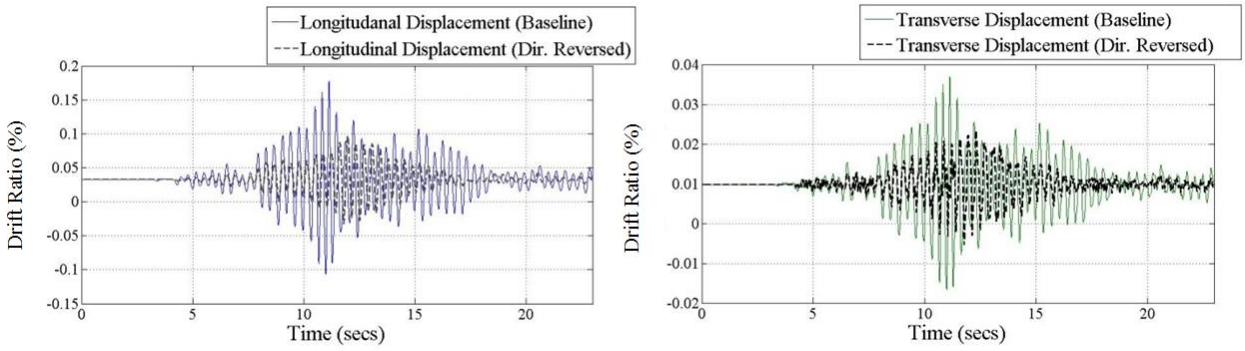

(a) (b)

Figure 5.4(a) Longitudinal and (b) Transverse Drift Ratios of Baseline Bridge with Reversed Input Direction - Top of Pier - Loma Prieta Time-history (Location 1)

5.7. *Effect of Support Condition*

Another parameter investigated is the effect of a non-integral abutment support. The analysis showed that small variations in support condition significantly affect the excitation and subsequent distribution of actions in the bridge model. Imposing a typical abutment support, the integral abutments are replaced with bearing pads and reinforced with shear keys. The support connection is modeled by restraining translation in the vertical and transverse directions and rotation about the vertical and longitudinal axes. In addition, a three-inch gap spring is used to represent the typical longitudinal expansion allowed between the superstructure and abutment. The results from the analysis show that the use of a bearing type connection releases the structure in the longitudinal direction, increasing the period of vibration and subsequently reducing the demand on the structure. Modal analysis yields an increased period of 0.394 sec and induces equivalent modes of vibration to the baseline model.

The dynamic time-history analyses results show that with the change in abutment condition, a lower demand is generated across the piers. In fact, a very low demand is generated that induces little to no additional strain on the pier columns. In addition the bearing supports develop significantly smaller forces, with transverse force and moment 12.3% and 33.6% lower than those of the integral abutment, respectively. At the pier connection, actions developed across all DOFs were 53.7% lower than those developed with an integral abutment. This may infer that there are significant advantages for CDOT to employ bearing type (or longitudinally released) supports at the abutments for curved and skewed bridges where seismic performance is a concern. On the other hand, if bearing supports are adopted, bridge designers should make appropriate considerations to potential pounding effects, as well as the strength of transverse support components such as shear keys, despite it not being a concern for this specific bridge configuration and loading scenario.

5.8. *Effect of Soil Stiffness*

A series of models were constructed to specifically investigate the effect of a varied spring soil condition around the abutments. To achieve this 5 additional models were constructed with varying soil stiffness's, as shown in Table 5.3. Each model varies the spring force by the resistance factor that is the ratio between the new spring force and the spring force for the benchmark model.

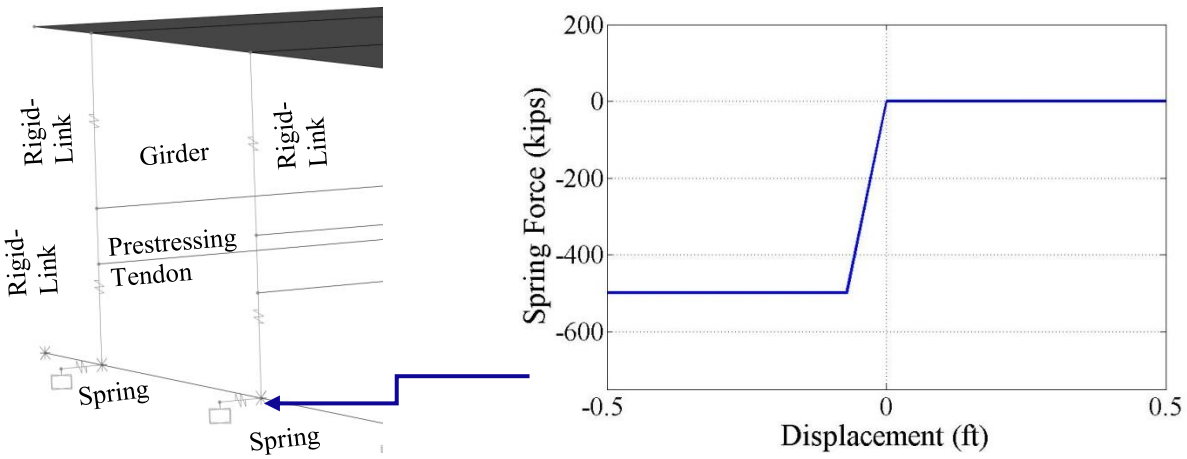

Figure 5.5 Abutment Spring and Force-Displacement Relationship

Table 5.4 Soil stiffness

	Model 1	Model 2	Model 3 (BM)	Model 4	Model 5	Model 6
Soil Stiffness (kN/m)	15	75	150	225	300	6000
Soil Resistance Factor	0.01	0.5	1	1.5	2	4

Time-history analysis of various soil conditions impacts the dynamics of the structure and consequent distribution of forces. With an increase in soil stiffness, the bridges dynamic response is reduced (Table 5.4). This in turn leads to a lower displacement in the longitudinal direction, which is characterized by a lower column drift. It also diminishes effects of torsion from skew, reducing the transverse column displacement and rotation. This is accompanied by a reduction in both shear and bending forces in the substructure (Figure 5.6). An increase in soil stiffness also leads to an increase in the axial compression forces developed. This has both positive and negative effects by increasing the section capacity in bending, but decreasing the capacity of the section to resist shear forces.

Table 5.5 Soil Stiffness Results

Model #	Soil Force Abutment (kips)	Drift Ratio (long.)	Drift Ratio (transv.)	Axial Force (kip)	Long. Shear (kip)	Trans. Shear (kip)	Long. Moment (kip-ft)	Trans. Moment (kip-ft)
1	78.7	0.18%	0.058%	816.5	408.7	129.3	1596	6757
2	316.2	0.17%	0.056%	804.6	366.0	121.4	1492	6050
3	505.7	0.16%	0.055%	821.2	371.8	114.9	1401	6167
4	641.2	0.16%	0.054%	827.8	372.7	114.2	1398	6201
5	730.4	0.16%	0.051%	830.4	373.4	112.9	1375	6164
6	898.4	0.15%	0.048%	837.4	357.9	107.0	1283	5890

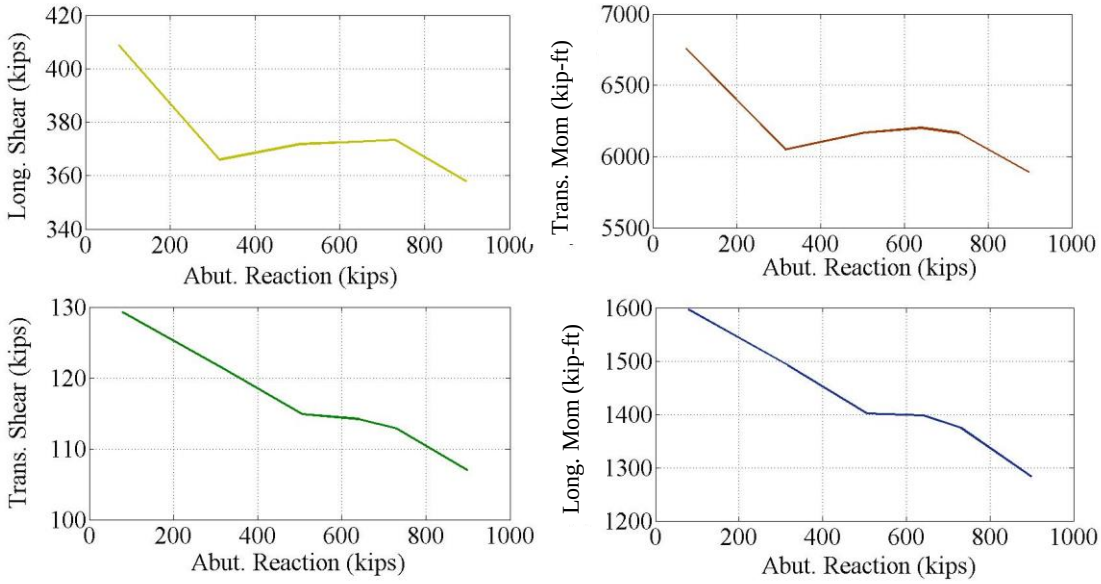

Figure 5.6 Soil Effects on Pier Column

5.9. *3-Span Parametric Study Results – Curved and Skewed Bridge Configurations*

The analyses described above evaluate the impacts of design considerations for the base line model. In this section, the effects of curvature and skew are further analyzed. The results of the

baseline models are used as a reference for comparison of trends, while the benchmark model (no skew or curvature) is used as a control for evaluating geometric effects.

5.9.1. Drift Ratios of Pier-Columns

The excitation of the bridges induces relatively low deformation, regardless of geometric configuration (Fig. 5.7). The displacements in both directions are observed to be minimal, with relatively higher longitudinal displacements observed in the primary axis of loading. The bridge configurations are composed of non-slender reinforced concrete members that are connected integrally to abutments and piers. Subsequently, large deformations are not easily incurred without significant damage to members or connections. Behavioral effects observed in the model sets would likely be amplified in less structurally rigid bridges with more flexible supports.

Planar rotation in the substructure is observed in skewed bridges, characterized by higher percentages of translational drift and lower percentages of longitudinal drift, measured at pier caps. Effects from curvature on the bridge translational motion are not observed due to the constraining nature of the abutments. Despite the limited deformation observed, the bridge geometries incorporating skew and curvature result in trends of higher resisting forces in the substructure and abutment.

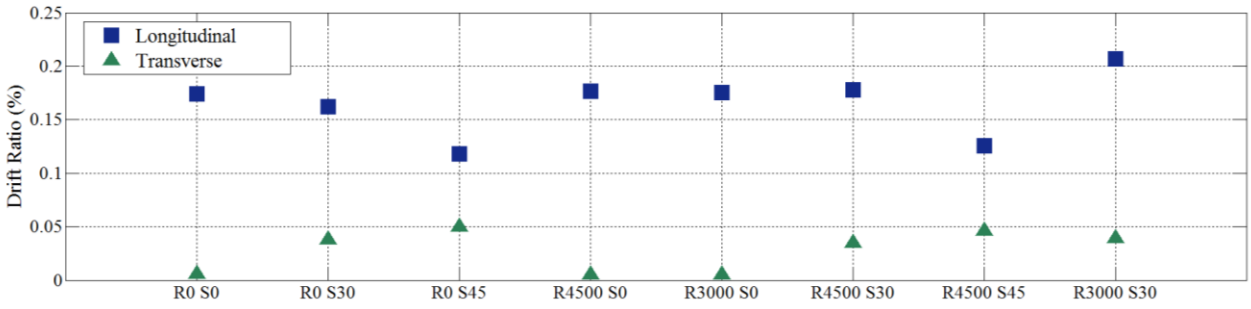

Figure 5.7 Longitudinal and Transverse Drift Ratios at Pier

5.9.2. Soil Resistance

The resistance of the soil at the abutment is a function of the induced vibration from effects of geometry, and the resultant displacement in the longitudinal direction. The non-skewed bridge configurations induce primarily longitudinal vibration and therefore, yield the highest resistance from soil springs (Fig. 5.8). Skewed bridges induce more planar rotational motion about the center of the superstructure. This causes substantially higher forces on the transverse supports of the abutments, and less stress longitudinally on the backing soil. Alternative abutment configurations where initial transverse resistances are comparable, such as shear keys or wing walls, would be heavily loaded in the scenarios involving skewed geometries and may exceed expected capacities.

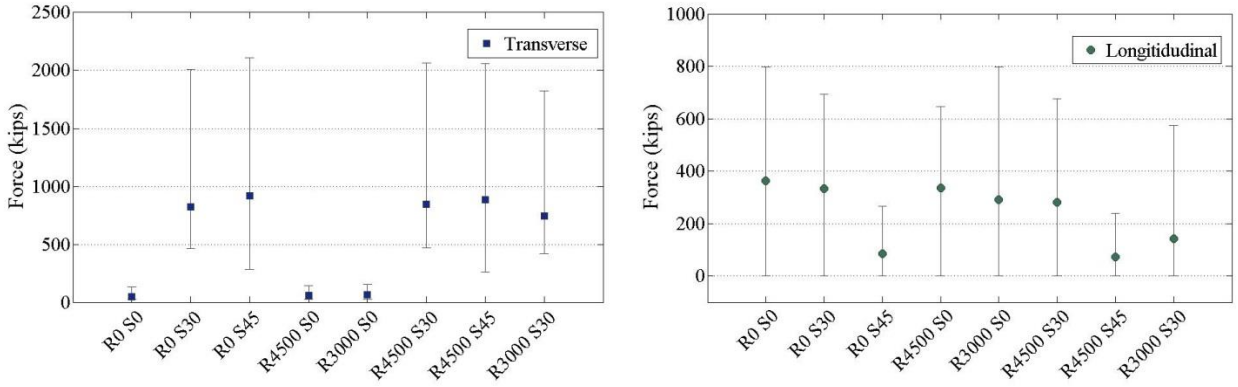

Figure 5.8 Reaction Force at Abutment – (Global)

5.9.3. Shearing Forces in the Pier-Columns

The shear capacity of the pier-columns was calculated using section 5.8.3.3 of the AASHTO LRFD Bridge Specifications for determination of nominal shear resistance of concrete

members (American Association of State and Highway Transportation Officials, 2007). The shear capacity of the section is heavily dependent on axial, moment and shear demand, thus a comparison of the capacity to the longitudinal and transverse shear loading over the span of the time history is made (Critical long. direction shown in Fig. 5.10). A summary of the critical shear D/C ratios for each of the configurations is also made, as presented in Fig. 5.11. The shear force observed in the substructure of skewed bridges shows significant dependence on the angle of skew. In both skewed bridges, skew causes a reduction in the transverse column shear, and a substantial increase in longitudinal shear. The longitudinal shear in the 45 degree skewed bridge is the highest at 650.2 kips, and exceeds the capacity of the section at the two boxed intervals shown in Fig. 5.9. The longitudinal and transverse shear observed in the pier-columns of curved bridges decrease for higher radii of curvature. In the combined geometries, the shearing forces are comparatively higher in the transverse directions and varied in the longitudinal direction. The longitudinal shear forces observed in all the skewed bridge configurations are near or exceed 1.

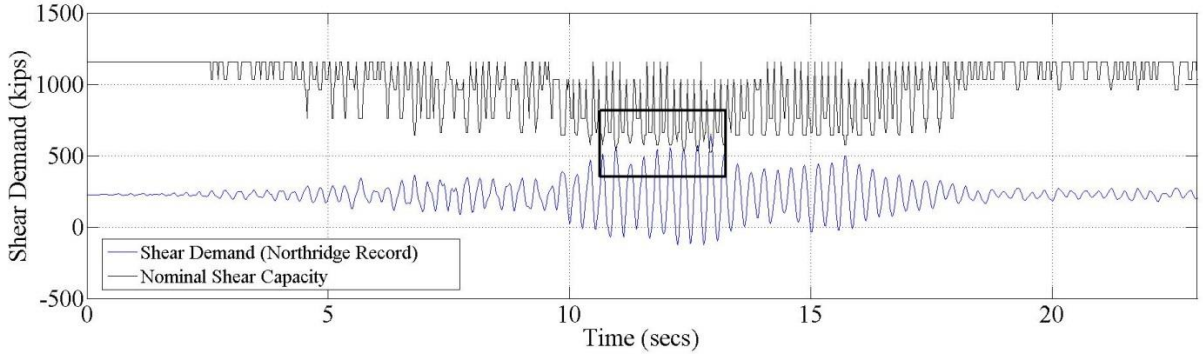

Figure 5.9 Pier Shear Force/ Nominal Capacity – Northridge Time-history

5.9.4. Axial Force and Moment Demand on Pier-Columns

In comparison to the benchmark model (of no skew or curvature) the bridge configurations with skew and curvature independently yield higher D/C ratios in the substructure. An evaluation of the pier-columns is conducted first through force-uniaxial moment D/C ratios, then by use of force-biaxial moment surface interaction. The D/C ratios represented in Figs. 5.10a-b are for the time-history and column location yielding the highest demand, although the analysis and discussion is equally accurate for the average behavioral trends. In all model sets, the distribution throughout the pier-columns shows the highest concentration of demand at the bases of pier-columns.

Imposing skew on the bridge structure directs bending in the substructure away from the weak axis of the columns and also causes cross coupling of actions between adjacent columns. In the longitudinal (weak) axis of the pier-columns: the normally critical longitudinal moment decreases proportional to the skew angle (Fig. 5.10a). This is accompanied by an amplification of the moment in the strong axis, which becomes critical in the 45-degree skew configuration. In the curved bridge configurations, although equivalent deformation is observed, longitudinal moment increases proportional to higher degrees of curvature, and is substantially more critical than transverse moments. In the combined geometries, interaction between skew and curvature leads to a stacking effect where higher moments are observed in both the longitudinal and transverse directions. This results in the longitudinal and translational moment reaching 87.9 % and 66.6 % of nominal capacity respectively in combined configurations.

To evaluate the pier-column capacities for axial forces with bidirectional moments, the column demand was evaluated with respect to the force-biaxial moment surface capacity. For each bridge configuration the most critical time-point is selected from the time history, and the resulting demand is plotted against the triaxial surface capacity (Fig. 5.10b). The plot of the

analysis shows the demand exceeding the capacity of the pier-column sections in 3 out of 8 bridge configurations, primarily attributed to moment in the longitudinal moment direction. Some damage may occur in the curved bridge configuration of lowest radii (3000 ft.), due to higher induced longitudinal moment from curvature in combination with induced transverse moment and low axial compression. In the combined curved and skewed bridge configurations, higher longitudinal moments (caused by curvature) combined with higher transverse moment (caused by skew) lead to exceedance of capacity in both 3000 ft and 4500 ft curved, 30-degree skew bridges. Exceedance of capacity does not occur in the 4500 ft curved, 45-degree skew bridge configuration due to reduced longitudinal moment attributed to the skew angle. The triaxial analysis performed on the range of geometric configurations illustrates the importance of examining combined loadings, particularly in complex geometries where demands are high in both directions.

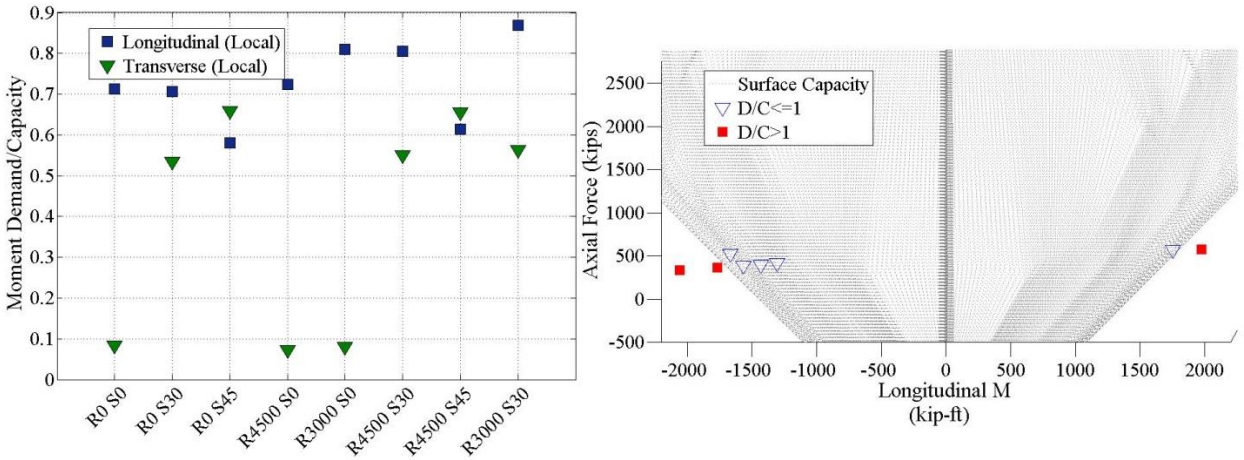

Figure 5.1 (a) Section Analysis – Unidirectional Moment Demand/Nominal Section Capacity at Critical Pier (b)Triaxial D/C Ratios of Pier-Columns in Various Bridge Configurations

Analysis of the different geometries also identifies critical locations for higher seismic demand and locations where damage may occur (Fig. 5.11). For the curved configurations, the

two interior columns consistently display higher D/C ratios compared to exterior columns, where the separation is proportionally larger for higher degrees of curvature. For the curved bridge model of highest curvature, this effect leads to exceedance of nominal capacity in interior columns. For skewed bridge configurations, coupling of actions in diagonally opposite pier-columns is observed. Higher force and moment demand in skewed bridges is higher, and focused in front interior and back exterior locations due to coupling and planar rotational. The separations between column sets are also more apparent for higher degrees of skew. The behavior observed in curved and skewed bridges is evident in combined geometries and a stacking effect is observed. Both skew and curvature have in common the interior front column location as a focus point for high concentrations of demand. This location yields higher shearing forces as well as higher axial and moment demands, which in two of the three combined geometries leads to exceedance of nominal capacity.

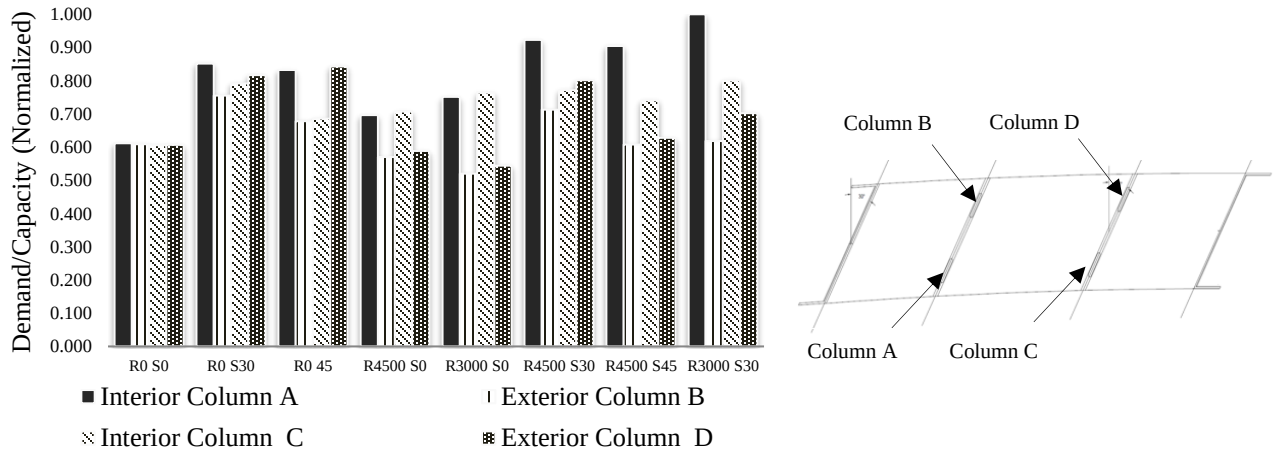

Figure 5.2 Normalized Triaxial Demand Ratios at Critical Pier-Columns

5.10. Section Analysis of Bridge Components

In order to evaluate the remaining structural components of the bridge against seismic based loading, a section analysis is performed for the integral abutments, bent-caps and girder components. In the section analyses, each section is subject to a large range of axial stresses. To be consistent, the axial force used to determine the section capacity is taken conservatively as zero for each section. For the 3-span bridges, the demand is determined from the critical geometry and time-history from the entire set of geometries. Based on the section performance, insight is provided on the impact of geometrical effects.

Table 5.6 Section Analysis of Integral Abutment: 2-Span Bridge

		Peak Demand	Nominal Section Capacity	D/C
Axial	Kip	-119.4	635.4, -7005.1	0.02
V2	Kip	-112.0	659.1	0.17
V3	Kip	-11.7	448.9	0.03
T	Kip-ft	-270.3	299.3	0.90
M2	Kip-ft	13.8	2537.1	0.01
M3	Kip-ft	363.2	739.2	0.49

Table 5.7 Section Analysis of Integral Abutment: 3-Span Bridges

		Peak Demand	Nominal Section Capacity	D/C
Axial	Kip	-192.3	597.6, -7549.9	0.03
V2	Kip	46.2	786.6	0.06
V3	Kip	-251.8	457.4	0.55
T	**Kip-ft**	**-1489.2**	**533.6**	**2.79**
M2	Kip-ft	447.2	3327.5	0.13
M3	Kip-ft	154.9	637.9	0.24

The integral abutment is analyzed across the *x*-section that spans between girders. The highest demand was observed at interior and exterior span locations. The main issue with the abutment is its resistance to the torsional moment created by the skew of the bridge

superstructure. This is particularly of concern for the 3-span bridges with larger skew angles that result in larger torsional moments. The SAP models do utilize full fixity in this DOF as a representation of the integral abutment support provided by the pile foundation and backing soil. Although beyond the scope of this project, a soil-interaction study at this location may be helpful on providing more accurate insights, which is recommended for future study.

Table 5.8 Section Analysis of Bent Cap: 2-Span Bridge

		Peak Demand	Nominal Section Capacity	D/C
Axial	Kip	-192.3	1459.2, -10179.0	-0.04
V2	Kip	-362.57	682.9	0.48
V3	Kip	326.27	1246.3	-0.04
T	Kip-ft	-49.97	876.1	0.65
M2	Kip-ft	566.76	3487.2	0.08
M3	Kip-ft	282.99	2884.4	-0.28

Table 5.9 Section Analysis of Bent Cap: 3-Span Bridges

		Peak Demand	Nominal Section Capacity	D/C
Axial	Kip	-684.41	1755.89, -9728.7	0.07
V2	Kip	497.37	680.20	0.73
V3	Kip	97.90	580.46	0.17
T	**Kip-ft**	**1181.82**	**1145.00**	**1.03**
M2	Kip-ft	549.01	2322.50	0.24
M3	Kip-ft	-2589.77	6404.43	0.40

In the analysis of the bent cap under seismic ground motion, the section is exposed to large moment and torsional demand. In bending, the section capacity is large enough that the integrity of the member is unscathed. Under seismic loading, an integral diaphragm connection between the pier-columns and the superstructure can create large torsional moments on the bent cap section. This could potentially be alleviated by using a bearing type connection, or strengthening the cross-section for larger torsional forces. Of the various bridge geometries, these demands

were observed to be the largest on bridges incorporating larger degrees of skew and curvature. Peak torsional demand was observed in bridge sets that involved both components together.

Table 5.10 Section Analysis of Girder: 2-Span Bridges

		Peak Demand	Nominal Section Capacity	D/C
Axial	Kip	-921.11	-3715.7	0.25
V2	Kip	102.03	712.59	0.14
V3	Kip	-6.12	681.59	0.01
T	Kip-ft	15.69	52.00	0.30
M2	Kip-ft	43.57	233.36	0.19
M3	Kip-ft	-1122.91	3734.89	0.30

Table 5.11 Section Analysis of Girder: 3-Span Bridges

		Peak Demand	Nominal Section Capacity	D/C
Axial	Kip	-842.31	-3196.90	0.26
V2	Kip	-83.92	1056.99	0.08
V3	Kip	-8.35	671.67	0.01
T	Kip-ft	3.69	69.45	0.05
M2	Kip-ft	57.80	67.37	0.86
M3	Kip-ft	-1221.89	5542.25	0.22

In the analysis of the seismic demand on the superstructures girders, no exceedance of the nominal section capacity was observed. Some lateral bending moments were induced due to skewed and curved plan geometries. However, they were not large enough to exceed the girder member's capacity. The highest concentration of bending forces and demand were observed at the ends of the span, and particularly at the connection to the integral abutment.

5.11. *Summary of Analytical Results*

Over the course of this study, two and three-span RC bridge configurations were subjected to 7 different earthquake ground motions. The geometric and support configurations of the three-span bridges were varied to include different components of skew and curvature, as well as the effects of support boundary conditions and soil conditions. FE bridge models were created for each configuration and subjected to nonlinear time-history-analysis. The following summarizes the results from the numerical analyses conducted:

Analysis of 2-Span Bridge J-17-AA:

In the pier-columns of the substructure, the 2-span bridge with a radius of 2000’ and 40 degree skew performs well under axial and shear demands imposed by the earthquake sets. The axial forces reach a peak D/C ratio of 0.64, and the shear demand reaches a peak in the translational direction of 0.65. In bending, the column is not vulnerable in the translational direction (about the weak axis). The moment demand in the longitudinal direction of the column exceeds the bending capacity by D/C of 1.08. Through the section analysis, it was found that the integral abutment may also encounter some issues with torsional demand as the D/C ratio for the section reached a peak of 0.9. Analysis of the bent cap and I-girders yielded no major issues under seismic loading.

Analysis of 3-Span Configurations

Similar to the 2-Span bridge model, large deformations are not observed on the 3-span bridges due to the rigid nature of abutment supports and integral pier connections. Generalizing

all geometric configurations analyzed, peak drift ratios are measured at a 0.21% and 0.05% in the longitudinal and transverse directions, respectively.

Under axial and bending forces, a biaxial demand section analysis indicates high D/C ratios, but none exceeds unity. Triaxial demand analysis shows potential bending damage in the bridge of lowest curvature (3000 ft) due to higher induced longitudinal moments in the interior column. Similarly, capacity exceedance is also observed in the two 3000 ft and 4500 ft radius curved, 30 degree skewed bridges. This is attributed to higher longitudinal moments caused by curvature, combined with higher transverse moments caused by the skew angle. The lengthwise shear demand induced in the pier-columns of the substructure also yields a potential damage point for all bridges involving skew levels of 45 degrees, and also in the 910 m radius, 30 degree skew bridge.

Through the section analysis conducted, it is observed that some damage may be sustained to the integral abutment under the torsional demands induced by the superstructure. Although the demand may be significantly alleviated by the displacement of the foundations (not included in the model), analysis of FE models yields peak D/C ratio of 2.8. Similarly, analysis of the bent cap section yields that the torsional demand exceeds section capacity by a marginally higher ratio of 1.03. The girder section capacities do not yield any particular vulnerability to seismic loads, which is consistent with most observations in other earthquake studies.

Effect of Earthquake Input Direction

Ground motion applied primarily in the global longitudinal direction (100/40) was confirmed to control the design and analysis. Loading shifted to (100/40) in the transverse axes yielded a 55.5% reduction in the column D/C ratios, lower deformations at pier caps, and lower resistance

forces generated at supports. Dynamic time-history analysis per the AASHTO codes utilizes a (100/30) ratio for applied earthquake time-histories. If a single direction is applied; a primarily longitudinal combination is likely to induce larger demands on the bridge.

Effect of Support Condition

Integral abutments were found to induce substantially higher actions and deformations in the structural model compared to a bearing support. A standard bearing support if adopted and properly designed, can increase the period of vibration, reduce bridge excitation, and substantially lower the demand on columns, abutments and pier cap connections.

Effect of Soil Stiffness

The bridge displacement is reduced as the resistance force and soil stiffness increase. The increase of soil stiffness also reduces the effects of torsion, characterized by a reduction in column rotation. With a reduction in the displacement of the deck and superstructure, a trend of reduction in both shear and bending forces is observed in the substructure. It also leads to an increase in the axial compression forces developed which can have a net positive effect by increasing the section capacity in bending, but reduces shear capacity.

Analysis of 3-Span Bridge D-17-DJ Geometric Configurations:

Effect of Skew

Skewed bridge geometries induced coupling effects between diagonally opposite columns and directed seismic induced actions away from the primary axes. The result exhibits a sharp increase in the observed longitudinal shear and transverse moment in the local axes of the

substructure, supplementing a decrease in longitudinal moment and transverse shear. The effect of skew was observed to be directly proportional to the skew angle and an established difference was readily visible at the supposed conservative skew level of 30 degrees. The increase in longitudinal shear attributed to skew exceeded the capacity of pier-column members in the 45-degree skew bridges and 30-degree skewed bridges with low radii.

Effect of Curvature

Curved bridge models induced higher longitudinal moments and overall lower shear demand in the substructure compared to the benchmark model. The interior columns of the bridge with respect to the center of curvature experienced the highest longitudinal moment demand and exceeded the capacity of the member in the analysis of triaxial demand. The demand on the interior, in contrast to exterior, pier-columns was observed to be much higher and increase proportionally to the level of curvature.

Effect of Curvature and Skew in Combined Geometries

Curved and skewed bridge models exhibited mixed effects proportional to the influence of each geometric parameter. The result is higher observed D/C ratios in the columns, and higher transverse deformation of the superstructure. In some cases mixed effects were observed to counteract each other leading to more conservative behavior than the single geometrical contribution. Bridges incorporating both geometrical components should be evaluated more rigorously, because they develop larger actions in the substructure with concentrations at specific column locations (shown in previous parts).

6. Comparative Study on Different Girder-bent Connections

As discussed earlier, depending on the actual design and construction of the connection details, the connection between the interior bent and the girder may be modeled in different ways for seismic analysis. Regardless of the design intention, how an actual connection would behave is more complex than people typically thought. In previous sections, the connection between the continuous superstructure and the interior bent cap was modeled as fixed connection. In engineering practices, similar connection is often chosen to be modeled as pin or roller supports by ignoring the moment resistance and even shear resistance of the connection details. Such seemingly over simplification of the connection representation (i.e. ignoring moment resistance) sometimes may lead to non-conservative results. In this section, a comparative study is carried out to investigate the influence of different connection modeling choices on the seismic response of the prototype bridge.

6.1. Bridge configuration

Among all the bridge configurations studied previously, four three-span bridges with varying curvature and skew are examined in this section (Table 6.1). Other geometric and material parameters are the same for the four bridges. The plan view of a bridge with skew of 30 degrees and curved radius of 3000-ft is shown in Figure 6.1. Each bridge has the same side span and middle span length of 72’-6” and 96’-8”, respectively. A typical cross section of a bridge is shown in Figure 6.2. The superstructure consists of 8-in concrete slab deck and eight 5’-8” deep

pre-stressed concrete I-girders. The substructure is composed of 5-ft deep pier caps, 12-ft×3-ft interior piers, integral abutments and 3'-7" caissons.

Table 6.1 Bridge configurations

Bridge Name	Skew (degrees)	Curvature Radius (ft)	Super Elevation (degrees)
R0S0	0	0	0
R0S30	30	0	0
R3000S0	0	3000	6
R3000S30	30	3000	6

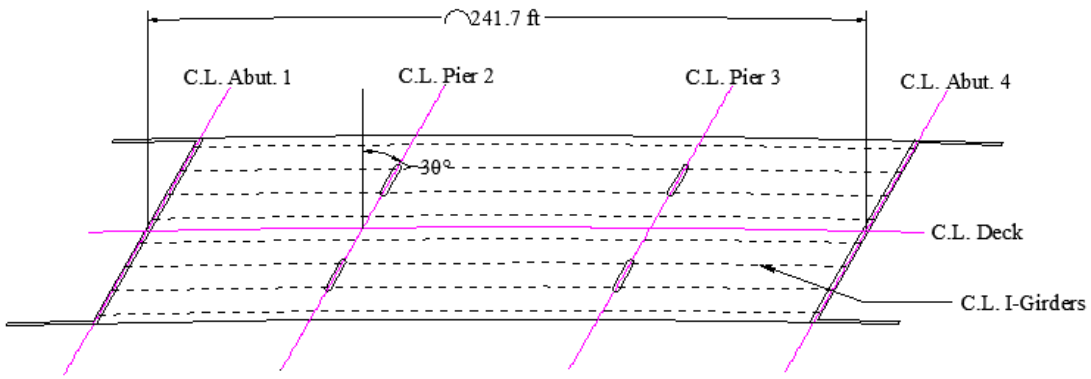

Figure 6.1 Plan view of bridge R3000S30

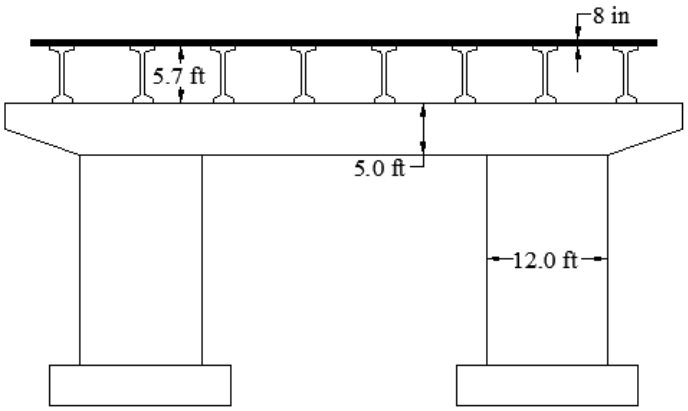

Figure 6.2 Typical cross section

6.2. SAP modeling and three connection types

SAP2000 is used to model and analyze the bridges. The finite element model of bridge R3000S30 is shown in Figure 6.3. Frame elements are used to model the I-girders, pier caps, piers and abutments. The deck slab is modeled using shell elements. The girders and deck are connected by rigid link elements. Prestressing tendons are simulated with equivalent load which follow the geometry of the tendons at each girder. The columns are fully constrained at the bottom. To consider the plastic behavior of columns, plastic hinges are assigned at the two ends of columns. The connections between the integral abutments and girders are modeled as fixed. The abutments are assumed as fixed by the surrounding soil and pile foundation in all translational and rotational directions. A tri-linear, longitudinal, compressive spring is used to model the stiffness of backing soil behind the abutment.

After the cast-in-place diaphragm and bridge deck are made, the original simple-supported girders become continuous on the superstructure. The focus of this study is on the connection between the continuous girder-diaphragm superstructure and the bent cap. In order to examine different connection assumptions, three types of support conditions are studied, including fixed, pin and roller supports as shown in Figure 6.4. These support conditions are modeled by link elements. The fixed support implies that the bent cap and girder are rigidly connected in all directions. After releasing rotations about the transverse axis and longitudinal axis based on the assumption that rotational constraint will be failed during earthquake due to concrete crushing, a pin support is formed. Additionally, if the translational constraints in the transverse and

longitudinal directions are also assumed to have failed during an earthquake, the connection would essentially become a roller support (Figure 6.4).

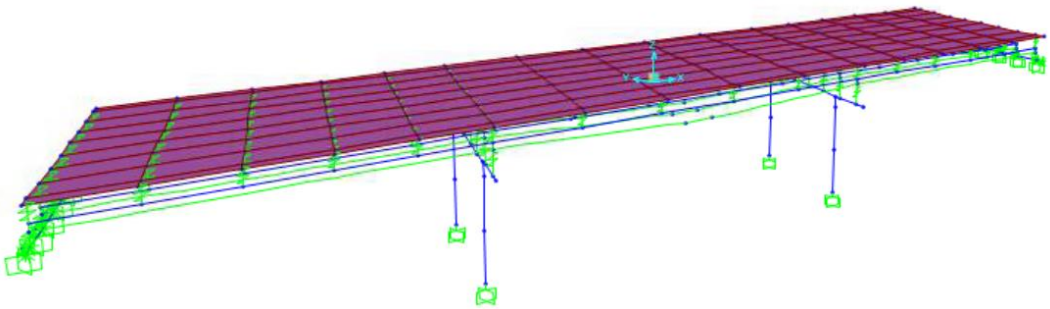

Figure 6.3 Finite element model in SAP2000

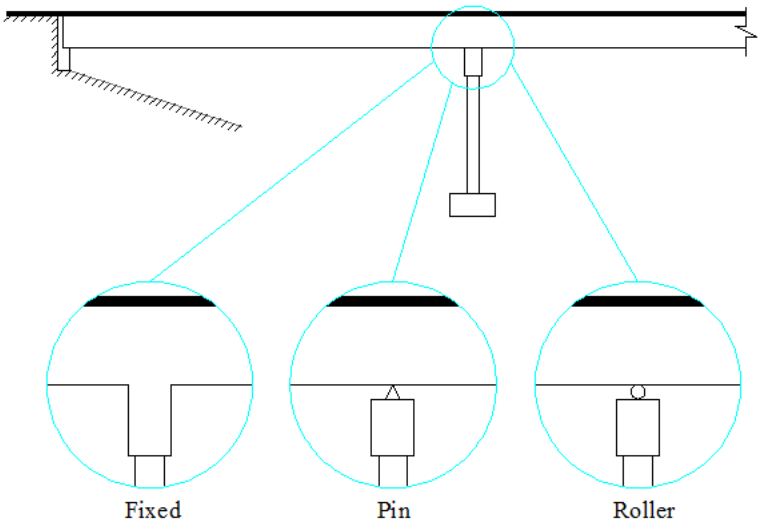

Figure 6.4 Support conditions at intermediate pier

6.3. Ground motion record and earthquake scaling

In order to carry out seismic analysis of the selected bridges, seven earthquake records are selected from the Pacific Earthquake Engineering Research (PEER) Center strong motion

database. Response spectrum-based scaling method is used to scale the ground motions. A stiff soil profile for Denver is selected, and a design response spectrum is developed using the USGS database and AASHTO Guide Specifications. Response spectrums of the seven earthquake records are obtained by using software SeismoSignal.

For the three different connections as shown in Figure 6.4, three different SAP analytical models are developed for each bridge configuration. After the modal analyses are conducted for each bridge, the corresponding fundamental frequencies are obtained. By matching the design response spectrum as specified by AASHTO LRFD design specification to the average of the response spectrums of the seven earthquake records at the fundamental period of the bridge structure, the scaling factors are computed for both fault normal direction and fault parallel direction.

6.4. Analytical results

Modal results

Modal analyses are carried out for three different bridges, each with three different girder-bent connections and the fundamental modal properties are shown in Table 6.1.

Table 6.1 Fundamental modal property (Unit: s)

Bridge /support	**R0S0**		**R0S30**		**R3000S0**		**R3000S30**	
	Period (s)	Mode type	Period (s)	Mode type	Period (s)	Mode type	Period (s)	Mode type
Fixed support	0.206	Deck longitudinal translation	0.186	Deck longitudinal translation & torsion	0.205	Deck longitudinal translation	0.199	Deck longitudinal & torsion
Pin Support	0.198	Deck longitudinal translation	0.193	Deck longitudinal translation &	0.339	Deck vertical bending	0.474	Deck vertical bending

				torsion				
Roller Support	0.294	Pier bending about transverse axis	0.312	Pier bending about transverse axis	0.368	Deck vertical bending	0.542	Deck vertical bending

As shown in Table 6.1, after the rotational constraint is released from fixed connection for the straight bridge (R0S0), the fundamental period of the longitudinal movement remains almost the same with a very slight reduction. Given the fact that the bridge has integral abutments, the rotational release does not affect the longitudinal stiffness considerably. When the translational constraints of the straight bridge are also released, the fundamental mode shifts from longitudinal translation of superstructure to pier bending with an increased period (0.198 s to 0.294 s). The skewed-only bridge (R0S30) exhibits similar modal properties as the straight bridge (R0S0) and the fundamental modes are mostly controlled by longitudinal movements, mixed with torsional movement because of the skew nature. Slightly different from straight bridges, the rotational release of the intermediate support for the skew-only bridge (R0S30) causes an increase of the fundamental period from 0.186 s to 0.193 s for the translation and torsion modes, respectively. Further release of translational constraints at the superstructure-bent cap connection causes the fundamental mode to shift from longitudinal translation of superstructure to pier bending about the transverse axis with an increased period from 0.193 s to 0.312 s.

For curved bridges (R3000S0 and R3000S30), the fundamental periods generally increase to varying extents for different bridges. For bridges with curvature, the release of rotational constraints causes considerable increase of fundamental periods and shifts the fundamental mode shape from longitudinal translation to vertical bending. For curved bridge, rotation release of the superstructure-bent connection causes the deck to lose local rotational restraint from the

bearings, shifting the fundamental mode shape from longitudinal translation of deck to a coupled local vibration of bending and torsion of deck. Meanwhile, the fundamental period is increased by 65.4% and 138.2% for bridge R3000S0 and R3000S30, respectively. Translational release of the support causes the substructure to fully lose longitudinal restraint from superstructure. Because the ratio of average spectrum acceleration to design spectrum acceleration decreases as the fundamental periods increases, the earthquake scaling factors increase with the increase of fundamental periods. Thus, the release causes larger increases in both scaling factors and earthquake loads for curved bridges (30.4% and 51.8%) in comparison to the non-curved bridges (0.8% and 15.8%).

Moment Demand at pier base

The results of the moment demand at the base of the intermediate pier for different bridges and constraints are listed in Figure 6.5. For the straight bridge, the release of rotational constraint can considerably decrease the longitudinal moment demand from that of the fixed connection. The release of translational constraint will further reduce the longitudinal demand. However for the transverse moment, the release of rotational constraint does not cause much change from that of the fixed support, which also confirms the rationality of fixed connection assumption in transverse directions for multi-column bent recommended by Priestley et al. (2007).

As shown in Figure 6.5, there is a general trend for both longitudinal (about transverse axis) and transverse moments (about longitudinal axis) for other three curved and/or skewed bridges. The general trend is that the longitudinal and transverse moment demands of the “pin support” model are typically smaller than those of the “fixed support” models. The release of translational

constraint ("roller support") will cause further decrease of the moment demands at the bottom of the bent pier primarily because of the reduction in load transfer from the superstructure to the pier. However, the transverse moment demand of bridge R3000S0 and longitudinal moment demand of bridge R3000S30 do not follow the same pattern. For the curved and skewed bridge (R3000S30), the longitudinal moment demand for the pin support is very close to that of the fixed support, which indicates the pin design may not always lead to reduced demands in terms of longitudinal moment for curved and skewed bridge as people usually assumed for straight bridges. For the curved-only bridge (R3000S0), the transverse moment demand of the pin support is actually slightly higher than that of the fixed support. It is also found that the curvature will usually cause the increase of longitudinal moment, while the skew nature will cause the increase of transverse moment at the base of the pier.

As discussed earlier, the constraint release affects the fundamental periods and in turn the scaling factor for the earthquake in addition to the load transfer paths as affected by the release. For the roller support, the translational forces cannot be transmitted to the piers, and in turn significant reduction on the base moment and shear of the pier is observed.

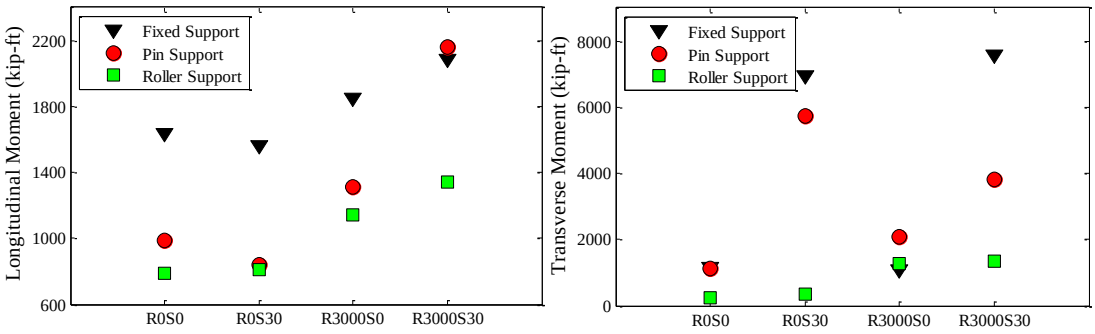

Figure 6.5 Moment demand at pier base

Shear forces at pier base

The shear forces at pier base follow similar patterns as the moment demands (Figure 6.6). However, the transverse shear of bridge R3000S0 does not follow the same pattern. This is also the result of the complex outcome, both advantageous and disadvantageous, from constraint release. In this case, increased transverse shear force due to the increased earthquake loads exceeds reduced shear force due to modified load path, as a result, leading to a resultant increase. Moreover, the variation of shear forces corresponds well to that of moment demand in two directions. Similarly, it is found that fully fixed support may result in non-conservative result for curved bridges. In-plane rotation also causes larger transverse shear for skewed baseline and "pin support" bridges.

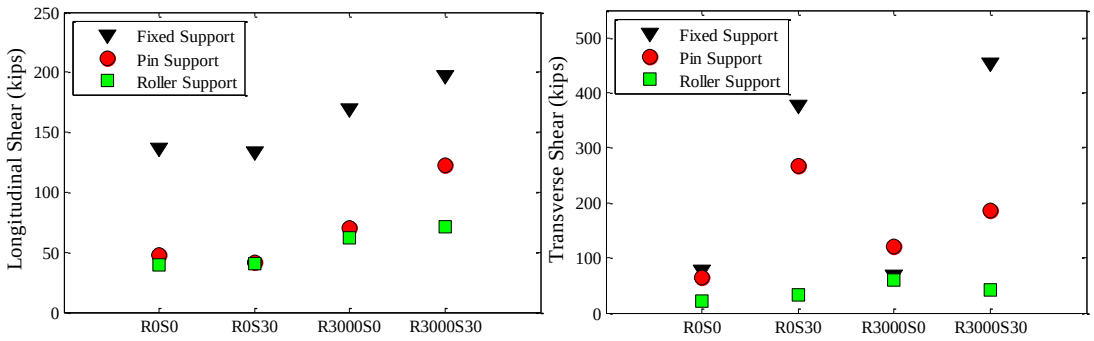

Figure 6.6 Shear forces at pier base

Drift ratio of pier

For the non-curved bridges, the drift ratios remain unchanged or slightly reduced after rotation release and translation release in general (Figure 6.7). For the curved bridges, the drift ratios increase first after rotation release and then decrease after translation release. It can also be explained by the combined effect from both earthquake loads and also modified structure and load path. Rotation release affect bridge R3000S30 the most, causing 82% increase in

longitudinal drift ratio and 169% increase in transverse drift ratio. This is because rotation release leads to relatively large seismic demand increase for bridge R3000S30, and the resulted negative effect is much larger than the positive effect. Lager transverse drift ratio in skewed bridges is also partially due to the planar rotation of superstructure. For curved and skewed bridges, the increased drift ratio at the pier top for the pin-support may cause some design issue.

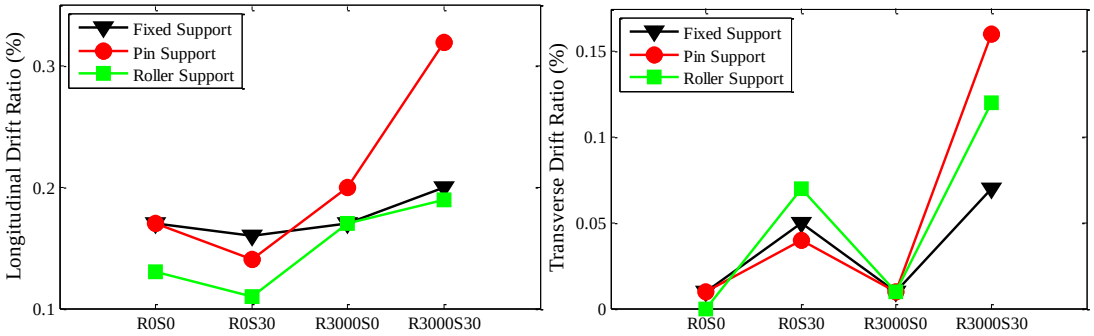

Figure 6.7 Drift ratio of pier

Resistance behind integral abutment

Figure 6.8 summarizes the results of the resistance force behind integral abutments of bridges with different connections. After rotation release and translation release, the longitudinal force acting on the abutment from soil springs increases in general as compared to the "fixed" model. Due to the loss of longitudinal restraint from girder and deck after translation release, most longitudinal earthquake load acting on the superstructure is shifted from the piers to the abutments. Translation release leads to an increase in longitudinal force and a reduction in transverse force on the abutments for skewed bridges. Planar rotation in skewed bridges also causes significant larger transverse reaction at abutment. For abutments, fixed support conditions always lead to non-conservative design as expected. Particularly, for curved bridges (R3000S0 and R3000S30), those with pin–support connections will generate considerably larger

longitudinal forces on the abutments, which may pose some design challenges on the abutment depending on the actual soil conditions. For skewed bridges (R0S0 and R3000S30), the transverse reaction forces are much larger than those non-skewed bridges.

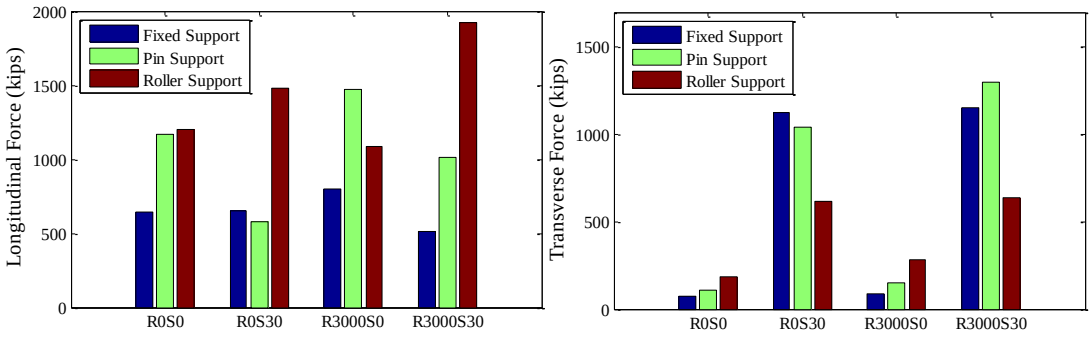

Figure 6.8 Resistance force behind the abutment

6.5. Discussions

Joint effect of scaled earthquake loads and structural system

It is found that support release causes both advantageous and disadvantageous effects in terms of seismic performance. In order to quantify the respective contributions, three time-history analysis cases for bridge R3000S0 under San Fernando earthquake are compared (Figure 6.9). Case 1 uses the fixed-support model and the corresponding scaling factor. Case 2 uses the same scaling factor as Case 1 but with the pin support. Case 3 uses the pin support model and the corresponding scaling factor. It is can be seen from Figure 6.9 that under same earthquake load, moment demand of Case 2 is 48.2% less than that of Case 1 because of the modified structure connection. In other words, by only considering the structure with released constraints, the moment demands at the pier base can be reduced by about a half. Comparing Case 2 and Case 3, the moment demand of Case 3 is 58.2% greater than that of Case 2 (equivalent to an increase about 30% of the Case 1 demand), and such an increase is attributable to the seismic load change due to the updated fundamental period, scaling factor, and in turn earthquake loads. In other

words, for the exactly same structure, by using the updated earthquake load, the moment demands increase more than 50%. As a summary, for the R3000S0 bridge, it was found that the constraint releasing alone and the seismic load change alone cause about 52% reduction and 30% increase from the longitudinal moment demand of the fixed support (Case 1) respectively, resulting in about 22% total reduction by considering the combined effects. For any bridge with released constraints, the ultimate structural response is approximately the superposition of two types of effects. For a particular bridge, depending on which part of influence (advantageous one or disadvantageous one), the resultant effect from constraint releasing can be complex and a general trend cannot be made at this point.

For this particular study, fixed support condition overall gives more conservative results for the base moment and shear for the most part. In some cases such as curved bridges, fixed support condition may lead to non-conservative estimation. If the displacement at the pier top is of concern, pin support may actually cause the largest response particularly for both curved and skewed bridge.

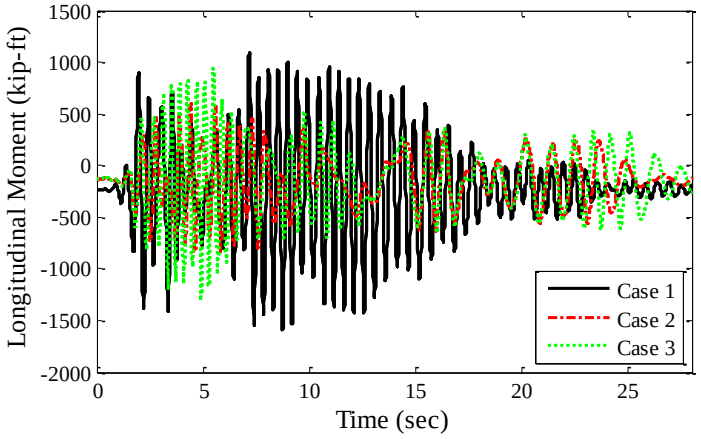

Figure 6.9 Time-history of moment demand at pier base of bridge R3000S0

Support assumptions

In order to further analyze the support assumptions, internal demands of some critical connections are quantified. For the fixed support, the moment demand at the fixed connection is evaluated, which may be used to assess the assumption rationality of any specific connection detail. Because of the adoption of rigid link element, the moment at the element on the top of the bridge pier, rather than the link itself, is shown in Figure 6.10. The peak moments in longitudinal and transverse directions are about 1000 and 450 kip-ft, respectively. Similarly, the shear forces of the element on the top of the pier are also assessed to provide information in terms of whether translational constraints would fail, causing a constraint release. As shown in Figure 6.11, for the pin support, the shear forces are about 25 and 40 kips in longitudinal and transverse directions, respectively. For the given connection detail one can determine the capacity of the connection and evaluate whether or not failure (i.e. release) of the detail is really expected. The detailed capacity analysis of the specific connection details is not conducted here.

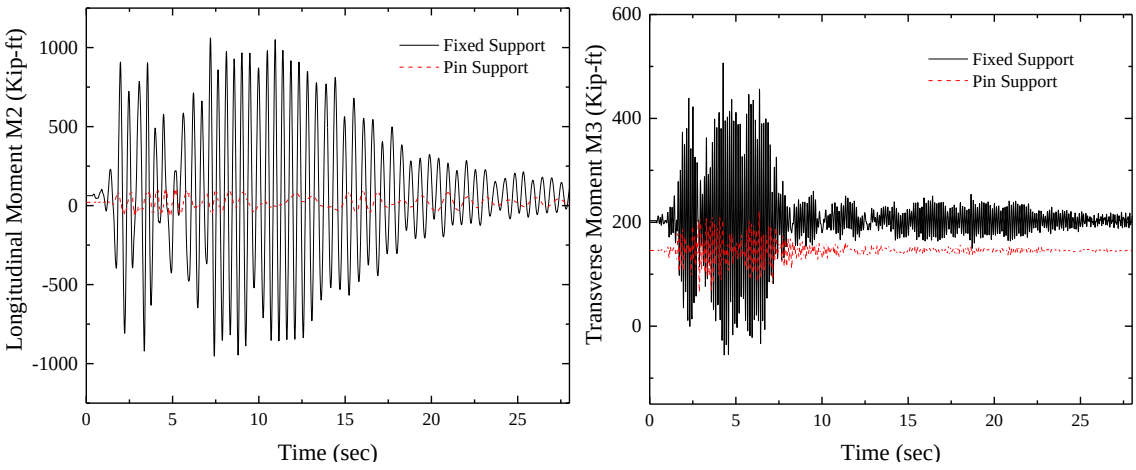

Figure 6.10 Moment demand at the top of the pier of bridge R0S0

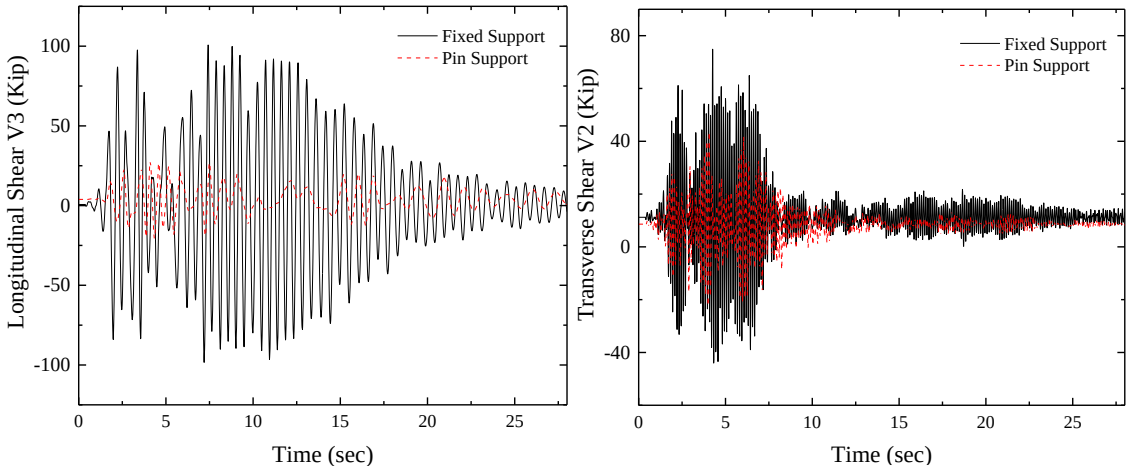

Figure 6.11 Shear force at the top of the pier of bridge R0S0

6.6. Summary

The comparative study of four different bridge models was made by appropriately scaling the respective time-history earthquake records. The main findings from this comparative study are summarized below:

1) In terms of bridge pier base shear and moment response, fixed connection usually gives the most conservative results for straight bridges and also most scenarios of curved and/or skewed bridge. For curved bridges, releasing the rotation at the girder-pier connection may not always reduce the shear and moment demands at the base of the bridge pier. For the both curved and skewed bridge, the rotation constraint release also considerably influences the transverse moment and shear for multi-column pier, which is very different from the straight bridge.
2) Release of constraints usually does not cause much difference on the pier top displacement for the straight bridge. However, such release can cause considerable

increase of the top displacement for the curved and skewed bridge. This observation suggests that the constraint release may increase the risk of excessive drift ratio for curved and skewed bridge.

3) It was found that the release of constraints at the connection part may affect the fundamental period, scaling actor and in turn earthquake loads. In addition, the constraint release will also modify structural load path and the response. The resultant influence on the bridge response will depend on the combined effects from both factors, which are specific to bridge configurations. For the R3000S0 bridge as an example, it was found that the constraint releasing alone and the earthquake load adjustment alone cause about 52% reduction and 30% increase from the longitudinal moment demand of the fixed support (Case 1) respectively, resulting in about 22% total reduction by considering the combined effects.
4) For straight bridge with multi-column piers, to model the connection between the top of the interior pier and diaphragm support with a pin may have some advantages such as reduced longitudinal moment and shear demands on the pier end at the cost of the increased pier top longitudinal displacement. For curved and skewed bridge, releasing rotation constraints will reduce transverse moment even for multi-column piers, however the pier top displacement will be considerably increased along with large abutment reaction forces, which may cause some design challenges.
5) For the pier-diaphragm connection of the prototype bridge, the realistic scenario is probably a type of semi-rigid connection during earthquake with limited capacity of some constraints regardless of what was the design intention. This is more critical to low seismic region than to high seismic region because of limited demands acting on those

connections. An accurate capacity analysis is needed for those connections in order to assess what is the more realistic connection assumption based on how the bridge actually behaves during earthquakes.

7. Discussion about displacement-based and force-based designs for bridges

The underlying design philosophy for designing bridge against seismic demands, known as Capacity Design, is to design a bridge with sufficient ductility and deformability to resist the expected demand. The deformability in the system is typically achieved through ensuring adequate movement in the bridge joints which the ductility is ensured through the formation of plastic hinges in the piers or possibly through components of the superstructure such as steel cross bracings and end diaphragms connecting two adjacent girders. It is important to note that typically an engineer would have to determine the joints and components that can be utilized to achieve the required deformability and ductility, respectively. The remaining components are then designed to remain elastic without losing their strength such that they can provide the required load path and accommodate the expected actions (forces and moments) and deformations (displacements and rotations) imposed on the joints and components that are utilized to achieved the desired deformation and ductility.

Traditionally, seismic provisions have relied on force-based capacity approach to resist the earthquake effects expressed as a set of horizontal actions defined as a proportion of the weight of the structure. In the past two to three decades, there has been a shift towards using ductility instead of strength as the main approach for seismic design of structures. The motivation of utilizing the ductility-based methods, also called displacement-based method, is due to the significant uncertainty in estimating the seismic demand using the force-based method. On the other hand, the ductility method is much less sensitive to unexpected increase in the force demand imposed on it than its strength-designed counterpart. In addition, the use of the ductility-

based method is likely to result in less material being required and hence produce lighter structures. However, the ductility method typically requires extensive detailing to ensure proper energy dissipation as manifested by plastic hinge formation. Therefore, more workmanship is expected and could drive the fabrication cost higher. Both the force-based method and the displacement-based methods are adopted by the AASHTO Specification. Specifically, the force-based method is included in the AASHTO LRFD Specification while the displacement-based method has recently been adopted by the AASHTO Guide Specification for Seismic Bridge Design.

Both methods hinge on the determination of the demand through seismic analysis, designing the bridge elements to meet the required demand, and finally comparing and evaluating the demand/capacity ratio. Various analysis methods and techniques can be used to determine the expected demand on the bridge include both static and dynamic analysis. The static analysis include 1) equivalent static, 2) conventional pushover, and 3) adaptive pushover, while dynamic analysis could be conducted using 1) multi-modal spectral analysis, response time-history analysis, and 3) incremental dynamic analysis. Performing the analysis requires the generation of the numerical model, selecting the analysis method, and acquiring the forces and displacements from the analytical results for which elements and component will be designed to withstand. Undoubtedly, the complexity of the numerical analysis process is governed by the required level of geometrical representation of the bridge when generating the models and the level of seismic input hazard which can affect the ability of models to achieve convergence.

Force-based Method: The force-based method is customarily used in the ASHTO LRFD Bridge Design Specifications. In this method, yielding in specified elements is ensured through computing the elastic forces from an elastic demand analysis then reducing the forces, for which the element is to be designed, to ensure the development and progression of yielding in these elements. The reduction in forces is achieved through the use of Response Modification Factors (R). In other words, the yield force is equal to the peak elastic force divided by a force modification factor, R. In Figure 7.1 below, the elastic response line represents the response of the bridge when no yielding occurs. The elastic force is then reduced using the R factor to ensure the presence of ductile behavior. However, as indicated previously estimating the inelastic force is rather challenging due to the large uncertainty associated with estimating the R factor and often times the displacements are accurately predicted as opposed to member forces.

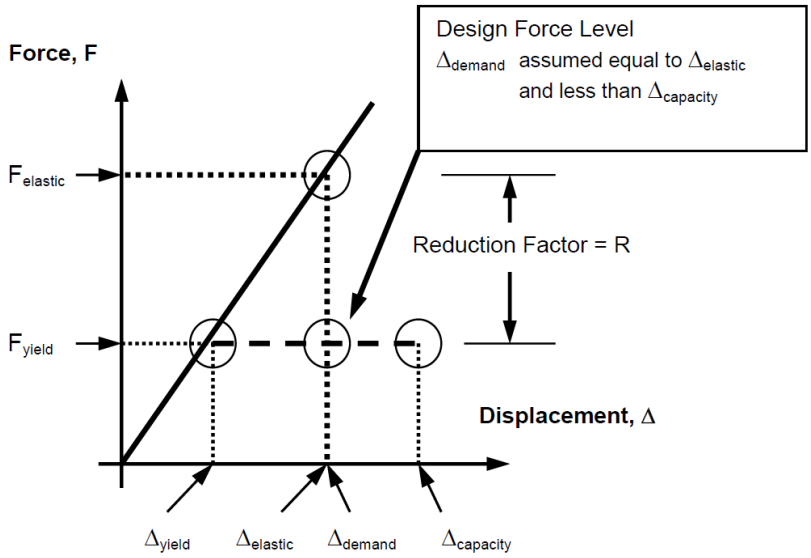

Figure 7.1 Calculation of Design Force Level and Displacement Demand in Force-Based Method (FHWA-NHI-15-004, 2014)

Displacement-based Method: Used in the AASHTO Guide Specification, the displacement-based method essentially seeks to provide the needed performance requirements of those of force-based design; that is deformability and ductility. In this method design forces for the yielded elements

are not computed. Instead, the system can be proportioned by the designer such that the displacement demand on the bridge is less than the displacement capacity at each pier while ensuring that minimum lateral strength, typically represented by base shear and overturning moment, is provided. This is depicted in Figure 7.2 where the displacement capacity is larger than the displacement demand. In this method the required displacement is ensured through specific detailing requirements that are with specific guidelines provided to avoid brittle failure.

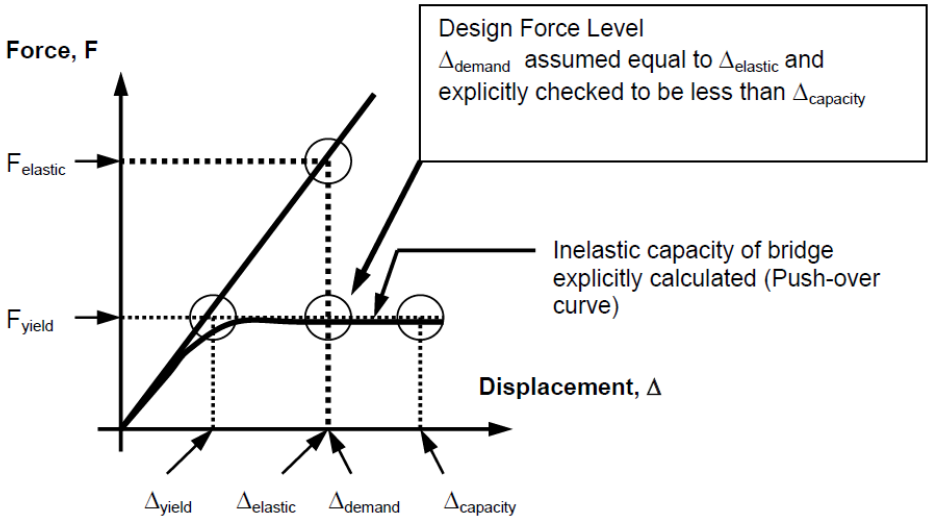

Figure 7.2 Calculation of Design Force Level and Displacement Demand in Displacement-Based Method (FHWA-NHI-15-004, 2014)

8. Conclusion

This report summarizes the analytical studies on the seismic performance of typical Colorado concrete bridges, particularly those with curved and skewed configurations. A set of bridge models with different geometric configurations derived from a prototype bridge selected in Denver area were studied. Some discussions about the connection modeling are carried out in terms of the interior bent support. For the displacement-based and force-based designs, due to the lack of design details that may be adopted for different Colorado bridges, some specific recommendations cannot be made at this point without detailed analyses of all possible detailing options. Therefore, some general observations of these two design concepts are summarized in the end of the report. In the appendices, the design examples of 2-span and 3-span bridges are listed to help the engineers to conduct bridge seismic analysis in Colorado.

The SAP2000 modeling example and four design examples are included in the Appendices of this report.

9. Sources Cited

Abdel-Mohti, A., & Pekcan, G. (2008). Seismic Response of Skewed RC Box-Girder Bridges. *Earthquake Engineering and Engineering Vibration*, *7*(4),

American Association of State and Highway Transportation Officials. (2007). *AASHTO LRFD Bridge Design Specifications* (4th ed.). Washington, DC: AASHTO.

American Association of State and Highway Transportation Officials. (2011). *AASHTO Guide Specifications for LRFD Seismic Bridge Design* (2nd ed.). Washington, DC: AASHTO.

American Society of Civil Engineers. (n.d.). *FEMA 356-Prestandard and Commentary for the Seismic Rehabilitation of Buildings*. *Washington DC: Federal Emergency Management …*. Washington, DC.

Aviram, A., Mackie, K., Stojadinovic, B. (2008). Guidelines for Nonlinear Analysis of Bridge Structures in California. *Pacific Earthquake Engineering Research Center Report (PEER 2008/03)*.

Baker, J. W., & Allin Cornell, C. (2006). Spectral shape, epsilon and record selection. *Earthquake Engineering & Structural Dynamics*, *35*(9), 1077–1095. doi:10.1002/eqe.571

Berman, E. (2008). *Estimated Annualized Earthquake Losses for the United States*. *FEMA 366*.

Bignell, J. L., LaFave, J. M., & Hawkins, N. M. (2005). Seismic vulnerability assessment of wall pier supported highway bridges using nonlinear pushover analyses. *Engineering Structures*, *27*(14), 2044–2063. doi:10.1016/j.engstruct.2005.06.015

Bisadi, V., Asce, S. M., Head, M., & Asce, A. M. (2011). Evaluation of Combination Rules for Orthogonal Seismic Demands in Nonlinear Time History Analysis of Bridges, (December), 711–717. doi:10.1061/(ASCE)BE.1943-5592.0000241.

Burdette, N. J., Elnashai, A. S., Lupoi, A., & Sextos, A. G. (2008). Effect of Asynchronous Earthquake Motion on Complex Bridges. I: Methodology and Input Motion. *Journal of Bridge …*, (April), 158–165.

Button, M., Cronin, C., & Mayes, R. (2002). Effect of vertical motions on seismic response of highway bridges. *Journal of Structural Engineering*, (December), 1551–1564.

California Department of Transportation. (2006). Caltrans Seismic Design Criteria, (1.6), 161.

Charlie, W. A., Battalora, R. J., Siller, T. J., & Doehring, D. O. (2002). Magnitude Recurrence Relations for Colorado Earthquakes. *Earthquake Spectra*, *18*(2), 233. doi:10.1193/1.1490546

Charlie, W., Battalora, R., Siller, T., & Doehring, D. (2006). Colorado Earthquakes and Active Faults, 20–34.

Computers and Structures Inc. (2011). *CSI Analysis Reference Manual*. Berkeley, California, USA.

Cooper, J., Sharpe, R. L., Fox, G. F., Gates, J. H., Goins, V. M., Hourigan, E. V, … Martin, G. A. (1981). *ATC- 6 Seismic Design Guidelines for Highway Bridges*. Berkeley, California, USA.

Donnell, A. P. O., Beltsar, O. A., Kurama, Y. C., & Taflanidis, A. (2011). Evaluation of Ground Motion Scaling Methods for Nonlinear Analysis of Structural Systems Erol Kalkan Unites States Geological Survey. In *Proceedings of 2011 NSF Engineering Research and Innovation Confernence*. Atlanta, Georgia.

Elnashai, A. S., & Luigi Di Sarno. (2008). *Fundamentals of Earthquake Engineering* (1st ed., p. 347). John Wiley & Sons, Ltd.

Housner, G. W. (1952). Spectrum Intensities of strong-motion earthquakes. *Proceedings of the 1st World Conference on Earthquake Engineering,, 1*.

Itani, A. M., & Pekcan, G. (2011). *Seismic Performance of Steel Plate Girder Bridges with Integral Abutments*. *Federal Highway Administatrion.*

Kalkan, B. E., & Kwong, N. S. (2010). Documentation for Assessment of Modal Pushover-Documentation for Assessment of Modal Pushover-Based Scaling Procedure for Nonlinear Response History Analysis of "Ordinary Standard" Bridges.

Kalkan, E., & Chopra. (2010). Practical guidelines to select and scale earthquake records for nonlinear response history analysis of structures. *US Geological Survey Open-File Report*.

Kappos, A. J., Paraskeva, T. S., & Sextos, A. G. (2005). Modal pushover analysis as a means for the seismic assessment of bridge structures. In *4th European Workshop on the Seismic Behaviour of Irregular and Complex Structures*. Thessaloniki, Greece.

Kirkham, R. (1986). An interpretation of the November 7, 1882 Colorado earthquake. *Colorado Geological Survey*, (Open File Report 86-8).

Kirkham, R. M., & Rogers, W. P. (1985). Colorado Earthquake Data and Interpretations 1857 to 1985. *Colorado Geological Survey*, *46*, 94.

Krawinkler, H., & Seneviratna, G. D. P. K. (1998). Pros and cons of a pushover analysis of seismic performance evaluation. *Engineering Structures*, *20*(4-6), 452–464. doi:10.1016/S0141-0296(97)00092-8

Kunnath, S. K., Larson, L., & Miranda, E. (2006). Modelling considerations in probabilistic performance-based seismic evaluation: case study of the I-880 viaduct. *Earthquake Engineering & Structural Dynamics*, *35*(1), 57–75. doi:10.1002/eqe.531

Kurama, Y. C., & Farrow, K. T. (2003). Ground motion scaling methods for different site conditions and structure characteristics. *Earthquake Engineering & Structural Dynamics*, *32*(15), 2425–2450. doi:10.1002/eqe.335

Marsh, L., Buckle, I., Kavazanjian, E. (2014). LRFD seismic analysis and design of bridges reference manual: *NHI Course no. 130093 and 130093a*.

Mwafy, A. M., & Elnashai, A. S. (2007). Assessment of seismic integrity of multi-span curved bridges in mid-America, (April). Retrieved from http://www.ideals.illinois.edu/handle/2142/8782

NCHRP (2004). Connection of Simple-Span Precast Concrete Girders for Continuity. NCHRP Report 519.

Sheehan, A. F., Godchaux, J. D., & Hughes, N. (2003). COLORADO FRONT RANGE SEISMICITY AND SEISMIC HAZARD. *Colorado Geological Survey Special Publication 55*, (15), 1–21.

Spence, W. (1999). Colorado's Largest Historical Earthquake. *USGS Fact Sheet 098-99*, (098-99).

Spence, W., Langer, C. J., & George, L. C. (1996). Rare , Large Earthquakes at the Laramide Deformation Front Colorado (1882) and Wyoming (1984), *86*(6), 1804–1819.

Stover, C. W., & Coffman, J. L. (1993). Seismicity of the United States, 1968-1989 (Revised). *U.S. Geological Survey Professional Paper 1527*, 418.

Washington Department of Transportation. (2011). *WSDOT Bridge Design Manual*.

Widmann, B. L., Kirkham, R. M., & Rogers, W. P. (1998). *Preliminary Quaternary Fault and Fold Map and Database of Colorado*. *Colorado Geological Survey* (Vol. Open-File). Denver, Colorado.

INVESTIGATION OF SEISMIC PERFORMANCE AND DESIGN OF TYPICAL CURVED AND SKEWED BRIDGES IN COLORADO

Appendix

The appendices A-C include the SAP modeling example and four design examples.

DISCLAIMER

In order to provide related specification requirements for engineers to follow the design examples, some formulas and graphs from AASHTO LRFD and Guide Specifications are directly cited. The copyrights of the cited information belong to the original owner.

Table of Contents

Appendix A: SAP 2000 Modeling Example

The following section describes the detailed steps taken to develop the 3-span bridge. The dimension and other information about the 3-span bridge can be found in Appendix B (B.1). The steps describe the general procedures taken, with additional information and guidelines that are specific to Colorado bridge design and seismic hazard. The FE models described have been used for research purposes and may be more detailed than required.

A.1 **AutoCAD data input into SAP2000**

It is often difficult to develop the geometries for the bridge models using the drawing tools provided in the analysis software. It is preferable to develop a spine structure in a drafting program that can be further built upon in SAP2000. AutoCAD is widely used in engineering as a drafting program and is compatible with most FE software to deal with complex structures. For non-complex structures, a model can be constructed more quickly through the templates and drawing tools found in SAP2000. The steps taken to developing the spine model for the 3-Span bridge using AutoCAD is discussed below.

Step A.1.1

In AutoCAD, the coordinates for the centroid of the bridge girders are calculated from the bridge plans and drawn in a 2-D plane.

Step A.1.2

Next, the outside edges of the deck, and centerlines of the abutments and bent caps are added to the drawing, again in the 2-D plane.

Step A.1.3

The super-elevation is added by rotating the plan geometry of the bridge to the super-elevation specified about the (0,0,0) coordinates.

Step A.1.4

While very simple, the basic spine used for SAP is shown in Figure 10; Additional bridge components may be added as to the spine model as necessary. The file is saved as a "*.dxf", which is easily imported with most FE software.

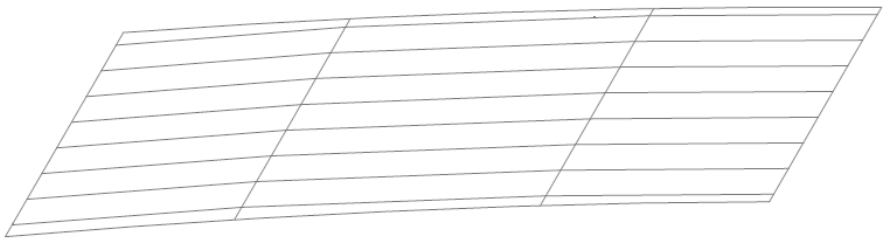

Figure A.1 AutoCAD Spine Model

Step A.1.5

A super elevation may be added by rotating the plan of the bridge about the (0,0,0) global coordinate. This assumes that each curve is drawn a distance equal to the radius of curvature from the (0,0,0) coordinate.

A.2*Model Construction in SAP 2000*

Step A.2.1

A new blank model is created in SAP2000; the default units are always kip-ft when the model is opened. The units can only be permanently changed in the file by using the Excel interactive database.

Step A.2.2

The .dxf file created in AutoCAD is imported into the blank model space. A check is made to ensure that the imported geometries and unit lengths are consistent with the CAD model. There should be a line element for each of the girders. The curved AutoCAD lines that span the outside of the deck will not import into SAP, however the nodes on each end of those lines are available and may be used for developing curved shapes.

Step A.2.3

The girder elements need to first be divided into 5 separate segments. This is done by selecting the frame element and selecting Edit>Edit Lines>Divide Lines>Divide Into Specified Number of Frames = 5.

Step A.2.4

The next step is to construct nodes for the deck. From the bridge plans, the distance between the centroid of the girders and the centroid of the deck (Call this distance Z*) is measured. Using the "draw special joint" tool, nodes are constructed that are offset by Z* in the positive global z-direction. The nodes are created at an offset from all of the imported girder, abutment and bent-cap nodes.

Step A.2.5

The outside edges of the deck also need to be drawn. Using the tool for a curved frame element, the abutment and pier nodes are connected in each span at the exterior and interior edge of the deck; for this the two-point and radius tool should be selected. The default section (FSEC1) may be used, as this will be a place holder for the shell elements. The curved frame element is discretized into 5 straight sections, per span. SAP does not support curved frame elements but will discretize a curve into a number of straight line elements.

Once the elements are discretized, construction nodes for the abutment and bent cap sections are added; using the "draw special joint" tool, nodes are constructed at the centroid of the bent cap and abutment members. The model then resembles Figure A.2.

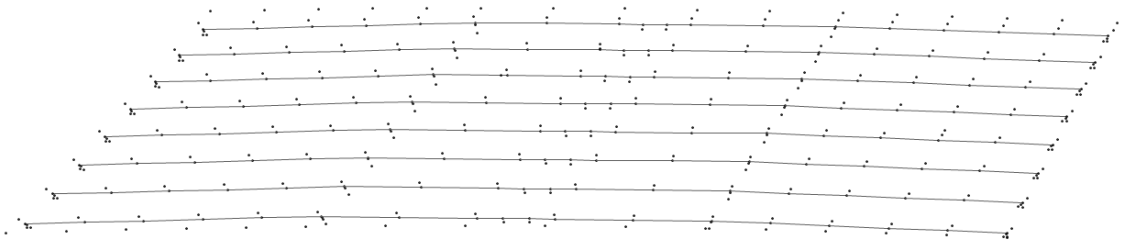

Figure A.2 SAP2000 Model – Early Stages

Step A.2.6

Subsequently, a check is made to ensure that the nodes of the deck are discretized into equivalent quadrants. To model the deck slab, shell elements using the default section are drawn in each quadrant created. A sample model at this point is shown in

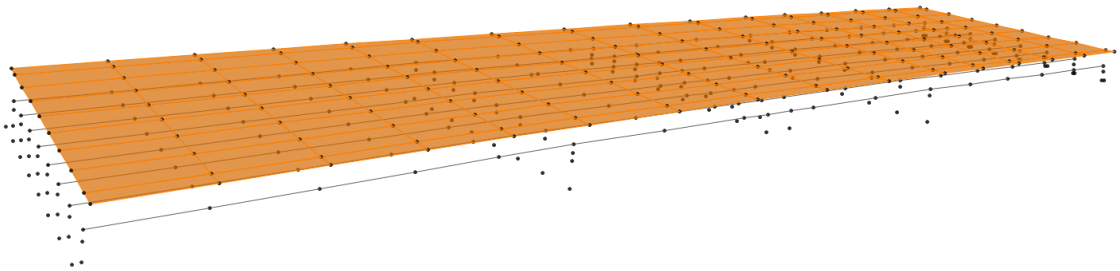

Figure A.3.

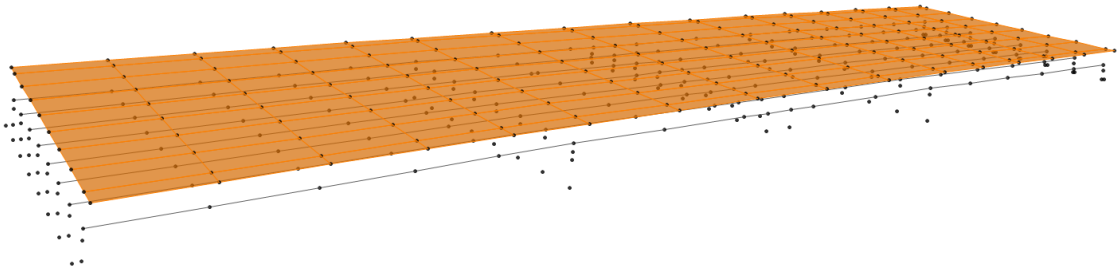

Figure A.3 SAP Model with Girder Elements, Shell Elements, and Nodes for Abutment and Bent Cap

Frame elements are then drawn through the construction nodes at the bent cap and abutment, again using the default FSEC1 section. Specific sections will be assigned to members in a later step.

Step A.2.7

Following the same procedure as illustrated in Step 7, nodes are added at the intersections between the column and the bent cap and the column and the footing. The adjacent nodes are connected using frame elements to represent the pier-column.

A.3***Materials***

Material definitions are created for the structural components of the bridge. A new material is defined by using the following steps.

Step A.3.1

A custom material is defined by Define>Materials>Add New Material

Step A.3.2

Enter the properties of the material in the dialogue boxes for other material properties under "Advanced Property Display". (See Figure A.4a)

Step A.3.3

Alternatively a predefined material may be used by adding a "New Material Quick". Figure A.4b shows the characteristics of predefined A992 steel.

Step A.3.4

The steps above may be repeated to create material properties for the reinforcing steel, all strengths of concrete, prestressing steel and other pertinant materials that will be used in the model.

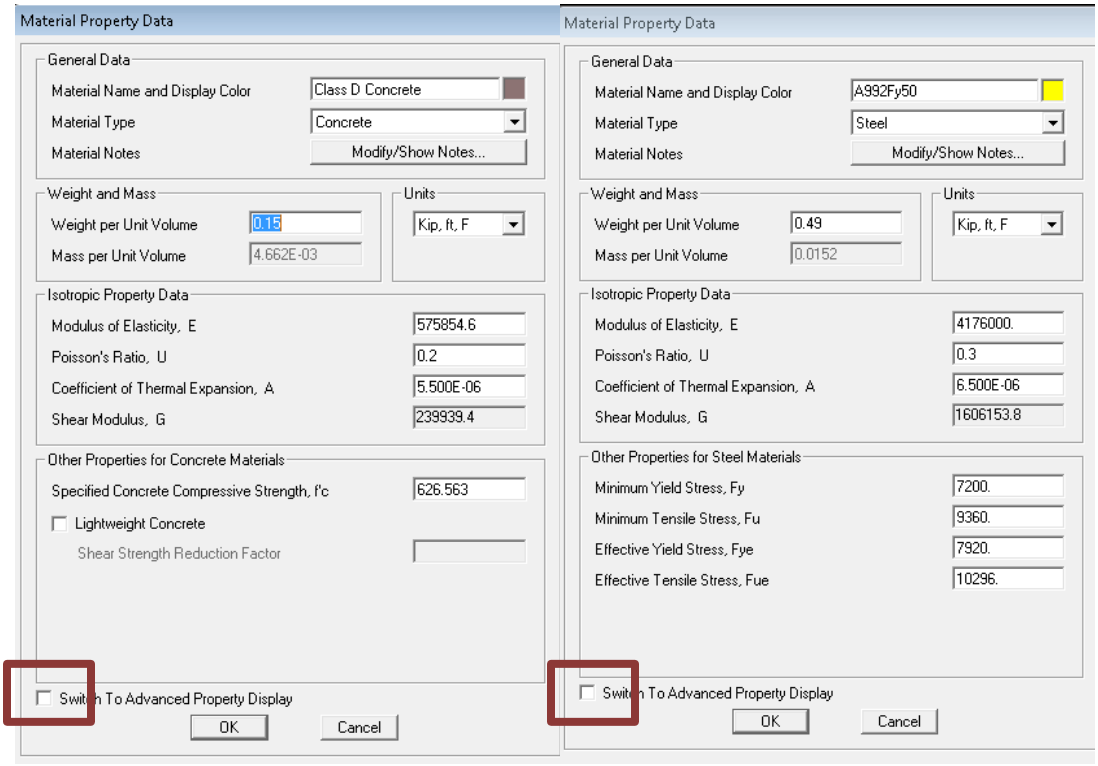

Figure A.4 (a) and (b) SAP2000 Custom and Predefined Material Properties

A.4*Section Definitions*

A member section may be defined in a few different ways with SAP 2000. A section may be created based on predefined geometries, or custom sections may be produced with the section designer.

Step A.4.1

A new frame section is defined using Define>Section Properties>Frame Sections.

Step A.4.2

Under “Other”, “Section Designer” is selected and the “Section Designer” tab is selected to begin drawing a custom section.

Step A.4.3

Custom sections may be created by using the drawing tools to create the structural shapes and to add the layout of the reinforcement. In addition, the properties of the section may be modified under the C-model to add stirrups and confined properties of the concrete section. (See Fig. 6.5)

Step A.4.4

With variable geometry members as shown in Figure A.5, two tools become useful. The first is the guideline tool, where the outline of a shape may be drawn with guidelines using coordinates. The next is the polyshape tool that can create a shape from the nodes of the guidelines. Using these two tools, a non-typical shape may be created as shown below. While non-linear material properties for the concrete have been provided to SAP, it is unlikely that they will be invoked in the SAP analysis.

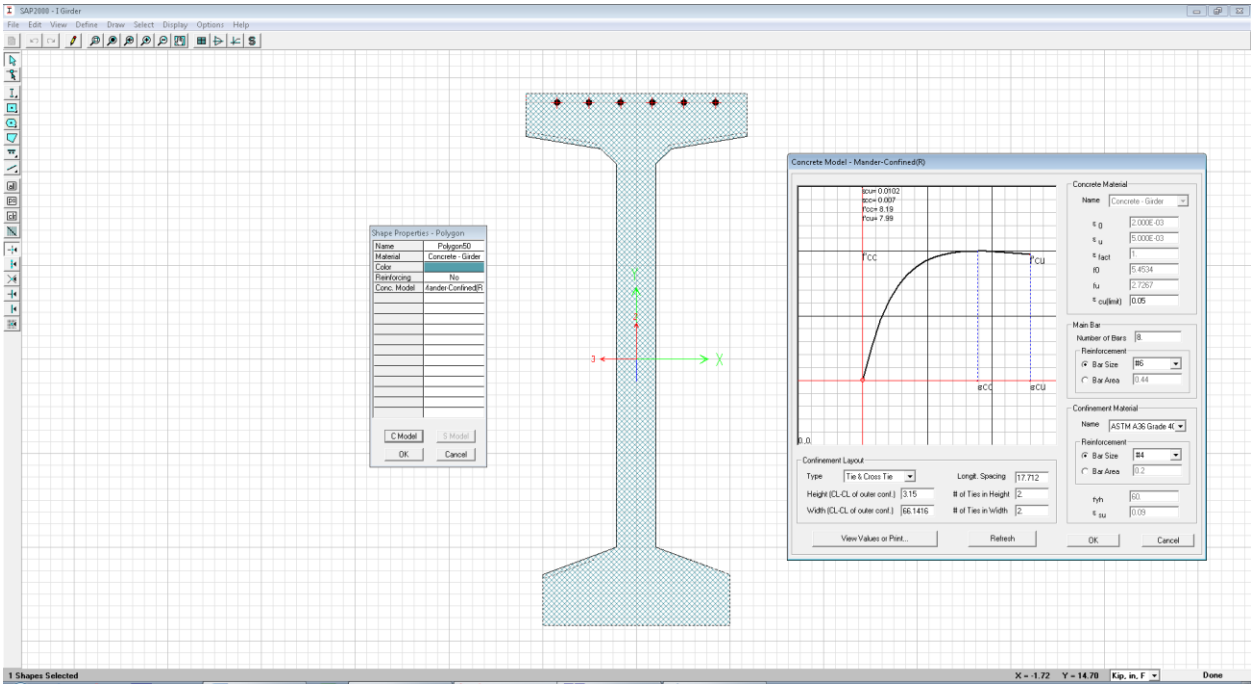

Figure A.5 Custom Girder Section

Step A.4.5

Following the preceding steps, sections for the remaining structural members are created. After material properties and sections have been created, the corresponding members are selected and using the Assign>Frame Sections command, a frame section is assigned to each of the frame elements as applicable. Assigning different colors to different frame sections and setting the Set Display Options to displaying by section color allows for easy differentiation between various member sections of the model; this can reduce clutter and avoid errors in the structural model.

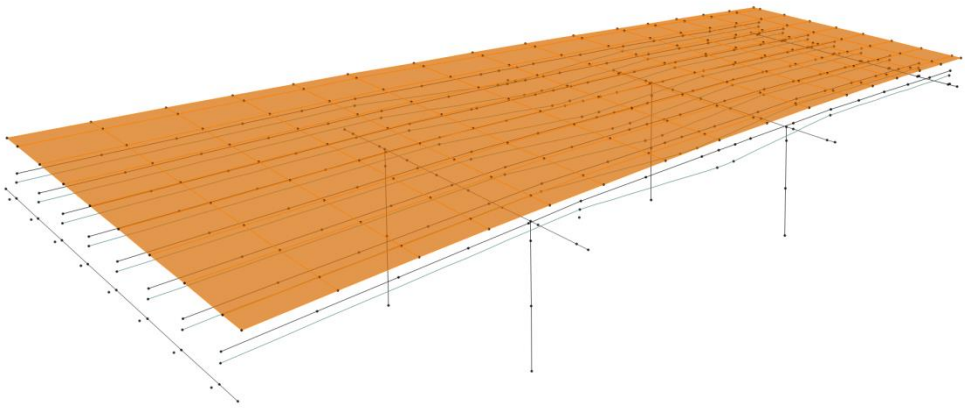

Figure A.6 SAP2000 Bridge Model with Bent Cap and Abutment Sections

A.5***Links***

In FE models, links are useful to model connections between adjacent nodes where a connection or interaction exists but cannot be modeled using frames or constraints. In the example shown, the superstructure is integral so fixed connections are used. At the abutments, the soil in the longitudinal direction is represented by nonlinear springs that are also modeled using link elements. The method of employing both links is described below

Step A.5.1

In order to model the connections between integral parts of the bridge, rigid links are used to connect adjacent frame elements.

Step A.5.2

A new link section is defined by selecting Define>Section Properties>Link/Support Properties and adding a new property.

Step A.5.3

Linear is selected under Link/Support Type and the “fix all” option is selected at the bottom of the dialogue box. This restrains displacement and rotation in all degrees of freedom between the two nodes of the link. The newly defined link will be used to model the integral behavior described above.

Step A.5.4

Using the ‘rigid link’ defined in the previous step, the girder nodes are connected to the deck at each intermediate node. This is done using the Draw>Draw 2 Joint Link – and selecting the rigid link section defined in the previous step. In addition a fixed connection is made between the nodes of the bent cap and girders, and the girders and the abutment. The configuration of the links should resemble the model shown below (ignore the links behind the abutment as they are added in a later step).

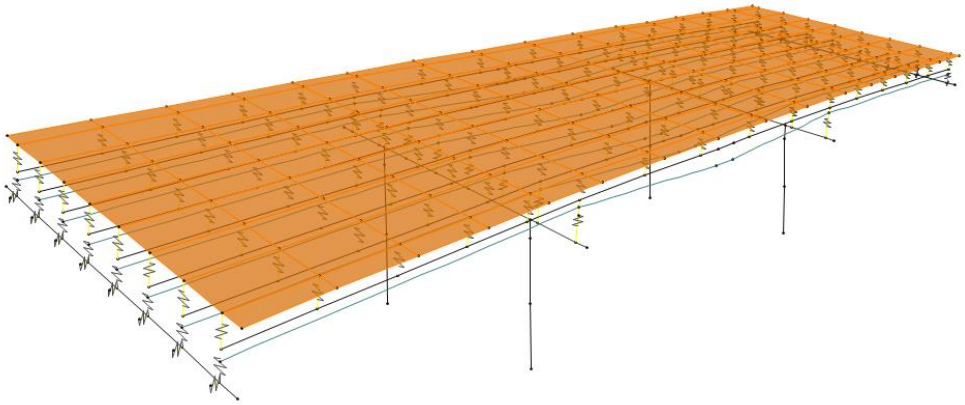

Figure A.7 SAP2000 Link Elements Implemented

A.6***Support Condition***

Step A.6.1

Next the support conditions of the bridge need to be defined. This is achieved through implementing nodal constraints at the appropriate locations of the bridge. The bridge modeled in this study utilizes integral abutments and a spread footing beneath each pier column. For the intent of this study and simplified representation of the global dynamic behavior, the spread footing support is modeled as a fixed support in all 6 DOF. The integral abutment is modeled as fixed in 5 DOF, while the backing soil in longitudinal (UX) direction is represented by a multi-linear spring.

The spread footings are modeled by selecting the nodes at the base of each column. Using the Assign>Joint>Restraints option – restrained displacement is implemented at the base of the member in all translational and rotational degrees of freedom.

Step A.6.2

The previous step is repeated for the nodes that support the abutment; however, translation in the global longitudinal direction (corresponding to UX) is not restrained. Note that it is also possible to change the local axes of the nodes by using the Assign>Joint>Local Axes

Step A.6.3

The next step involves creating a multi-linear spring for the backfill. This method is based on section 7.8.1 of the CALTRANS Seismic Design Criteria for the longitudinal abutment response for a stiff soil condition (SDC 1.6, 2010). The completed model is shown in Figure A.8.

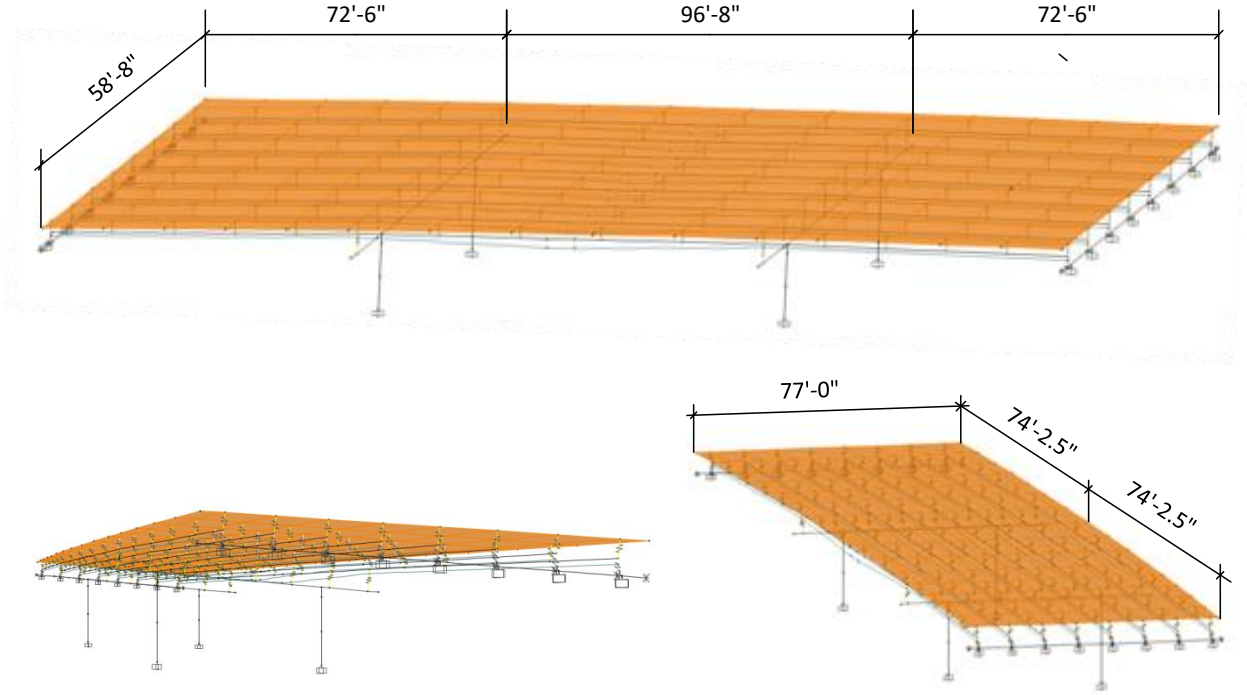

Figure A.8 Global SAP Models

A.7*Analysis Methods*

Once the model has been created, a series of different analyses may be performed. The analysis methods covered in this example include a dead load analysis, modal seismic analysis, seismic response spectrum analysis, and seismic time-history analysis.

A.7.1 Dead Load Analysis

Step A.7.1.1

To perform a dead load analysis, a load case must be created for the dead load, however, prior to defining the load case, the load pattern must be defined.(Define>Load Patterns>Add New Load Pattern) is selected and a new load pattern is defined.

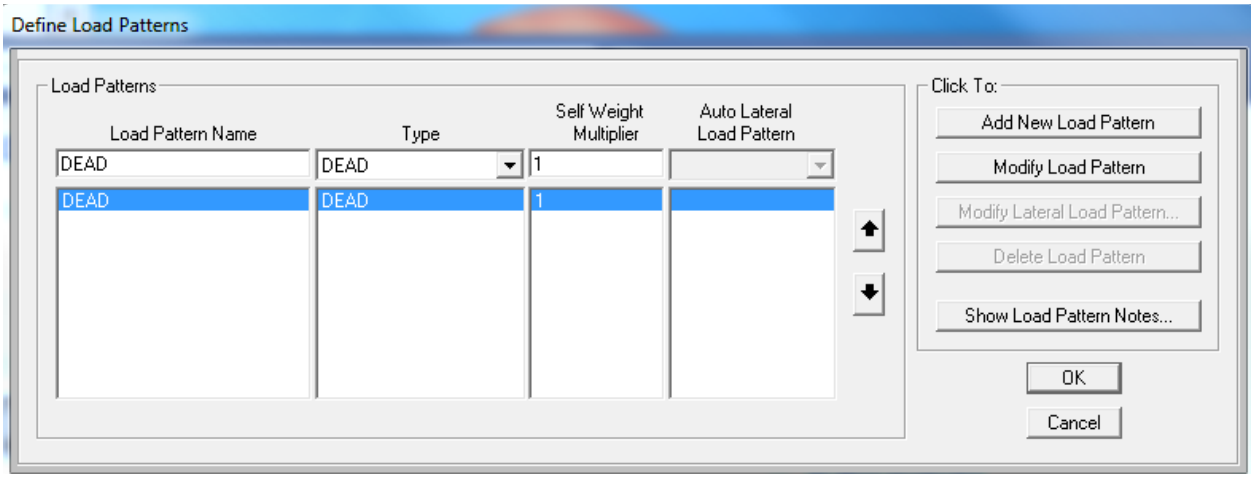

Figure A.9 Defining Load Pattern

Step A.7.1.2

Following creating the dead load pattern, a load case is created. (Define>Load Cases>Add New Load Case). The new load case is named DEAD and static and nonlinear is chosen under the

load case and analysis type. Load Pattern is chosen under Load Type and DEAD is selected under Load Name and a scale factor of 1 is applied.

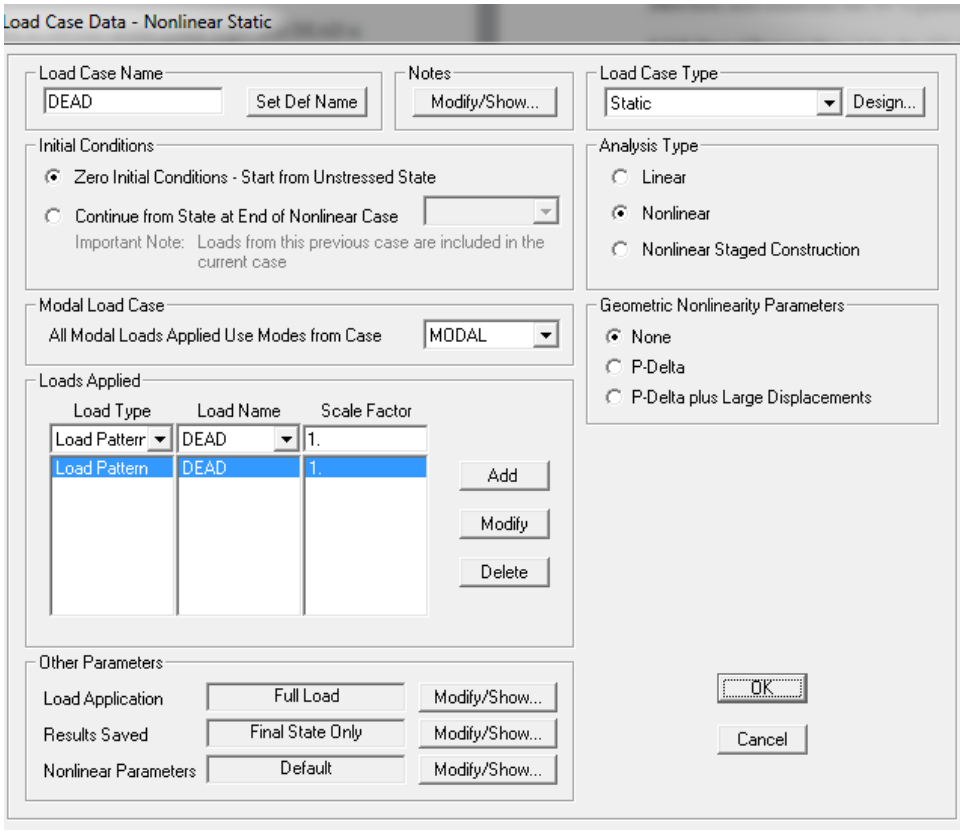

Figure A.10 Load Case Data - Dead Loads

Step A.7.1.3

Due to limitations of this study, the effects of bridge live load were not considered. A traffic loading may be considered at this stage however, SAP no longer has this capability and it would be necessary to use CSI Bridge or a similar product. Additionally, AASHTO does not have any firm requirements for the value of γ_{EQ}, the load factor for live load in the Extreme Event I (Earthquake) Load combination.

A.7.2 Modal Analysis

Step A.7.2.1

Another load case named MODAL is created. Modal is selected under Load Case Type and Ritz Vectors are employed. The maximum number of modes specified is 30, which may vary depending on model complexity; at a minimum, enough modes must be considered to capture 95% of the structure mass and in this case, 30 modes are sufficient. Depending on the intent of the analysis, the stiffness used in the analysis may be selected as an unstressed state or using the stiffness at end of nonlinear case and selecting dead. It is the recommended that the stiffness at the end of the dead load analysis be used, thus the dead loads will be applied during the nonlinear case.

Step A.7.2.2

Under “Loads Applied”, add a load with an Acceleration Load Type, UX direction and maintain the 99 % participation ratio as shown in Figure A.11.

Step A.7.2.3

Repeat Step 2 for the UY direction in the same load case.

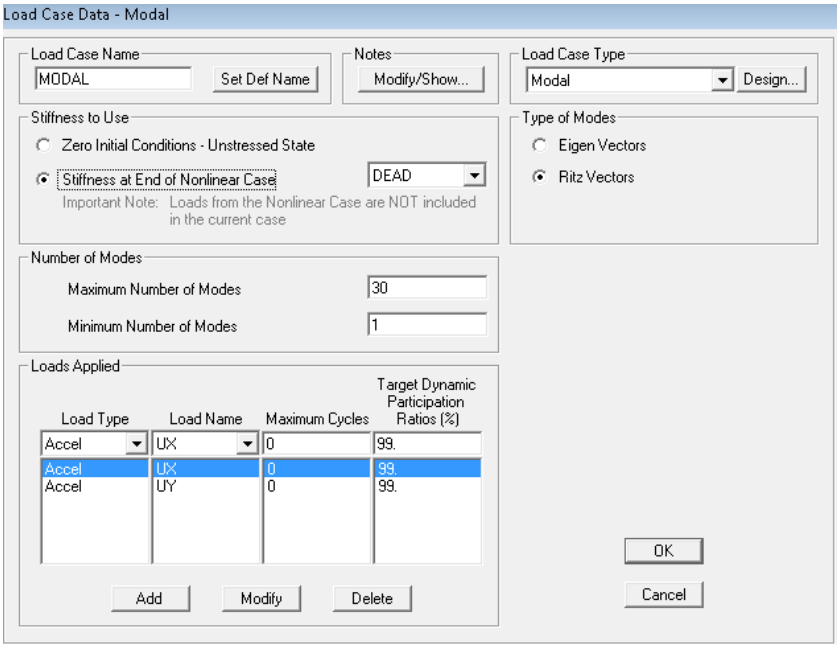

Figure A.11 Modal Load Case

A.8 ***Response Spectrum Analysis***

Although it is not employed in the analysis performed in this study, Response Spectrum analysis provides a quick way to estimate the seismic demand on a structure. The following steps describe a quick method of conducting this type of analysis per the AASHTO 2011 Guide Specifications. In order to estimate the seismic demand, a response spectrum must be created for the geographic location and site condition. This can alternatively be created directly in SAP2000 through their tool, on the USGS website, or through the hazard maps in either AASHTO Bridge Design specification. This example utilizes a USGS tool developed for the AASHTO 2011 Guide Specification with a return period of 1000 years.

Step A.8.1

Using the tool below, a response spectrum for Site Class D - a stiff soil is assumed for site for Denver, Colorado using the AASHTO Guide Specification (2011) as the base design code.

http://earthquake.usgs.gov/designmaps/us/application.php

Step A.8.2

The report that is generated using the link above contains information on the site class definitions in conjunction with the articles of the code. The report also develops a Design Response Spectrum and partitions which Seismic Design Category that specific site falls into.

Step A.8.3

Using the data supplied in the report and the equations given in section 3.4.1 of the GS, the design response spectrum in tabular form can be generated. This can be readily computed in a program like Microsoft Excel.

Step A.8.4

Once the periods and corresponding spectral accelerations have been generated, the data is copied and pasted into a .txt file (notepad preferable) and saved. The response spectrum can now either be used to analyze a frame directly or be indirectly used in a time-history analysis.

Step A.8.5

The response spectrum curve is input into SAP 2000 by using the. Define>Functions>Response Spectrum> select "From File" under "Choose Function Type to Add" and click Add New Function.

Step A.8.6

“Browse” is selected and the text file containing the response spectrum is selected. "Time and Function Values” under "Values are:" are used and a check box is selected. So the parameters "Header Lines to Skip" match the data imported. "Display Graph" is used as a final check to ensure the correct RS is generated.

Alternatively, one can add a new function directly by going to Define>Functions>Response Spectrum and manually input the data

Step A.8.7

In the SAP model, a new load case is created and named RS. A new Response Spectrum type load case is defined and the defaults are left as is. Under Loads Applied, a U1 load case is applied with the response spectrum function and original scale factors multiplied by 32.2 (ft/s^2) to account that the spectrum is input as a percentage of gravity.

Step A.8.8

This step is repeated for another load case with the applied load in the U2 direction. Alternatively, a load case should be used for comparative purposes, which applies 100% load in the U2 direction, and 30% in the orthogonal U1 direction. This simulates the fact that the direction of the earthquake is unknown. In addition a load case to consider 100% U1 plus 30% U2 analyzed.

A.9 ***Nonlinear Time-History Analysis***

Time-history analysis is the most rigorous and accurate analysis method used by code standards and researchers alike. It can be used in both linear and nonlinear structural models, and typically requires large computational demand depending on the complexity of the model. The general steps to performing a generic time-history analysis are described below.

Step A.9.1

Earthquake records should be selected to simulate earthquake ground motion loading on the bridge. The AASHTO specifications require a minimum of three records for a suitable analysis (two horizontal and one vertical ground motion). The records should be characteristic of the tectonic setting and site characteristics. For Colorado, this is not feasible because of the limited seismic data in Colorado and records with similar tectonic characteristics. It is typically recommended (not per code) that records be selected based on a low PGA, similar to that of the DRS developed, a medium site distance, and from a primarily inter-plate database where records are generally more reliable. The PEER database (the link to which is shown below) is widely utilized in research and design and provides a strong motion database for earthquake selection.
http://peer.berkeley.edu/gmsm/documentation/

Step A.9.2

Once three records have been chosen, the ground motions must be scaled. Although different scaling methods provide various advantages and disadvantages (Section 4.1) a response spectrum based scaling approach is often used due to its accuracy, efficiency and code based origins.

Step A.9.3

Construct a design response spectrum using guidelines from the AASHTO Bridge or Guide Specifications.

Step A.9.4

Determine the fundamental period of vibration of the bridge by running a modal analysis, developed in 6.3.7. The fundamental period is determined by searching for the mass participation being excited in the direction of interest,

Step A.9.5

In an Excel spreadsheet, tabulate the response spectra from the structural code (ex. USGS - AASHTO 2011) as well as the fault normal and fault parallel components of the ground motion records. When using the PEER database, the response spectra are available through the "Save Search Spectra" option for the marked search results. Alternatively, a program like Seismosignal developed by Seismosoft, (http://www.seismosoft.com/en/seismosignal.aspx) provides a quick and free solution for processing earthquake signals.

Step A.9.6

The scaling factor is determined as the differential factor between the spectral acceleration of the DRS and the earthquake record at the fundamental period of the bridge. This factor is computed for the fault normal and fault parallel components. The scale factor is multiplied by 0.3* per design codes for the fault parallel (or smaller ground motion component).

**In the analyses described in the previous chapter, the perpendicular scaling factor used to evaluate bridge performances was multiplied by 0.4. A higher scaling factor was used for research purposes as to limit the probability of underestimation of seismic demand imposed by the earthquake ground motion. This was adopted from the following study (Bisadi and Head, 2011).*

Step A.9.7

After the scaling factors are computed, the records need to be processed and imported into SAP2000. Each record is imported into Seismosignal and a baseline correction is applied.

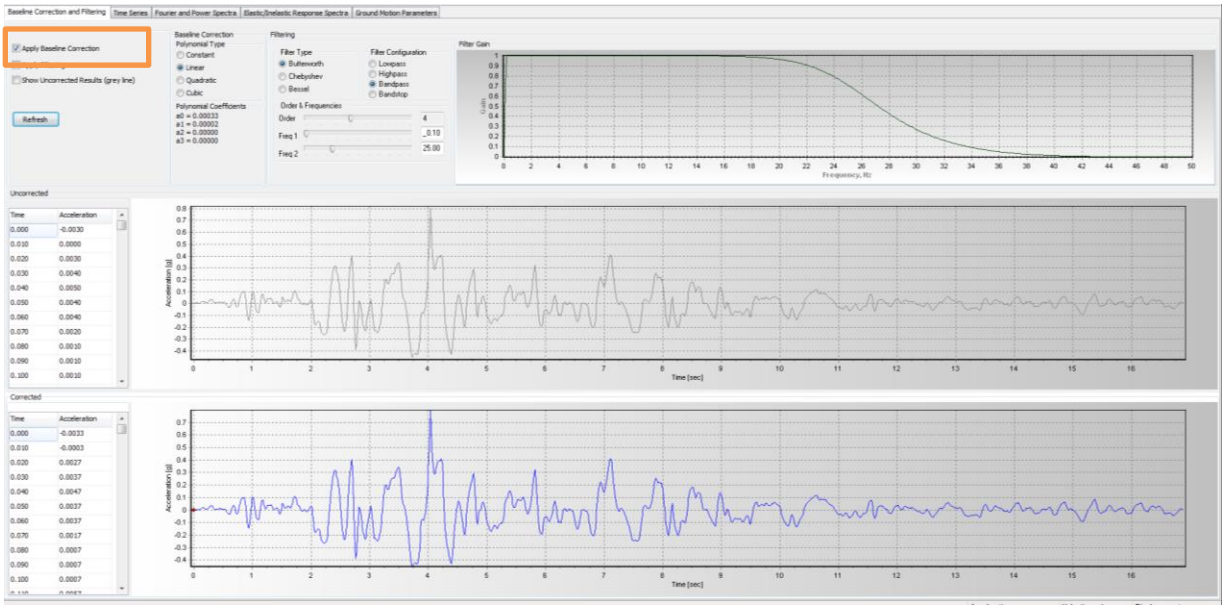

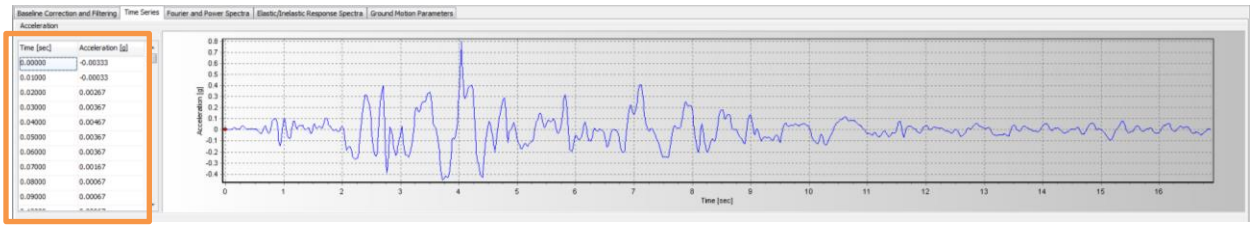

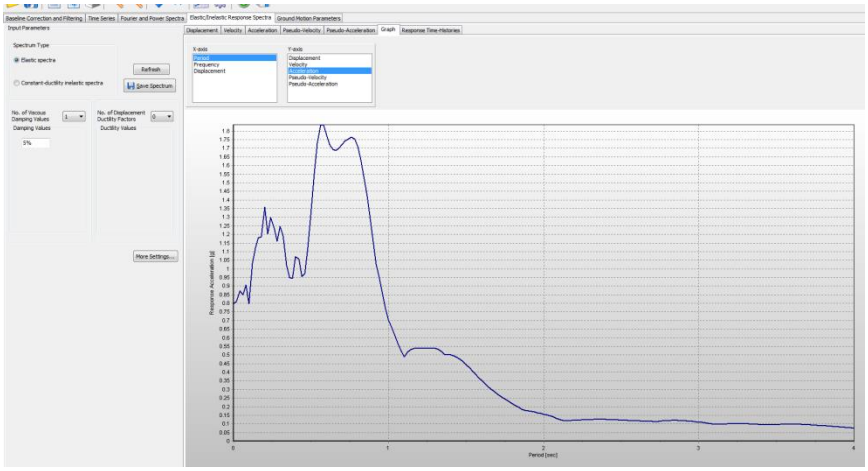

Figure A.12 Seismosignal Forms for Signal Processing

The time-history record in the dual column format is shown in the “Baseline Correction Filtering” tab under “Corrected” and can be copied and pasted into a .txt file. An independent text file is created for both the fault normal and fault parallel component of each earthquake. The response spectrum can also be found under the “Elastic/Inelastic Response Spectra” tab, this may be useful for *Step A.9.6.*

Step A.9.8

In SAP, a new load function is added through the Define>Functions>Time History>Add New Function (From File). Under browse, the text file is added and the parameters are completed to match the format of the record.

Step A.9.9

After the earthquakes have been processed, scaled and imported into SAP2000, a load case can be created. The important parameters of the load case are that it is Time History, Nonlinear,

Direct Integration, and considers P-Delta effects. It is also important to "Continue from State at End of Nonlinear Case: Dead" (Figure A.13).

Step A.9.10

The earthquake records are added as shown in the picture below and the time step and total number of output time steps matches that of the original earthquake record. Damping is defined by a 2% proportional Rayleigh damping of dynamic vibration for the first and second modes of vibration. The method of direct time integration is conducted through Hilber-Hughes-Taylor method.

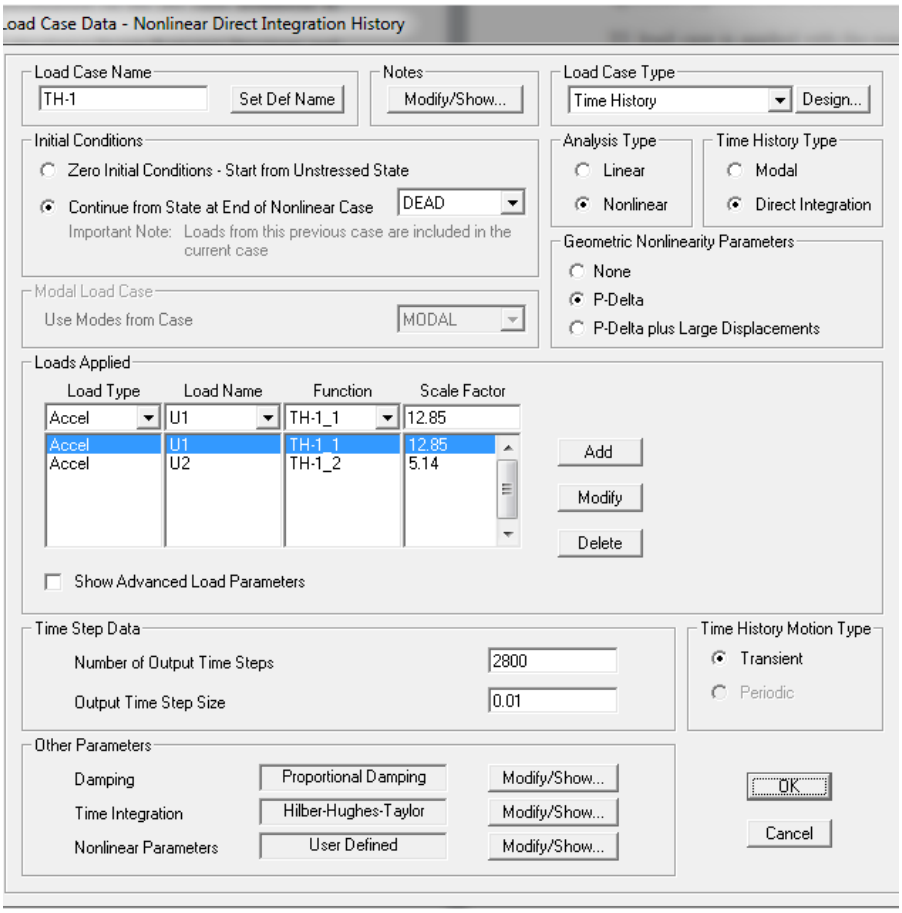

Figure A.13 Load Case Data - NLTH

A.10 ***Post Processing Methods***

A few different tools are available to easily post process the SAP models. Each of the following options has their advantages based on information provided and computation time.

I. Use the display options to display forces and displacements as shown below

The advantages to this option are that it is easily accessible, and can show a visual representation of the forces and moment diagram on the actual frame. It is also easy to right click on the frame to obtain action diagrams once it is displayed. The disadvantages are that for time-history analysis it necessitates large amounts of time to compute. It also has difficulties panning through the model to find results (i.e. it needs to update each time step).

II. Use the "Show Plot Functions" option.

The "Show Plot Function" allows a time-history plot of various components, such as a single nodal result (i.e. displacement or force). It is best used for further investigating components of the model once a global demand has been calculated. For example, in this study it was useful for finding a particular peak demand and the corresponding actions that develop at that time for a specific point in the earthquake time-history. Additional post processing is easiest computed by exporting the results from this section to a .txt file and subsequently importing into MATLAB, Excel or other software for further processing. Alternative select step-by-step under the "Show Tables" option discussed below.

III. Utilizing the "Show Tables" option

Most of the post processing can be conducted using this option. It is recommended that the engineer select the frames or nodes that are of interest – select “Show Tables” and select the results that are desired from the analyses in order to avoid being overloaded with data. This method is the recommended option as it provides the maximum developed actions and displacements in a clean format that can be formatted and post processed directly in Excel.

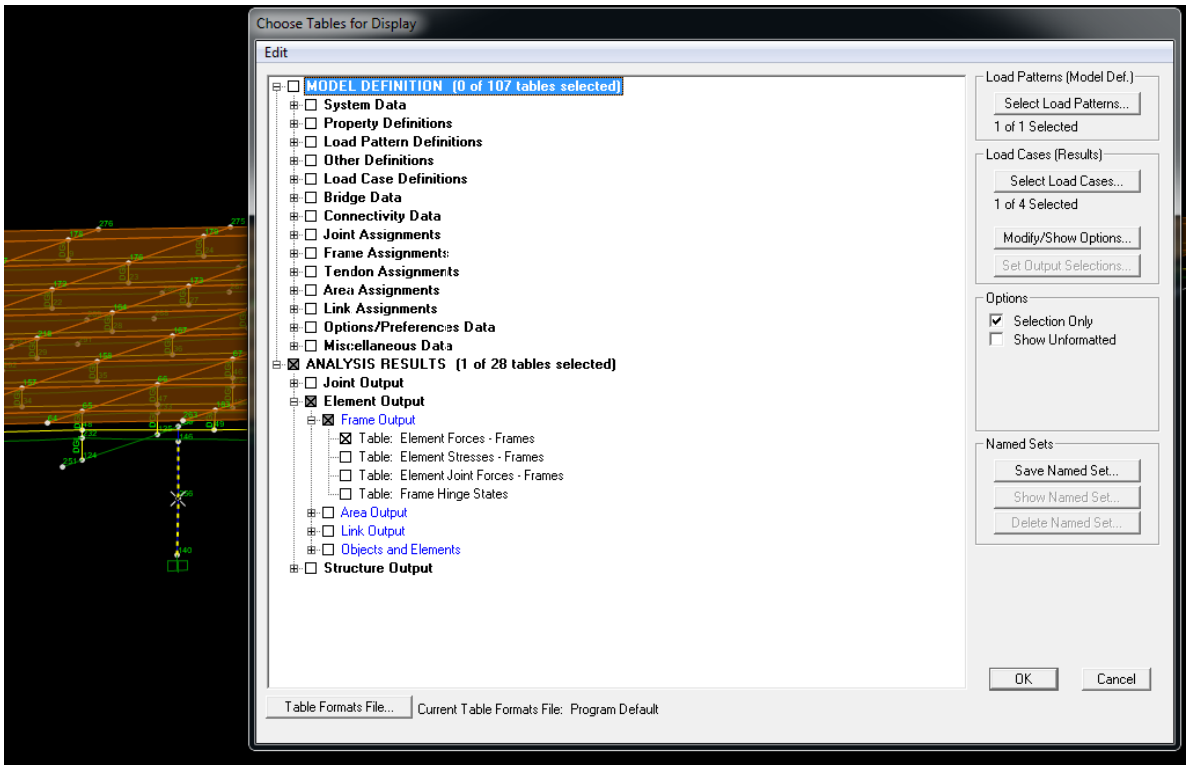

Figure A.14 Display Tables

For time-history analysis, the output will only display the largest demand observed over the entire earthquake. For analyses that require more than one demand component, this can lead to conservative and un-conservative design values. Therefore option B is recommended for identifying particular critical time points.

Appendix B: Design Examples 1 and 2 for SZ I & SDC A

AASHTO Bridge Design Code Examples 1 & 2 are based on LRFD and Guide Specification respectively for the 3-span bridge in SZ I & SDC A. The basic information of the 3-D bridge (referred to “D-17-DJ bridge” in some following text) is shown below.

B1. **3-span bridge Information**

Three-span bridge layout and construction information is shown in Figures B1-B5.

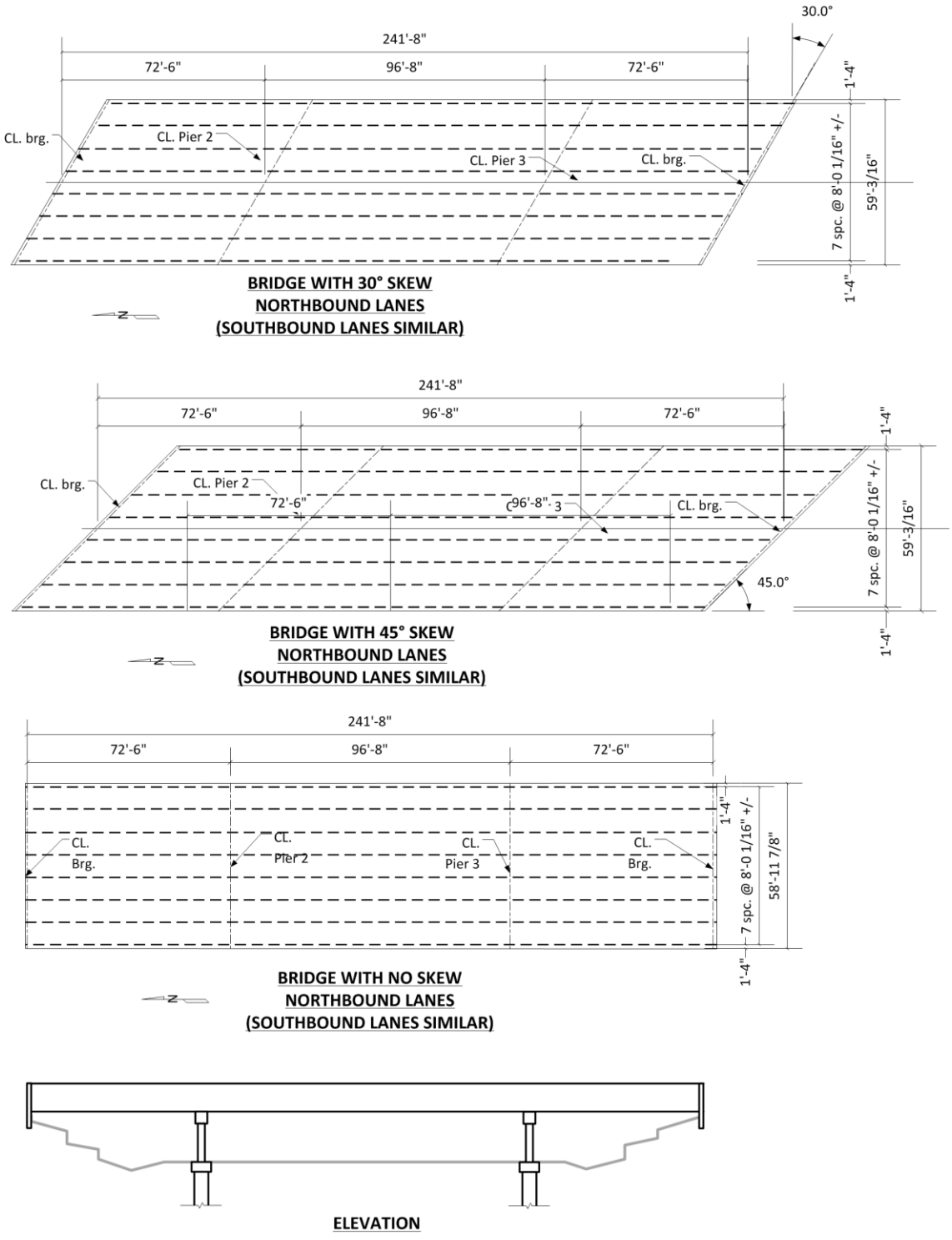

Figure B.1 - Three Span Bridge - Plans and Elevation (D-17-DJ bridge)

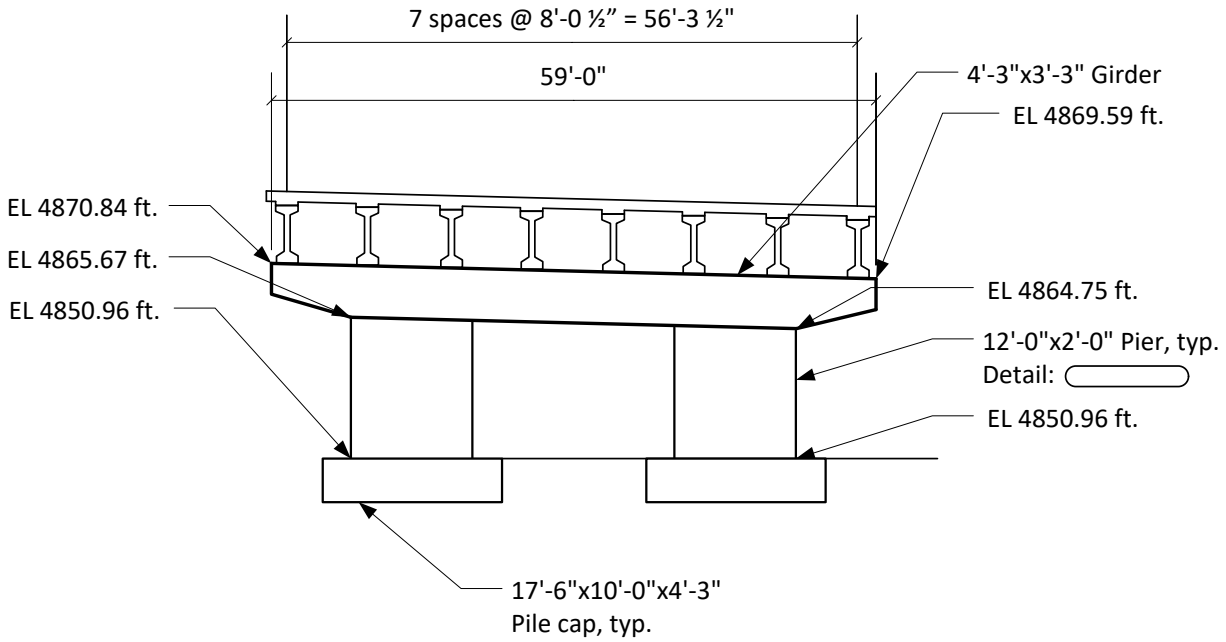

Figure B.2 – Three Span Bridge Section at Pier

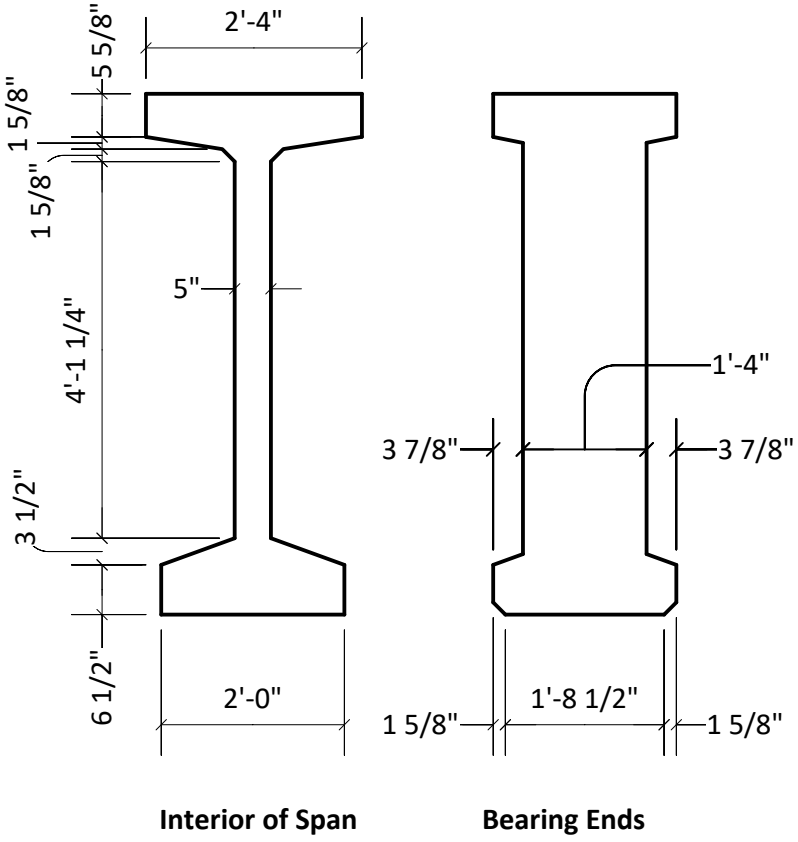

Figure B.3 – Three Span Bridge - Precast I Sections

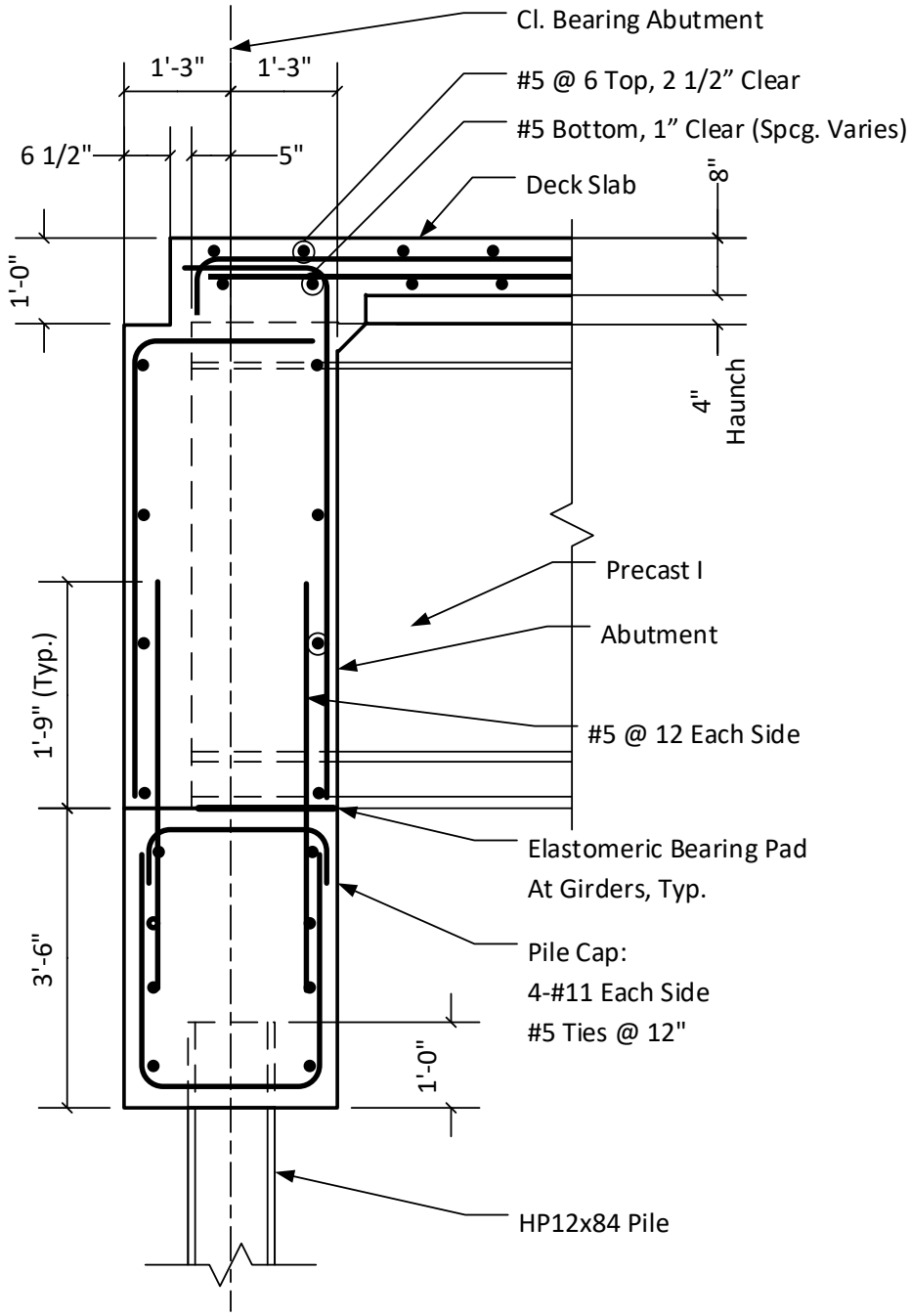

Figure B.4 – Three Span Bridge - Section at Abutment

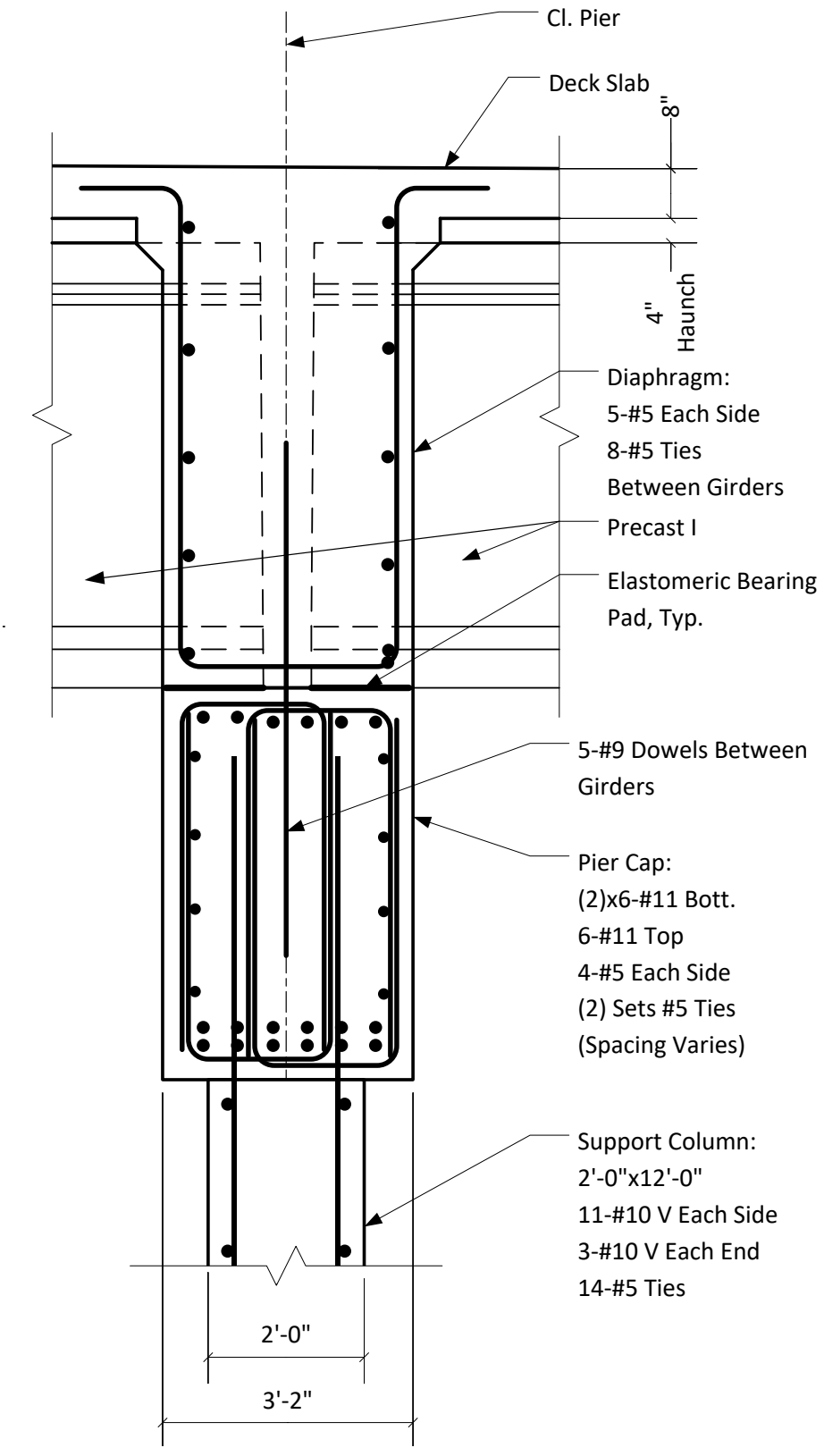

Figure B.5 – Three Span Bridge - Section at Pier

B2. **Design Example No.1 (LRFD Design Specification-SZ I)**

This design example is based on AASHTO LRFD Bridge Design Specifications – Customary U.S. Units (2012)

The following section describes the seismic design procedures required for bridges in Seismic Zone 1. The bridge selected for the design example carries the northbound and southbound lanes of Interstate Highway I25 over State Highway 119 at Del Camino (Firestone, Colorado). The bridge layout and construction are shown in Figures B.1 to B.5. The example is not comprehensive for all bridges in SZ-1 but rather serves as a general example for a typical bridge design with a few additional comments and insights.

The flowchart presented in Chapter 3, Appendix A3 of the AASHTO LRFD Code is the easiest way to follow the seismic design procedure and is thus followed herein. The organization of the design example is categorized by article title and follows the general structure of the design flowcharts.

B2.1 Earthquake Demand:

B.2.1.1 **AASHTO Article 3.10 Earthquake Effects: EQ**

AASHTO Article 3.10.1 introduces the general methodology of the seismic design, and also describes the applicability of the specifications.

There are two possible options for determination of the seismic hazard factors:

Option A. Use the articles and procedures presented in AASHTO subsections 3.10.2, 3.10.4, and 3.10.6 to identify the seismic hazard factors from hazard maps , develop a design response spectrum, make adjustments with respect to the soil condition, and select the seismic performance zone (SZ).

Option B. (Recommended):Use the USGS-AASHTO web-based tool to determine the same parameters but through an automated process available at the following address:

http://earthquake.usgs.gov/designmaps/us/application.php

This example uses AASHTO Option A for determination of the seismic hazard factors to provide a basis for comparison with Option B, which is used in a subsequent example. From **AASHTO Article 3.10.2 f**or the D-17-DJ bridge and a site location in Firestone near Denver, Colorado, accelerations are determined from Figures B.6-8 and are equal to PGA=0.06g, S_s = 0.12g, S_1 = 0.035g, respectively. Linear interpolation is used for locations that are between contour lines; the red circle indicates the location of the bridge in Firestone.

Figure B.6 - AASHTO Bridge Spec.: 3.10.2-1 Acceleration Coefficient for Conterminous United States (PGA) with Seven Percent Probability of Exceedance in 75 yr. (Approx. 1000-yr Return Period)

Figure B.7 – AASHTO Bridge Spec.: 3.10.2-2 Horizontal Response Spectral Acceleration Coefficient for the Conterminous United States at Period of 0.2 s (S_s) with Seven Percent Probability of Exceedance in 75 yr. (Approx. 100-yr. Return Period) and Five Percent Critical Damping

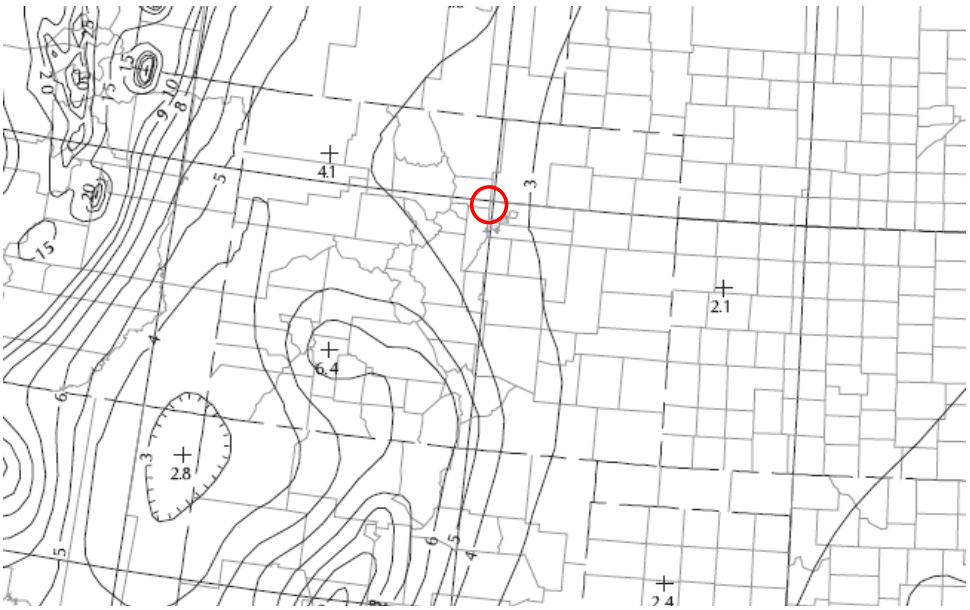

Figure B.8- AASHTO Bridge Spec.: 3.10.2-3 Horizontal Response Spectral Acceleration Coefficient for the Conterminous United States at Period of 1.0 s (S_1) with Seven Percent Probability of Exceedance in 75 yr. (Approx. 100-yr. Return Period) and Five Percent Critical Damping

B.2.1.2 **AASHTO Article 3.10.3 Site Class**

A site class is chosen based on the properties of the soil defined in **AASHTO Table 3.10.3.1-1**. For the prototype location in Firestone, Site Class D is selected for a stiff soil. Typically, the site class would be provided in the report of geotechnical investigation.

AASHTO Article 3.10.3.2 Site Factor

Based on **AASHTO Tables 3.10.3.2-1, 2 and 3** and the acceleration coefficients determined from the hazard maps, the following site factors were determined:

$F_{PGA} = 1.6$, $F_a = 1.6$, $F_v = 2.4$

B.2.1.3 **AASHTO Article 3.10.4 Seismic Hazard Characterization**

Using the equations and guidelines presented in **AASHTO Article 3.10.4**, a design response spectrum (DRS) was developed. Based on the equations, the following factors were calculated for the DRS:

$A_s = F_{pga}*PGA = 1.6*0.06g = 0.96g$

$S_{DS}=F_A*S_S = 1.6*.12g = 0.192g$

$S_{D1} = F_vS_1 = 2.4 * 0.035g = 0.084g$

$T_s= S_{D1}/ S_{DS} = 0.084/0.192 = 0.438s$

$T_0 = 0.2*T_s = 0.2 * 0.4375 = 0.875s$

B.2.1.4 **AASHTO Article 3.10.5 Operational Classification**

The owner shall determine the operational category of the bridge as Critical, Essential or Other. The operational category is used for determination of the appropriate response modification factor for the design of the substructure from **AASHTO Table 3.10.7.1-1** and from **AASHTO**

Table 3.10.7.1-2 for the connections. For the subject bridge supporting an interstate highway, the Critical category is chosen for which the response modification factor is 1.5 for vertical steel piles.

B.2.1.5 **AASHTO Article 3.10.6 Seismic Performance Zones**

Using the Seismic Hazard Parameters determined, the bridge may be assigned to a seismic performance zone. The Seismic Zone is determined from **AASHTO Table 3.10.6-1 (Table B.1)**.

Table B.1 - AASHTO Table 3.10.6-1 Seismic Zones

Acceleration Coefficient, S_{D1}	Seismic Zone
$S_{D1} \leq 0.15$	1
$0.15 < S_{D1} \leq 0.30$	2
$0.30 < S_{D1} \leq 0.50$	3
$0.50 < S_{D1} \leq$	4

$S_{D1} = 0.084 \leq 0.15$ which places the D-17-DJ bridge in Firestone, Colorado in Seismic Zone 1.

B.2.1.6 **AASHTO Article 3.10.7 Response Modification Factors**

The response modification factors for the connections are the same regardless of the response modification factor and are 0.8 for the superstructure to the abutment and 1.0 for columns to cap beam and columns to foundations.

B.2.1.7 **AASHTO Article 4.7.4 Analysis for Earthquake Loads**

Based on the Seismic Zone to which the bridge is assigned, this section is utilized to determine which analysis method is required. **AASHTO Table 4.7.4.3 (Table B.2)** presents each of the general analysis requirements. Based on a multi-span bridge type and seismic zone; for SZ-1, no seismic analysis is required.

Table B.2 - AASHTO Table 4.7.4.3

Seismic Zone	Single-Span Bridges	Multispan Bridges					
		Other Bridges		Essential Bridges		Critical Bridges	
		regular	irregular	regular	irregular	regular	irregular
1	No seismic analysis required	*	*	*	*	*	*
2		SM/UL	SM	SM/UL	MM	MM	MM
3		SM/UL	MM	MM	MM	MM	TH
4		SM/UL	MM	MM	MM	TH	TH

* = no seismic analysis required

UL = uniform load elastic method

SM = single-mode elastic method

MM = multimode elastic method

TH = time history method

For SZ-1 the next step is to meet the minimum requirements in AASHTO Articles 4.7.4.4 and 3.10.9. Starting with 4.7.4.4, the minimum support length requirements must be satisfied. The support length, *N*, is determined from:

$$N = (8 + 0.02L + 0.08H)(1 + 0.000125S^2)$$ **AASHTO Eqn. 4.7.4.4-1**

Where:

N = minimum support length measured normal to the centerline of bearing (in.)

L = length of the bridge deck to the adjacent expansion joint, or to the end of the bridge deck; for single -span bridge, L equals the length of the bridge deck (ft)

H = for abutments, average height of columns supporting the bridge deck from the abutment to the next expansion joint (ft)
for columns and/or piers, column, or pier height (ft)

S = skew of support measured from line normal to span (degrees)

In this case:

$L = 241.6$ ft., H ; 14 ft., $S = 0^o$

$N = (8 + 0.02 \times 241.6 + 0.08 \times 14)(1 + 0.000125 \times 5^2) = 13.99$ in. Say 14 in. minimum

AASHTO Article 3.10.9.2

Subsequently, the connection design forces are calculated per AASHTO Article 3.10.9.2 for a bridge in Seismic Zone 1.

Calculate the unit dead load of the bridge deck for determination of tributary vertical reactions in order to calculate resulting horizontal seismic forces at the piers and abutments.

Table B.3 – Unit weights for bridge superstructure components

Element	Weight	Factor	Unit Load (psf)
Precast I Beams	637 lb/ft.	8'-0 ½" Spacing	127.5
Slab + Haunches	6760 lb/ft (total)	59'-0" Width	59
Wearing Course	24 psf	1	24
Deck Forms	5 psf	1	5
Total	-	-	216

If A_s<0.05:

$$F_{long} \geq 0.15 \times (\text{Vert. Reaction based on influence area})$$

$$F_{lat} = 0.5 \times F_{long} = 0.15 \times (\text{Vert. Reaction based on tributary area})$$

If A_s <0.15:

$$F_{long} \geq 0.25 \times (\text{Vert. Reaction based on influence area})$$

$$F_{lat} = 0.5 \times F_{long} = 0.25 \times (\text{Vert. Reaction based on tributary area})$$

The next step is to calculate the influence area dead load of each span:

$$A_{span\ 1,3} = (72.5 \text{ ft})(59.1 \text{ ft}) = 4,285 \text{ ft}^2$$

$$A_{span\ 2} = (72.5 \text{ ft} + 96.8 \text{ ft})(59.1 \text{ ft}) = 10,006 \text{ ft}^2$$

$$W_{1,3} = (0.216 \text{ ksf})(4,285 \text{ ft}^2) = 926 \text{ kips} \text{ - Abutments}$$

$$W_2 = (0.216 \text{ ksf})(10,006 \text{ ft}^2) = 2161 \text{ kips} \text{ - Piers}$$

Next calculating the minimum connection force on the integral abutments and piers:

$$W_{1,3} = (0.216 \text{ ksf})(4,285 \text{ ft}^2) = 926 \text{ kips} \text{ - Abutments}$$

$$W_2 = (0.216 \text{ ksf})(10{,}006 \text{ ft}^2) = 2161 \text{ kips} \text{ - Piers}$$

Lastly calculating the minimum connection force on the center pier:

$$F_{Long} = (0.25)(2161 \text{ kips}) = 540 \text{ kips}$$

$$F_{Lat} = (0.5)(540 \text{ kips}) = 270 \text{ kips}$$

B.2.1.8 **AASHTO Section 5: Concrete Structures**

5.10.11 Provisions for Seismic Design

AASHTO Section 5.10.11.2 states that "For bridges in Seismic Zone 1 where the response acceleration coefficient, S_{D1}, specified in Article 3.10.4.2 is less than 0.10, no consideration of seismic forces shall be required for the design of structural components, except that the design of the connection of the superstructure to the substructure shall be as specified in 3.10.9.2."

For bridges in Seismic Zone 1 where $0.10 < S_{D1} \leq 0.15$, the transverse reinforcement requirements at the top and bottom of a column shall be as specified in **AASHTO Articles 5.10.11.4.1 d** and **4.10.11.4.1e**. For this design example, SD1=0.08 > 0.1, thus this section is not applicable.

B.2.1.9 **AASHTO Section 10: Foundations**

According to **AASHTO Appendix A10** a site specific investigation should be performed for sites with S_{D1}>0.1g, since S_{D1}<0.1g, no significant earthquake design factors need be considered

B.2.1.10 **AASHTO Section 11: Abutments, Piers and Walls**

The abutments are essentially concrete structures as they are caps supported by piles and thus, should be subject to the same design requirements, specifically, since S_{D1}<0.1g, no significant earthquake design factors need be considered.

The abutment walls carry no bridge load, vertical or horizontal and thus will not be subject to excitation from the bridge.

B3. **Design Example No.2 (Guide Specification-SDC A)**

This design example is based on AASHTO Guide Specifications for LRFD Seismic Bridge Design 2nd Edition (2011)

The following section describes the seismic design procedures required for bridges subject to the design requirements of Seismic Design Category A (SDC A) using the **AASHTO Guide Specifications (GS)**. The same bridge as used in design example No. 1 (D-17-DJ bridge) is selected, which carries the northbound and southbound lanes of Interstate Highway I25 over State Highway 119 at Del Camino (Firestone, Colorado) is considered. The center of the bridge is at coordinates 40.160654, -104.978964 based on Google.

B.3.1 *Earthquake Demand:*

B.3.1.1 GS *3.4 Seismic Ground Shaking Hazard*

Option A. Use the articles and procedures presented in *3.4 Seismic Ground Shaking Hazard* to develop a design response spectrum based on hazard maps, and make adjustments with respect to the soil condition.

Option B. (Recommended). Use the USGS-AASHTO tool to determine the same parameters but through an automated process.

http://earthquake.usgs.gov/designmaps/us/application.php

Using Option B, the following parameters were determined and may be used with the specifications in *Section 3.4.1-1* or taken directly from the USGS-AASHTO document to determine the design response spectrum:

Parameter	Value		
PGA	0.058g	$A_s = F_{PGA} * PGA$	0.093g
S_s	0.124g	$S_{DS} = F_a * S_s$	0.198g
S_1	0.033g	$S_{D1} = F_v * S_1$	0.079g
F_{pga}	1.60		
F_a	1.60		
F_v	2.40		

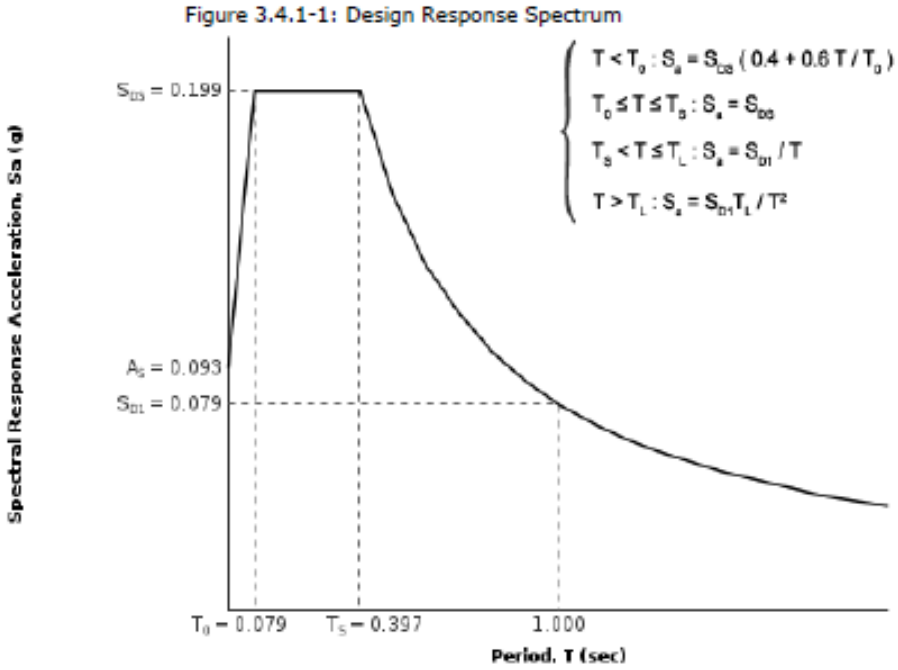

Figure B.6 - Design response spectrum – Origin: USGS – AASHTO 2014 Guide Spec. Seismic Hazard Tool

B.3.1.2 **AASHTO Article 3.5 Selection of Seismic Design Category (SDC)**

a. Utilize the specifications below and the S_{D1} parameter to determine the Seismic Design Category

AASHTO Table 3.5.-1 - Partitions for Seismic Design Categories A, B, C, and D

Value of $S_{D1} = F_v S_1$	SDC
$S_{D1} < 0.15$	A
$0.15 \le S_{D1} < 0.30$	B
$0.30 \le S_{D1} < 0.50$	C
$0.50 \le S_{D1}$	D

Based on the value of 0.079g for the S_{D1} parameter developed in the previous step, the Seismic Design Category is determined as **SDC A**. A review of the requirements for each step is shown below:

SDC A Requirements from **AASHTO Article 3.5** – Selection of Seismic Design Category (SDC)

a. No identification of ERS according to Article 3.3
b. No demand analysis
c. No implicit capacity check needed
d. No capacity design required
e. Minimum detailing requirements for support length, superstructure/substructure connection design force, and column transverse steel
f. No liquefaction evaluation required

B.3.1.3 **AASHTO Article 4.6 – Design Requirements for Seismic Design Category A**

Based on the requirements, determine the minimum design requirements that need to be met through Article 4.6. The acceleration coefficient A_s is the critical factor for calculation of the seismic forces on the connections in the restrained directions; for the subject connection A_s = 0.093.

For the 3-Span Bridge,

If A_s<0.05:

$$F_{min,conn,long} \ge 0.15 \times (\text{Vert. Reaction base on influence area})$$

$$F_{min,conn,trans} \ge 0.15 \times (\text{Vert. Reaction base on tributary area}) = 0.5 F_{min,conn,long}$$

If A_s <0.15:

$$F_{min,conn,long} \geq 0.25 \times (\text{Vert. Reaction base on influence area})$$
$$F_{min,conn,trans} \geq 0.25 \times (\text{Vert. Reaction base on tributary area}) = 0.5F_{min,conn,long}$$

This second case will be used since $0.05 < 0.093 < 0.15$.

Subsequently, the influence area dead load of each span is calculated (refer to **Table B.3** for unit values of component dead loads). The longitudinal loads should first be determined based on the influence areas:

$$A_{span\ 1,3} = (60.17\ \text{ft})(59.1\ \text{ft}) = 3{,}556\ \text{ft}^2$$
$$A_{span\ 2} = (60.17\ \text{ft} + 115.42\ \text{ft})(59.1\ \text{ft}) = 10{,}377\ \text{ft}^2$$

$$W_{1,3} = (0.216\ \text{ksf})(3{,}556\ \text{ft}^2) = 768\ \text{kips}\ \text{ - Abutments}$$
$$W_2 = (0.216\ \text{ksf})(10{,}377\ \text{ft}^2) = 2241\ \text{kips}\ \text{ - Piers}$$

Next calculating the minimum connection force on the integral abutment:

$$W_{1,3} = (0.216\ \text{ksf})(3{,}556\ \text{ft}^2) = 768\ \text{kips}\ \text{ - Abutments}$$
$$W_2 = (0.216\ \text{ksf})(10{,}377\ \text{ft}^2) = 2241\ \text{kips}\ \text{ - Piers}$$

Lastly, calculating the minimum connection force at the pier:

$$F_{Long} = (0.25)(2241\ \text{kips}) = 560\ \text{kips}$$
$$F_{Lat} = (0.5)(560\ \text{kips}) = 280\ \text{kips}$$

B.3.1.4 **AASHTO Article 4.12 Minimum Support Length Requirements**

The minimum required support lengths are specified in **AASHTO Article 4.12**. These specifications typically apply for bridges in Seismic Design Category A; however, the subject bridge has integral abutments and thus, does not need to satisfy this requirement.

B.3.1.5 **AASHTO Section 8: Reinforced Concrete Members**

8.2 – Seismic Design Category (SDC) A

For S_{D1}values equal to or exceeding 0.10, but less than 0.15 in SDC A, minimum shear reinforcement is required to meet the SDC B requirements for concrete members per **AASHTO Article 8.6.5**. In addition "When such transverse reinforcement is provided, the provisions of

AASHTO Article 8.8.9 should apply. The length over which this reinforcement shall extend shall be the plastic hinge region defined in **AASHTO Article 4.11.7**. Alternatively, this length may be that defined in **Article 5.10.11.4** of the AASHTO LRFD Bridge Specifications"

For the bridge under consideration, S_{D1}= 0.079 <0.1 and thus, does not need to satisfy these requirements.

B.3.1.6 **AASHTO Section 6: Foundation and Abutment Design**

Per **AASHTO Article 6.2.3,** "there are no special seismic foundation investigation requirements for SDC A".

Appendix C: Design Examples 3 and 4 for SZ II & SDC B

Design examples 3 & 4 are for both 2-span (J-17-AA bridge) and 3-span bridges (D-17-DJ bridge) in SZ II and SDC seismic zones based on the AASHTO LRFD Standard and Guide Specifications. The 3-span bridge information can be found at Appendix B (B.1). The 2-span bridge information is introduced in the below.

C1. **2-span bridge (J-17-AA bridge) Information**

Two Span Bridge Layout and Construction (J-17-AA bridge)

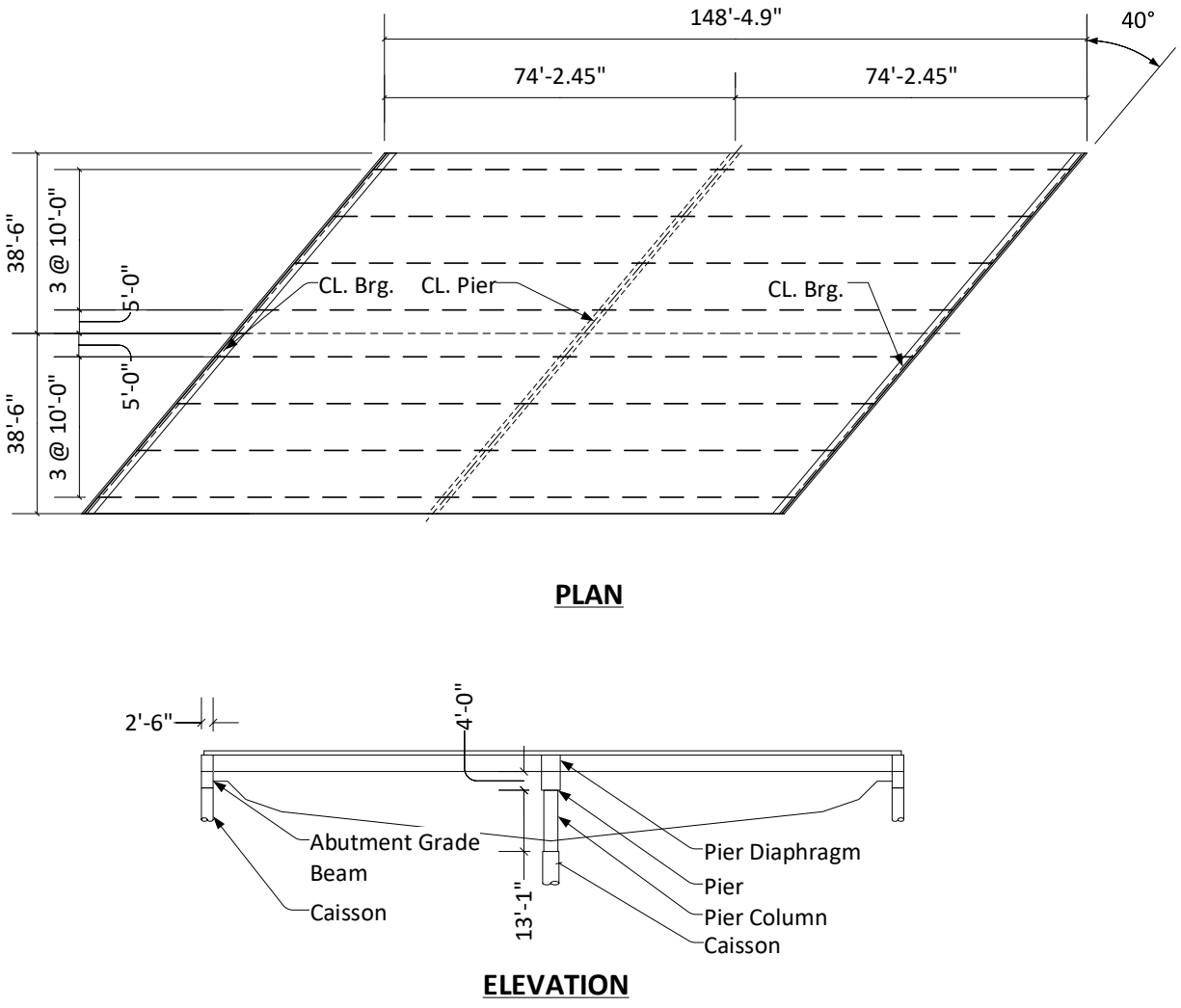

Figure C.1 - Two Span Bridge Plan and Elevation (J-17-AA bridge)

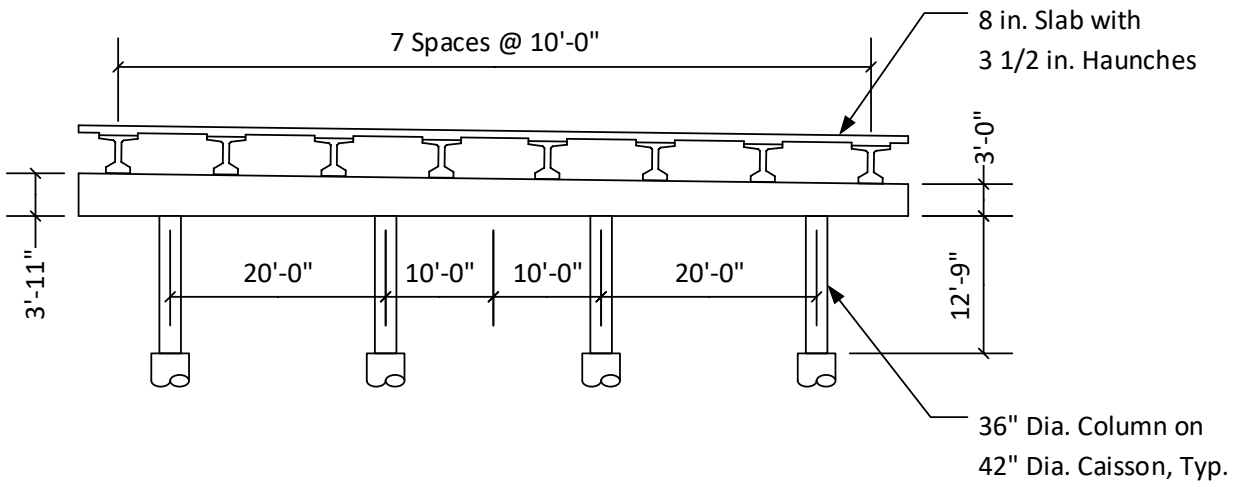

Figure C.2 - Two Span Bridge - Section at Pier

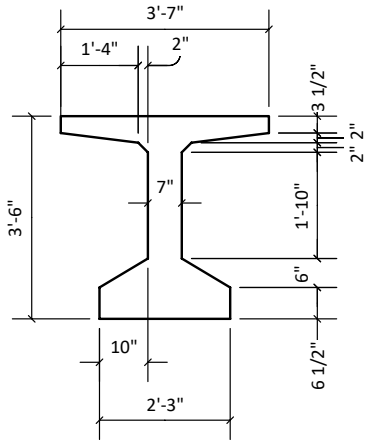

Figure C.3 - Two Span Bridge - I-Girder Cross Section

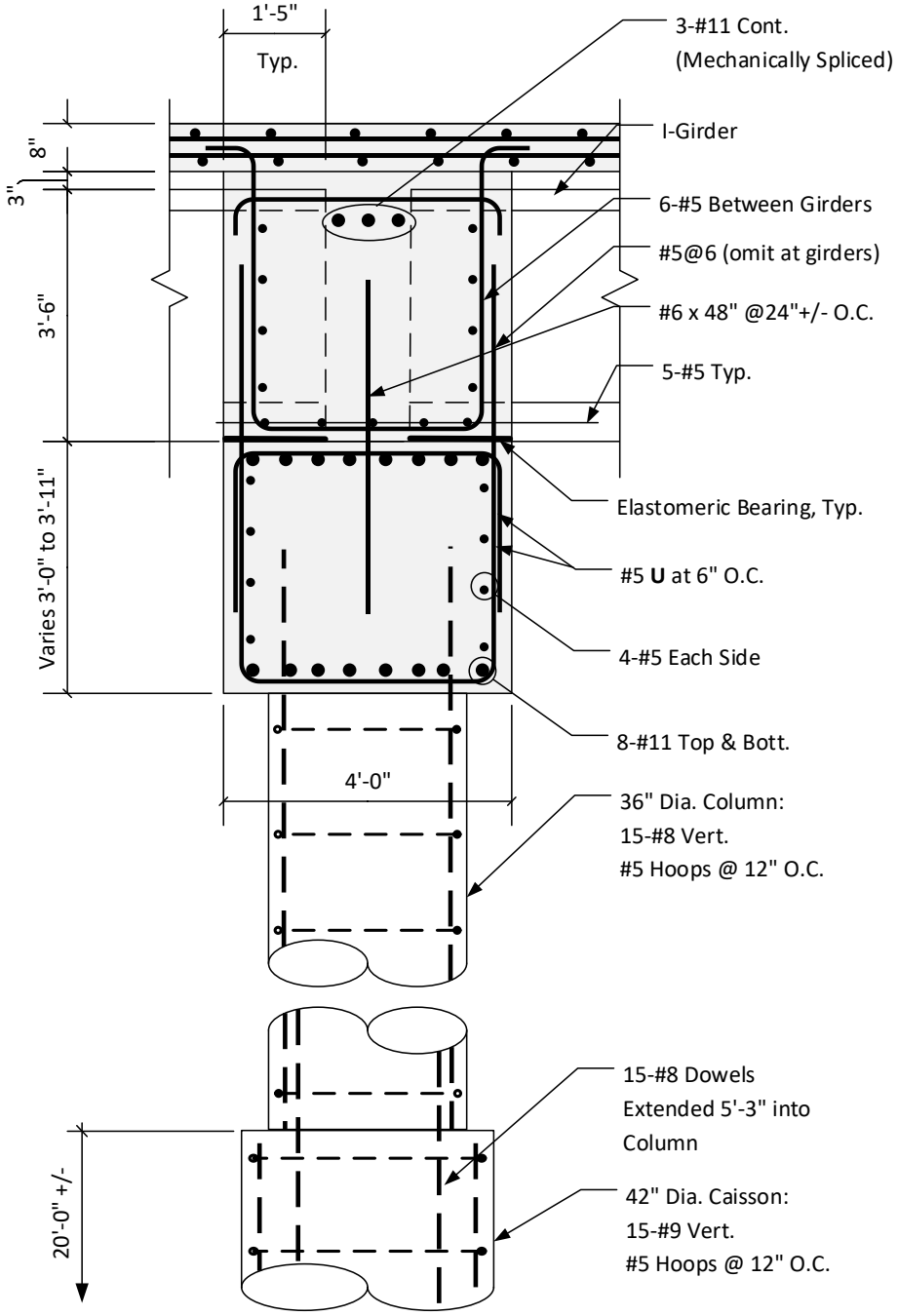

Figure C.4 - Two Span Bridge - Section at Pier

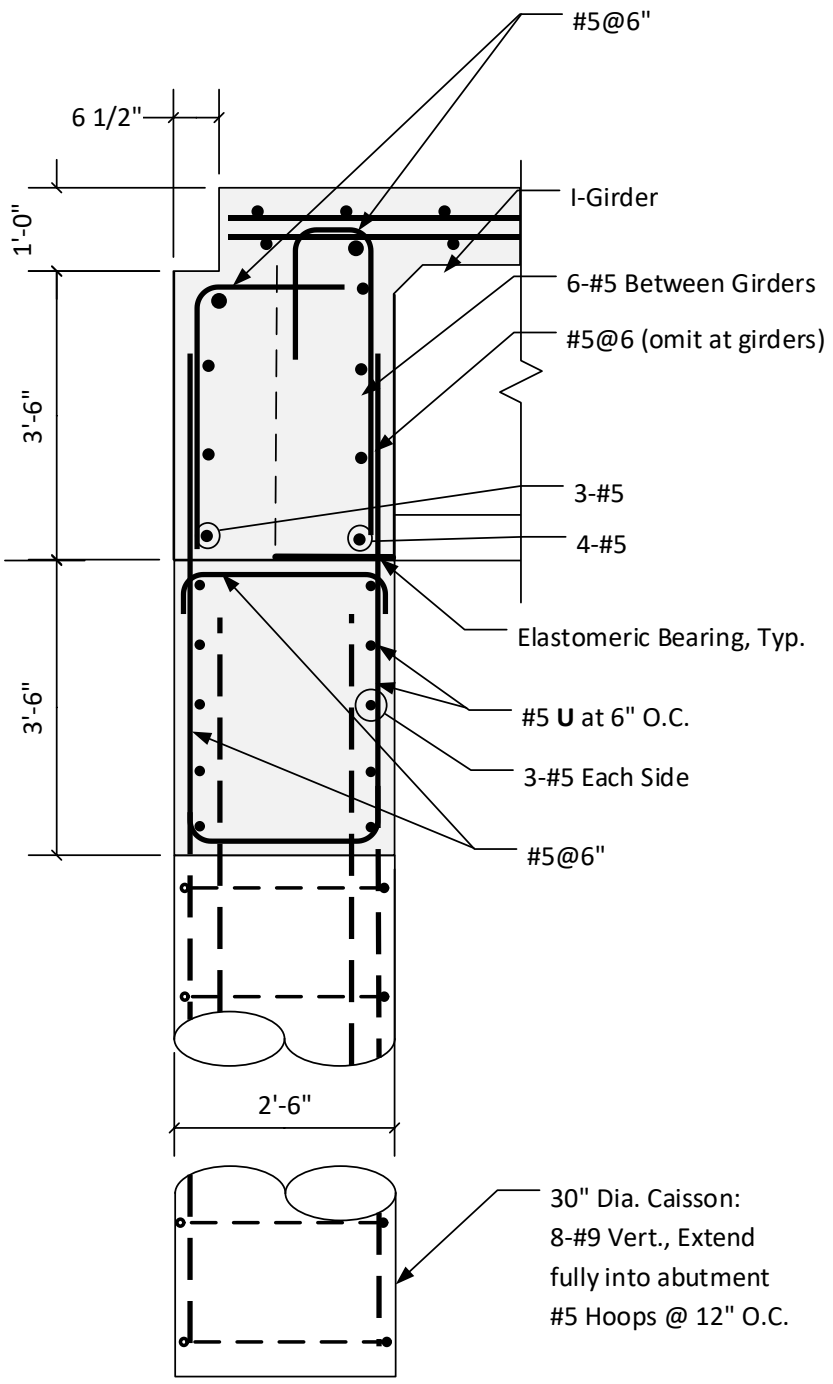

Figure C.5 - Two Span Bridge - Section at Abutment

C2. **SAP Analysis Results for the 2-span and 3-span bridges**

The portion of Colorado that falls into SDC B and SZ II in the AASHTO specifications is limited to a finite portion of the map, for a select soil condition. The select geographic area that falls in the higher seismic zone is limited to the portions of the South and West of Colorado, and for a softer (Site Class E and lower) soil condition. For this region and condition described a DRS is developed per the AASHTO Guide Specifications. The ground motion is then scaled and the imposed seismic demand is analyzed using the 2-span bridge, and a select 3-span bridge. The bridge geometry selected for the three-span bridge is Bridge #6 which has a radius of 4500 ft and skew angle of 30 degrees. Table C.1 shows the increased deformation of the model resulting from using SDC B/SZ II compared to SCC A/SZ I. Tables C.2 through C.7 present the increased structural demand of the model resulting from SDC B/SZ II.

Table C.1 Jt. Displacement: 2-Span & 3-Span Bridges

3-Span Bridge Jt. Displacements		
	U1 (Longitudinal)	U2 (Transverse)
Minimum	38%	49%
Maximum	122%	164%

2-Span Bridge Jt. Displacements		
	U1 (Longitudinal)	U2 (Transverse)
Minimum	18%	2%
Maximum	87%	62%

Table C.2 Jt. SDC B: 2-Span Bridge: **Column** Demand

		Peak Demand	% Increase from SDC A	D/C Ratio
Axial	Kip	-537.7	18.1%	0.12
V2	Kip	-83.51	52.8%	0.18
V3	Kip	181.3	62.8%	0.60
T	Kip-ft	20.15	34.4%	0.11
M2	**Kip-ft**	**1376.6**	63.4%	**1.24**
M3	Kip-ft	-503.8	49.7%	0.45

Table C.3 SDC B: 3-Span Bridge: **Column** Demand

		Peak Demand	% Increase from SDC A	D/C Ratio
Axial	Kip	-987.9	18.1%	0.07
V2	Kip	-843.0	73.9%	0.51
V3	**Kip**	**-276.3**	117%	**1.74**
T	Kip-ft	101.7	77.8%	0.53
M2	**Kip-ft**	**2930**	103%	**1.13**
M3	Kip-ft	-12460	78.0%	0.82

Nominal section capacities are not shown for components that are strongly influenced by fluctuating axial loads.

Table C.4 SDC B: 2-Span Bridge**: Bent Cap** Demand

		Peak Demand	% Increase from SDC A	Nominal Section Capacity	D/C
Axial	Kip	-643.1	52%	-9728.7	0.07
V2	Kip	385.8	26%	680.2	0.57
V3	Kip	82.5	92%	580.46	0.14
T	Kip-ft	700.2	131%	1145	0.61
M2	Kip-ft	393.2	99%	2322.5	0.17
M3	Kip-ft	-1274	36%	6404.43	0.20

Table C.5 SDC B: 3-Span Bridge**: Bent Cap** Demand

		Peak Demand	% Increase from SDC A	Nominal Section Capacity	D/C
Axial	Kip	-1014	52%	X,-10179	0.10
V2	Kip	583.7	26%	682.9	0.85
V3	Kip	-148.6	92%	1246	-0.12
T	**Kip-ft**	**1848**	131%	**876.1**	**2.11**
M2	Kip-ft	770.7	99%	3487	0.22
M3	Kip-ft	-3077	36%	2884	-1.07

Table C.6 SDC B: 2-Span Bridge**: Girder** Demand

		Peak Demand	% Increase from SDC A	Nominal Section Capacity	D/C
Axial	Kip	-959.4	12%	-3715.7	0.26
V2	Kip	-115.7	23%	712.59	0.16
V3	Kip	-7.21	29%	681.59	0.01
T	Kip-ft	17.0	33%	52	0.33
M2	Kip-ft	52.2	34%	233.36	0.22
M3	Kip-ft	-1216	15%	3734.89	0.33

Table C.7 SDC B: 3-Span Bridge**: Girder** Demand

		Peak Demand	% Increase from SDC A	Nominal Section Capacity	D/C

Axial	Kip	-948.7	29%	-3196.9	0.30
V2	Kip	-96.00	32%	1056.99	0.09
V3	Kip	-8.67	149%	671.67	0.01
T	Kip-ft	-4.69	104%	69.45	0.07
M2	**Kip-ft**	**-85.3**	165%	**67.37**	**1.27***
M3	Kip-ft	-1301	49%	5542.25	0.23

***It is unlikely that a significant compromise in structural integrity would result in this case. There are components of the superstructure such as the integral diaphragms between the girders that would increase the lateral moment (M2) capacity and were not included in the structural model.*

Table C.8 SDC B: 2-Span Bridge**: Integral Abutment** Demand

		Peak Demand	Nominal Section Capacity	D/C
Axial	Kip	-40.26	-7005.1	0.01
V2	Kip	84.49	659.1	0.13
V3	Kip	-157.2	448.9	0.35
T	**Kip-ft**	**-416.8**	**299.3**	**1.39**
M2	Kip-ft	277.2	2537.1	0.11
M3	Kip-ft	253.3	739.2	0.34

Table C.9 SDC B: 3-Span Bridge**: Integral Abutment** Demand

		Peak Demand	Nominal Section Capacity	D/C
Axial	Kip	-378.6	7549.9	0.05
V2	Kip	67.0	786.6	0.09
V3	Kip	-417.0	457.4	0.91
T	**Kip-ft**	**-2140**	**533.6**	**4.01**
M2	Kip-ft	-613.7	3327.5	0.18
M3	Kip-ft	267.2	637.9	0.42

With the increase in seismic excitation from the SDC B (SZ II) load case, the structural demand on the model increases significantly. The results exceed nominal capacities in shear and bending in the pier-columns, bent caps and girders. A large torsional demand is also observed on the integral abutment where damage is likely to occur. This is observed for both the 2 and 3-span bridge models. A suggestion for an improvement in cases where a Colorado bridge is exposed to either similar or higher seismic demand than imposed above, would be to implement bearing type supports. Allowing translation specifically in the longitudinal direction elongates the fundamental period and can dramatically reduce the excitation from seismic loads. In addition, it may be necessary to implement an Earthquake Resisting System (ERS) in the bridge, as discussed in the AASHTO Guide specifications. An ERS allows for concentrated yielding and energy dissipation to occur in targeted areas while maintain the structural integrity of the bridge. Further information on ERS details are provided in the AASHTO Guide Specifications.

C3. **Design Example No. 3: LRFD design specification and SZ II**

This design example is based on AASHTO LRFD Bridge Design Specifications – Customary U.S. Units (2012) a selected bridge in Seismic Zone (SZ) II.

The easiest way to maneuver through the bridge design specifications and complete a comprehensive seismic design is through the flow charts provided in Appendix A3 of the LRFD specification. The organization of Design Example 3 follows the structure of the flow chart.

C.3.1 *Earthquake Demand:*

C.3.1.1 **AASHTO Article 3.10 Earthquake Effects: EQ**

AASHTO Article 3.10.1 General

Applicability of the AASHTO Bridge Spec. to the seismic design of this bridge, along with supplemental information and is provided in this section

AASHTO Article 3.10.2 Seismic Hazard

> **Option 1:** Use the articles and procedures presented in AASHTO Articles *3.10.2-4,6* to develop a design response spectrum based on hazard maps, make adjustments with respect to soil condition, and determine seismic zone.
> **Option 2:** (Recommended) Use the USGS-AASHTO tool to determine the same parameters but through an automated process.

http://earthquake.usgs.gov/designmaps/us/application.php

Through Option 2, the following parameters were determined and can be used with the specifications in AASHTO Article *3.4.1-1* or taken directly from the USGS-AASHTO document to determine the design response spectrum:

Parameter	Value		
PGA	0.088g	$A_s = F_{PGA} * PGA$	0.219
S_s	0.117g	$S_{DS} = F_a * S_S$	0.443
S_1	0.045g	$S_{D1} = F_V * S_1$	0.156
F_{PGA}	2.50		
F_a	2.50		
F_v	3.50		

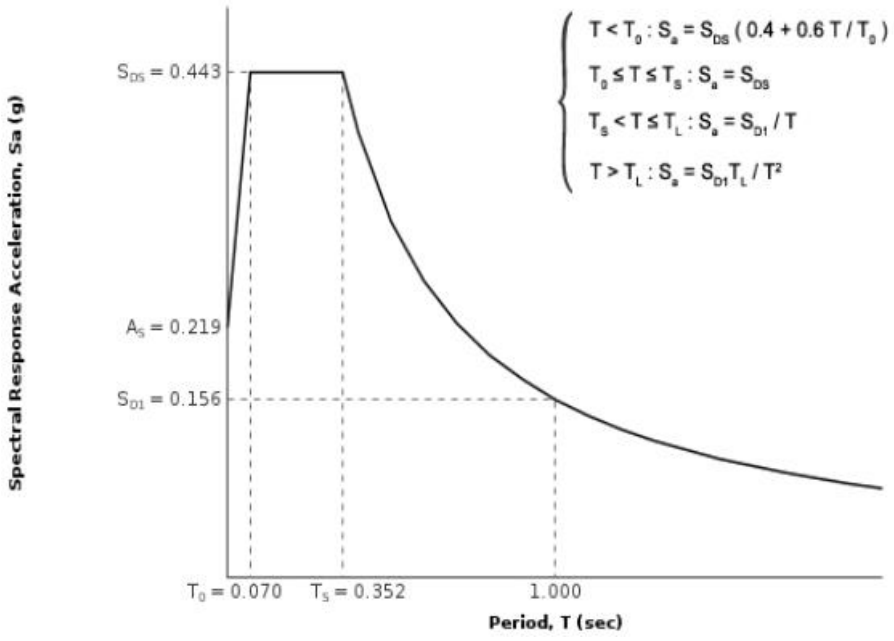

Figure C.6 – Origin: USGS – AASHTO 2011 Guide Spec. Seismic Hazard Tool

C.3.1.2 **AAHSTO Article 3.10.6 - Selection of Seismic Zone**

b. Utilize the specifications below and the S_{D1} parameter to determine the Seismic Design Category

Using the Seismic Hazard Parameters developed a DRS can be constructed and the Seismic Zone can be identified per Table 3.10.6-1

AASHTO Table 3.10.6-1 Seismic Zones

Acceleration Coefficient, S_{D1}	Seismic Zone
$S_{D1} \leq 0.15$	1
$0.15 < S_{D1} \leq 0.30$	2
$0.30 < S_{D1} \leq 0.50$	3
$0.50 < S_{D1} \leq$	4

$S_{D1} = 0.156 \geq 0.15$ which places the D-17-DJ bridge, for soft soil condition in Denver, Colorado, in Seismic Zone 2.

C.3.1.3 **AASHTO Article 3.10.5 Operational Classification**

"For the purpose of Article 3.10, the Owner or those having jurisdiction shall classify the bridge into one of three operational categories as follows:

i) Critical bridges
ii) Essential bridges, or
iii) Other bridges

For purposes of providing an example that is applicable to most designs, this bridge is designated as "Other" bridges

C.3.1.4 **AASHTO Article 3.10.7 Determine Response Modification Factors**

To apply the response modification factors, the structural details shall satisfy the provisions of Articles 5.10.2.2, 5.10.11, and 5.13.4.6.

AASHTO Table 3.10.7.1-1 Response Modification Factors Substructures

Substructure	Operational Category		
	Critical	Essential	Other
Wall-type piers-larger dimension	1.5	1.5	2.0
Reinforced concrete pile bents			
• Vertical piles only	1.5	2.0	3.0
• With Batter piles	1.5	1.5	2.0

Single Columns	1.5	2.0	3.0
Steel or composite steel and concrete pile bents • Vertical pile only • With batter piles	 1.5 1.5	 3.5 2.0	 5.0 3.0
Multiple column bents	1.5	3.5	3.0

It is evident that the substructure of the 3-span bridge has vertical steel piles (R = 5.0) supporting multiple concrete columns bents (R = 5.0).

AASHTO Table 3.10.7.1-2 Response Modification Factors – Connections

Connection	All Operation Categories
Superstructure to abutment	0.8
Expansion joints within a span of the superstructure	0.8
Columns, piers, or pile bents to cap beam or superstructure	1.0
Columns or piers to foundations	1.0

C.3.1.5 **Section 5: Concrete Structures**

C.3.1.5.1 **AASHTO Article 5.10.2.2 –Seismic Hooks (Section 5: Concrete Structures)**

"Seismic hooks shall consist of a 135 degree bend, plus an extension of not less than the larger of 6.0db or 3.0 in. Seismic hooks shall be used for transverse reinforcement in regions of expected plastic hinges. Such hooks and their required locations shall be detailed in the contract documents."

C.3.1.5.2 **AASHTO Article 5.10.11 Provisions for Seismic Design (Section 5: Concrete Structures)**

AASHTO Article 5.10.11.1 –General

Support length requirements as specified in Article 4.7.4.4 shall be met, otherwise longitudinal restrainers as specified in Article 3.10.9.5 shall be provided. The support length requirements are determined as follows:

$N = (8 + 0.02L + 0.08H)(1 + 0.000125S^2)$ (AASHTO 4.7.4.4-1)

where:

N = minimum support length measured normal to the centerline of bearing (in.)

L = length of the bridge deck to the adjacent expansion joint, or to the end of the bridge deck; for hinges within a span, L shall be the sum of the distances to either side of the hinge; for single-span bridges, L equals the length of the bridge deck (ft)

H = for abutments, average height of columns supporting the bridge deck from the abutment to the next expansion joint (ft).
for columns and/or piers, column, or pier height (ft)
for hinges within a span, average height of the adjacent two columns or piers (ft)

S = skew of support measured from line normal to span (degrees)

For the three-span bridge, the required bearing length calculated in accordance with AASHTO Eqn. 4.7.4.4.1 is:

$N = \left[8 + 0.02(169.4) + 0.08(14.25)\right]\left[1 + 0.000125(45)^2\right] = 15.7 \text{ in.} \approx 16 \text{ in.} < 20 \text{ in. OK}$

Therefore, no restrainers are required.

For the two-span bridge, the required bearing length is:

$N = \left[8 + 0.02(145.5) + 0.08(12.75)\right]\left[1 + 0.000125(40)^2\right] = 14.3 \text{ in.} \approx 15 \text{ in.} < 18 \text{ in. OK}$

Therefore, no restrainers are required.

Bridge structures located in SZ 2 shall also satisfy the requirements of **AASHTO Article 5.10.11.3.**

C.3.1.5.2 **AASHTO Article 5.10.11.3 – Seismic Zone 2**

"The requirements of Article 5.10.11.4 shall be taken to apply to bridges in SZ 2 except that the area of longitudinal reinforcement shall not be less than 0.01 or more than 0.06 times the gross cross-section area, A_g."

AASHTO Article 5.10.11.4.1 – Column Requirements

This article allows columns to be considered as piers for analysis and design if the ratio of the clear height to the maximum plan dimension of the support is less than 2.5.

For the three-span bridge, the columns are 24 in. x 144 in. x 14.7 ft. high.
The minimum ratio is 14.7/12 = 1.23 <2.5, thus, for design, these columns shall be considered as piers for the long direction and columns for the short direction.

For the two-span bridge, the columns are 24 in. diameter x 13.08 ft. high.
The ratio is 13.08/2 = 6.5>2.5, thus these supports shall be considered as columns for design.

C.3.2 *Flexible Resistance:*

AASHTO Article 5.10.11.4.1b Flexural Resistance

According to this section, biaxial strength in flexure should not to be taken as less than specified in **AASHTO Article 3.10.9.4**, however, this is contradicted by **AASHTO Article 3.10.9.3 – Seismic Zone 2**, which indicates that the appropriate response modification factor, *R*, be used. Thus, it seems logical that the biaxial strength should be evaluated based on the latter in accordance with **AASHTO Article 3.10.8.** Review of **AASHTO commentary C3.10.9.3** recommends that foundations of critical and essential bridges in SZ 2 use forces determined in **AASHTO Article 3.10.9.4.3f**; however, both bridges have been considered to be "Other Bridges" and thus AASHTO Article 3.10.9.3 shall be used for calculation of design forces, which "shall be determined by dividing the elastic seismic forces obtained from AASHTO Article 3.10.8 by the appropriate response modification factor, *R*, specified in AASHTO Table 3.10.7.10.1"; in this case, *R* = 5.0 (multiple column bents, other).

For the extreme event limit state (earthquake), resistance factors as dictated in **AASHTO Article 5.5.4.2** for columns shall be 0.9 for columns with either spiral or tie reinforcement.

C.3.3 *Column shear and transverse reinforcement:*

AASHTO Article 5.10.11.4.1c Column Shear and Transverse Reinforcement

Factored shear force, V_u, in each principal axis and pile bent shall be determined using **AASHTO Article 3.10.9.4** and, specifically, AASHTO Article 3.10.9.4.3c as it regards determination of elastic hinging forces, as follows:

The steps involved in the determination of forces at the pier bents are presented in the following paragraphs. Note that the force effects must not only be determined in the plane of the bent, but also perpendicular to the plane of the bent (AASHTO Table 3.10.7.1-1)

The following procedure is for a two column bent:

Step 1

Determine the column overstrength resistances (AASHTO Table 3.10.7.1-1). Resistance factor, $\phi = 1.3$ for reinforced concrete. The overstrength moment, $M_{os} = 1.3\ M_n$.

Step 2

Determine the column overstrength shear forces (V_{os}) based on the overstrength moment determined in step 1, $V_{os} = M_{os} / L_{col} = 1.3M_n/L_{col}$, where L_{col} = Column length.

Step 3

Apply V_{os} to the center of the mass of the superstructure above the pier and determine the corresponding axial forces in the pier. For two columns, $A_{os} = V_{os}/S_{col}(L_{col})$, where A_{os} = overstrength axial load and L_{col} = column length.

Step 4

Use A_{os} determined in step 3 as EQ in the Extreme Event Load Combination I to determine the revised column moment overstrength resistance. On the basis of the revised moment resistance calculate the column shear forces and the maximum shear force for the bent. If the maximum

shear force is not within 10% of the value determined in Step 2, return to Step 3 with maximum shear force and repeat Steps 3 and 4.

The forces in the individual columns in the plane of a bent corresponding to column hinging shall be taken as:

- "Axial Forces – The maximum and minimum axial loads determined using Extreme Event Load Combination I, with the axial load determined from the final iteration of Step 3 taken as *EQ* and treated as plus and minus.
- Moments – The column overstrength moment resistances corresponding to the maximum compressive axial load specified above.
- Shear Force – The shear force corresponding to the column overstrength moment resistances specified above, noting the provisions in Step 2 above"

Transverse reinforcement should not less than specified in **AASHTO Article 5.8.3.**

Specific to end regions V_c should be taken per the requirements in **AASHTO Article 5.8.3** unless axial force component < $0.1f'_c*A_g$. Here V_c shall decrease linearly to zero with zero compression force.

The end regions (top and bottom) shall be taken as the greater of: 18", diameter of the column, and maximum cross section of column.

AASHTO Article 5.11.4.1d Transverse Reinforcement for Confinement at Plastic Hinges

Rectangular columns shall satisfy in each principal direction:

$$A_{sh} \geq 0.30s\, h_c \frac{f'_c}{f_y}[\frac{A_g}{A_c} - 1]$$

Or

$$A_{sh} \geq 0.12s\, h_c \frac{f_c'}{f_y}$$

where:

A_{sh} = total cross-sectional area of tie reinforcement, including supplementary cross-ties having a vertical spacing of s and crossing a section having a core dimension of h_c.

s = vertical spacing of hoops, not exceeding 4.0 in.

h_c = core dimension of tied column in direction of consideration

f'_c = 28 day compressive strength

f_y = yield strength of reinforcing bars

A_c= area of column core

A_g = gross area of column

All cross-ties shall have seismic hooks as specified in Article 5.10.2.2

AASHTO Article 5.10.11.4.1e – Spacing of Transverse Reinforcement for Confinement

Short provisions on minimum detailing requirements for transverse reinforcement are provided in this section.

AASHTO 5.10.11.4.1f – Splices

Provisions for splice lengths types are provided in this section.

C.3.4 *Column reinforcement design:*

The column and resultant factored forces for the 3-span bridge are shown in Figure . The columns are 12'-0" long and 2'-0" wide. For preliminary purposes, the following assumptions are made:

Reinforcing clear distance = 2 in.

Vertical bars = 28 - #10

Ties = #5@16

Vertical cross ties = #5@16

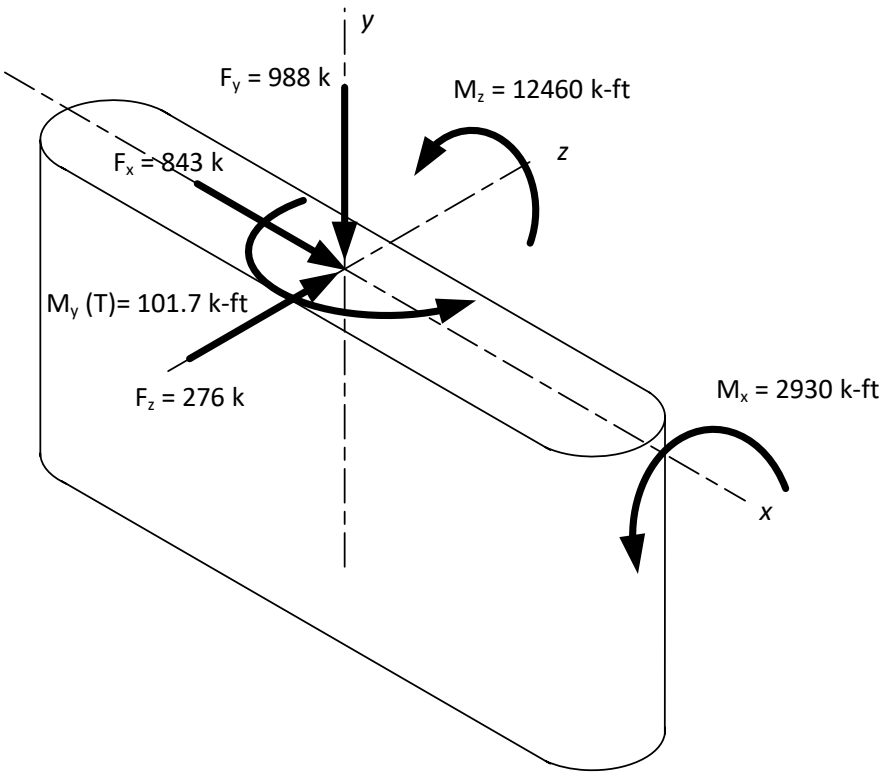

Figure C.7 - Resultant Factored Column Forces

Design and details of the column/pier reinforcing and shown following:

AASHTO 3.10.

This article specifies that for bending, two load cases must be considered based on combinations as follows:

- "100 percent of the absolute value of the force effects in one of the perpendicular directions combined with 30 percent of the absolute value of the force effects in the second perpendicular direction
- 100 percent of the absolute value of the force effects in the second perpendicular direction combined with 30 percent of the absolute value of the force effects in the first perpendicular direction.

When column connection forces are determined with plastic hinging of the column connection occurring, the resulting force effects may be considered individually without consideration of the combined effects above.

In this example these two load combinations become:

Case 1.

$M_x = 2{,}930$ k-ft

$M_z = 0.3(12{,}460 \text{ k-ft}) = 3{,}738$ k-ft

Case 2

$M_x = 0.3(2{,}930 \text{ k-ft}) = 879$ k-ft

$M_z = 12{,}460$ k-ft

The design of the bending reinforcing would determine the required size and spacing of bars on the longitudinal faces and at the ends to resist both cases.

AASHTO Article 5.8.3 – Sectional Design Model

This article discusses shear design where permitted in accordance with the provisions of AASHTO Article 5.8.1.

AASHTO Article 5.8.3.3 – Nominal Shear Resistance

Nominal shear resistance V_n, shall be the lesser of the following, which are modified for this example :

$V = V_c + V_s$ (AASHTO 5.8.3.3-1)

$V_n = 0.25 f_c' b_v d_v$ (AASHTO 5.8.3.3-2)

$V_c = 0.0316 \beta \sqrt{f_c'} b_v d_v$

$$V_s = \frac{A_v f_y d_v (\cot\theta + \cot\alpha)\sin\alpha}{s}$$

Where variables used are defined in AASHTO Article 5.8.3.3

AASHTO Article 5.8.6.3 – Regions Requiring Consideration of Torsional Effects

Torsional effects need not be investigated if

$T_u \le 1/3\phi T_{cr}$ (5.8.6.3-1)

in which:

$T_{cr} = 0.0632K\sqrt{f_c'}\,2A_o b_e$ (5.8.6.3-2)

$K = \sqrt{1 + \dfrac{f_{pc}}{00632\sqrt{f_c'}}} \le 2.0$ (5.8.6.3-3)

where:

$T_u =$ factored torsional moment (kip-in.)

$T_{cr} =$ torsional cracking moment (kip-in.)

$K =$ stress variable K shall not be taken greater than 1.0 for any section where the stress in the extreme tension fiber, calculated on the basis of gross section properties, due to factored load and effective prestress force after losses exceeds $0.18\sqrt{f_c'}$ in tension

$A_0 =$ area enclosed by the shear flow path of a closed box section, including any holes theein (in.^{2})

$b_e =$ effective width of the shear flow path, but not exceeding the minimum thickness of the webs or flanges comprising the closed box section (in.). b_e shall be adjusted to account for the presence of ducts

$p_c =$ the length of the outside perimeter of the concrete section (in.)

$f_{pc} =$ unfactored compressive stress in concrete after prestress losses have occurred

$\phi =$ resistance factor for shear specified in AAHSTO Article 5.5.4.2

For the bridge being considered, the values of the variables are as follows:

$T_u = M_y = 101.7$ k-ft. = 1220 k-in.

$f_c' = 4.50$ ksi

$K = \sqrt{1 + \dfrac{0}{0.0632\sqrt{f_c'}}} = 1.0 \le 1.0$ Okay

$A_o = 2[120 \text{ in.}(24 \text{ in.}) + 2(12 \text{ in.})^2 p/2] = 6665 \text{ in.}^2$

$b_e = 24$ in.

$f_{pc} = 0$

$f = 0.90$

$fT_{cr} = 0.90[0632(1.0)\sqrt{4.5}(2)(6665)(24)] = 38{,}600$ k-in

On the basis of the preceding:

$1/3\phi T_{cr} = 0.9(38,600)/3 = 11,580$ k-in.

$T_u = 1220$ k-in.<11,580 k-in., Okay

Thus, torsional effects need not be investigated.

C.3.5 *Seismic design load calculation:*

AASHTO Article 4.7.4.3 Multispan Bridges

For Seismic Zone II, either a single-mode or uniform load method may be applied to other regular bridges. The requirements for geometries of regular bridges are specified in AASHTO Table 4.7.4.3.1-2.

AASHTO Table 4.7.4.3.1-2 Regular Bridge Requirements

Parameter	Value				
Number of Spans	2	3	4	5	6
Maximum subtended angle for a curved bridge	90^0	90^0	90^0	90^0	90^0
Maximum span length ratio from span to span	3	2	2	1.5	1.5
Maximum bent/pier stiffness ratio from span to span excluding abutments	-	4	4	3	2

The subtended angle for all geometries evaluated of the D-17-DJ bridge ≤ 4.6 deg.

The span to length ratio: 29.5/22.1m = 1.33

The piers at all supports are the same dimensions and thus will have the same cross section properties ergo the pier stiffness ratio from span-to-span: 1:1

D-17-DJ bridges meet all requirements for regular bridges; and a Single-Mode Spectral Method is selected for analysis. The guidelines for the analysis methods are presented in the remaining sections of 4.7.4.3. The spectral method and other analysis methods are presented in 4.7.4.3.2-4.

C.3.5.1 **AASHTO Article 4.7.4.3.2b Single Mode Spectral Method**

I. LONGITUDINAL RESPONSE

1. Calculate the static displacements $v_s(x)$ due to an assumed uniform loading p_o

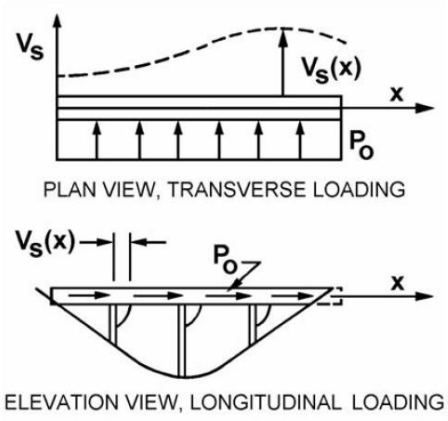

$$\alpha = \int v_s(x)dx\ (ft.^2)$$

(area under the deflection curve)

$$\beta = \int w(x)v_s(x)dx(k - ft.)$$

(area under the deflection curve x weight curve)

$$\gamma = \int w(x)v_s^2(x)dx\ (k - ft^2)$$

(area under the deflection curve squared x weight curve)

where:

p_o = arbitrary uniform load equal to 1.0 kip/ft

$v_s(x)$ = deformation corresponding to p_o (ft)

$w(x)$ = nominal, unfactored dead load of the bridge superstructure and tributary substructure

Using the SAP2000 structural model, a 1 kip/ft load is applied in the longitudinal direction.

$v_s(x)$ *=0 .0019 ft*

L = 241' 8"

w(x)= 16.26 kip/ft

$$\alpha = \int_0^{241.667\ ft} 0.0019\ (ft)\ dx$$

$$\alpha = 0.45917\ ft^2$$

$$\beta = \int w(x) v_s(x) dx$$

$$\beta = \int_0^{241.667\ ft} 16.256\ kip/ft\ * 0.0019\ (ft) dx$$

$$\beta = 7.464\ (kip - ft)$$

$$\gamma = \int w(x) v_s^2(x) dx$$

$$\gamma = \int_0^{241.667\ ft} 16.256\ kip/ft * (0.0019)^2\ dx$$

$$\gamma = 0.01418(kip - ft^2)$$

$$T_m = 2\pi \sqrt{\frac{\gamma}{P_o g \alpha}}$$

$$T_m = 2\pi \sqrt{\frac{0.01418}{1 * 32.17 * 0.45917}}$$

$$T_m = 0.195\ seconds$$

This period matches the estimated period generated in SAP2000.

T_m = period of vibration of the mth mode (sec.)

C_{sm} = dimensionless elastic seismic resonance coefficient (3.10.6.1-1)

T_m= period of vibration of mth modes (s) = 0.195 sec

T_0 = reference period used to define spectral shape

$T_0 = 0.2\ T_s\ (s) = 0.070$

Calculate C_{sm} using the 3.10.4.2-4 since $T_m > T_0 = 0.070$ sec. and $T_m \leq T_S = 0.352$ sec. (on linear portion of spectrum)

$$C_{sm} = S_{DS} = 0.443$$

T_s = corner period at which spectrum changes from being independent of period to being inversely proportional to period

$$p_e(x) = \frac{\beta C_{sm}}{\gamma} w(x) v_s(x)$$

$$p_e(x) = \frac{7.464 * 0.443}{0.01418} * 16.256 * 0.0019$$

$$\boldsymbol{p_e(x) = 7.20\ (kips/ft)}$$

The resultant loading can be applied to the structural model and yield the seismic response.

II. TRANSVERSE RESPONSE

Calculate the static displacements $v_s(x)$ due to an assumed uniform loading p_o

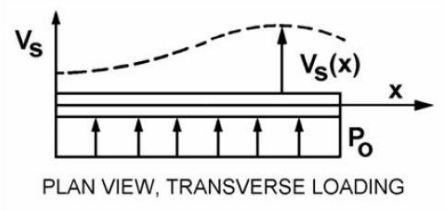

PLAN VIEW, TRANSVERSE LOADING

$$\alpha = \int v_s(x) dx$$

$$\beta = \int w(x) v_s(x) dx$$

$$\gamma = \int w(x) v_s^2(x) dx$$

$v_s(x)$ *=0 .0015 ft*

L = 241.667 ft

w(x)= 16.256 kip/ft

$$\alpha = \int_0^{241.667\ ft} 0.0015\ (ft)\ dx$$

$$\alpha = 0.363\ ft^2$$

$$\beta = \int w(x) v_s(x) dx$$

$$\beta = \int_0^{241.667\ ft} 16.256\ kip/ft\ * 0.0015\ (ft) dx$$

$$\beta = 5.893\ (kip - ft)$$

$$\gamma = \int w(x) v_s^2(x) dx$$

$$\gamma = \int_0^{241.667\ ft} 16.256\ kip/ft * (0.015)^2\ dx$$

$$\gamma = 0.00884(kip - ft^2)$$

$$T_m = 2\pi \sqrt{\frac{\gamma}{P_o g \alpha}}$$

$$T_m = 2\pi \sqrt{\frac{0.00884}{1 * 32.17 * 0.363}}$$

$$T_m = 0.173\ seconds$$

Actual modal period accounting for 60% transverse mass participation is 0.128 sec from SAP2000.

Calculate C_{sm} using the 3.10.4.2-4 since $T_m > T_0$ and $T_m \leq T_S$ (on linear portion of spectrum)

$$C_{sm} = S_{DS} = 0.443$$

$$p_e(x) = \frac{\beta C_{sm}}{\gamma} w(x) v_s(x)$$

$$p_e(x) = \frac{5.893 \ * 0.443}{0.00884} * 16.256 * 0.0015$$

$$\boldsymbol{p_e(x) = 7.20(kips/ft)}$$

The resultant loading can be applied to the structural model and yield the structural response.

C.3.5.2 **AASHTO Article 3.10.9.3 – Seismic Zone 2**

This section states "Structures in Seismic Zone 2 shall be analyzed according to the minimum requirements specified in Articles 4.7.4.1 and 4.7.4.3. Except for foundations (AASHTO Article 3.10.9.3), seismic design forces for all components, including pile bents and retaining walls, shall be determined by dividing the elastic seismic forces, obtained from Article 3.10.8, by the appropriate response modification factor, R, specified in Table 3.10.7.1-1.

C.3.6 *Seismic force combination:*

AASHTO Article 3.10.8 Combination of Seismic Force Effects

The specifications require two separate load cases to account for the uncertainty of the EQ direction:

Load Case 1: "100 percent of the absolute value of the force effects in one of the perpendicular directions combined with 30 percent of the absolute value of the force effects in the second perpendicular direction."

Load Case 1: $p_e(x)$ (longitudinal) applied 100% = 7.20 kips/ft

$p_e(x)$ (transverse) applied 30% = 2.16 kips/ft

Load Case 2: "100 percent of the absolute value of the force effects in the second perpendicular directions combined with 30 percent of the absolute value of the force effects in the first perpendicular direction."

Load Case 2 $p_e(x)$ (longitudinal) applied 30% = 2.16 kips/ft

$p_e(x)$ (transverse) applied 100% = 7.20 kips/ft

The loading developed is then applied to the structural model and evaluated using resistance factors and elastic response factors to verify capacities of the bridge structural elements.

C.3.7 *Minimum support length:*

AASHTO Article 4.7.4.4 – Minimum Support Length Requirements

The minimum support length to accommodate displacements is specified in *Article 4.7.4.4*. These specifications typically apply to bridges in SDC B; however the bridges analyzed in this scenario are integral abutment type and have integrally restrained displacement.

C.3.8 *Foundation:*

Foundations (AASHTO Section 10)

Foundations were not included in this design example. However the following sections are useful in aiding the seismic design portion if needed.

Settlement: 10.5.2.4 & 10.6.2.4

Battered Piles: 10.7.1.4

Concrete shafts and Piles: 10.5.2.4, 10.8.3.9.4 & 5.13.4.6

C.3.9 *Abutment and piers:*

Abutments, Piers and Walls (AASHTO Section 11)

AASHTO Article 11.6.5 covers seismic design for abutments and conventional retaining walls, however the abutments for the subject bridge are supported by piles and thus, non-conventional requiring advanced analysis, which is beyond the scope of this study.

C4. **Design Example No. 4: Guide specification and SDC B**

This design example is based on AASHTO Guide Specifications for LRFD Seismic Bridge Design 2nd Edition (2011)

The design example presented below utilizes the AASHTO Guide Specifications for seismic design and analysis of a select bridge in Seismic Design Category (SDC) B. The example is not comprehensive of all SDC B bridge design requirements and rather supplies only a guideline for a select seismic bridge design. The organization of Design Example No. 4 follows the structure of the flow chart. The bridges to which the GS are applicable are discussed in AASHTO GS Article 3.1.

C.4.1 *Earthquake Demand:*

C4.1.1 **AASHTO GS Article 3.4 - Seismic Ground Shaking Hazard**

Option 1: Use the articles and procedures presented in *3.4 Seismic Ground Shaking Hazard* to develop a design response spectrum based on hazard maps, and make adjustments with respect to the soil condition.

Option 2: (Recommended) Use the USGS-AASHTO tool to determine the same parameters but through an automated process.

http://earthquake.usgs.gov/designmaps/us/application.php

Through Option 2 the following parameters were determined and can be used with the specifications in **AASHTO GS Article 3.4.1-1** or taken directly from the USGS-AASHTO document to determine the design response spectrum:

Parameter	Value		
PGA	0.088g	$A_s = F_{PGA} * PGA$	0.219
S_s	0.117g	$S_{DS} = F_a * S_S$	0.443
S_1	0.045g	$S_{D1} = F_V * S_1$	0.156
F_{PGA}	2.50		
F_a	2.50		
F_v	3.50		

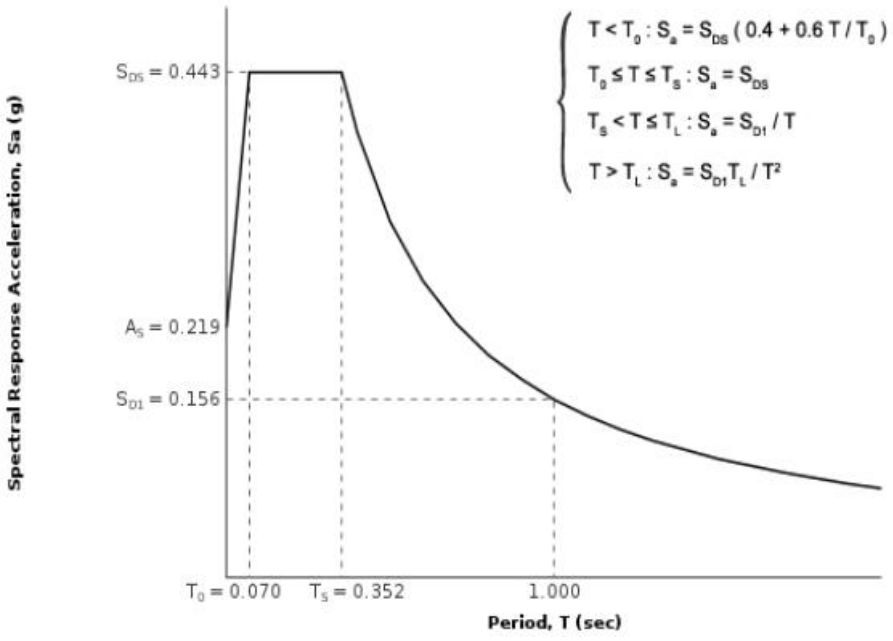

Figure C.8 Design response spectrum – Origin: USGS – AASHTO 2011 Guide Spec. Seismic Hazard Tool

C4.1.2 **AASHTO Article GS 3.5- Selection of Seismic Design Category (SDC)**

c. Utilize the specifications below and the S_{D1} parameter to determine the Seismic Design Category

AASHTO GS Table 3.5.1 - Partitions for Seismic Design Categories A, B, C, and D

Value of $S_{D1} = F_v S_1$	SDC
$S_{D1} < 0.15$	A
$0.15 \leq S_{D1} < 0.30$	B
$0.30 \leq S_{D1} < 0.50$	C
$0.50 \leq S_{D1}$	D

Based on the S_{D1} = 0.156 developed in the previous step, the Seismic Design Category is determined as category B. A review of the generalized requirements for each step is shown below.

SDC B Requirements taken from **AASHTO GS Article 3.6** – Selection of Seismic Design Category (SDC)

g. Identification of ERS according to Article 3.3 should be considered
h. Demand analysis
i. Implicit capacity check required (displacement, P-Δ, support length)
j. Capacity design should be considered for column shear; checks should be considered to avoid weak links in the ERS
k. SDC B level of detailing
l. Liquefaction check should be considered for certain conditions

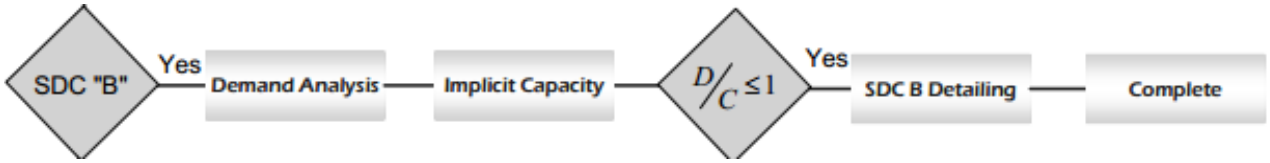

Figure C.9 AASHTO Bridge Spec. General Requirements

C4.1.3 **AASHTO GS Article 3.3 - Earthquake-Resisting Systems (ERS) Requirements for SDCSs C and D**

"For SDC C or D (see AASHTO GS Article 3.5), all bridges and their foundations shall have a clearly identifiable earthquake resisting system (ERS) selected to achieve the life safety criteria defined in AASHTO GS Article 3.2. For SDC B, identification of an ERS should be considered."

AASHTO GS Commentary C.3.3

"For SDC B, it is suggested that the ERS be identified. The displacement checks for SDC B are predicated on the existence of a complete lateral load resisting system; thus, the Designer should ensure that an ERS is present and that no unintentional weak links exist. Additionally, identifying the ERS helps the Designer ensure that the model used to determine displacement demands is compatible with the drift limit calculation."

C4.1.4 **AASHTO GS Article 4.2 –Selection of Analysis Procedure to Determine Seismic Demand**

To determine the seismic demands, the minimum analysis requirements are determined through AASHTO GS Section 4.2 and through use of the tables shown below.

For the D-17-DJ Bridge, the following specifications are determined:

AASHTO GS Table 4.2-1 Analysis Procedures

Seismic Design Category	Regular Bridges with 2 through 6 Spans	Not Regular Bridges with 2 or More Spans
A	Not required	Not required
B, C, or D	Use Procedure 1 or 2	Use Procedure 2

AASHTO GS Table 4.2-2 Description of Analysis Procedures

Procedure Number	Description	Article
1	Equivalent static	5.4.2
2	Elastic dynamic analysis	5.4.3
3	Nonlinear time history	5.4.4

The requirements for geometries of regular bridges are specified in Table 4.2.3.

AASHTO GS Table 4.2-3 Requirements for Regular Bridges

Parameter	Value				
Number of Spans	2	3	4	5	6
Maximum subtended angle (cur ed bridge)	30º	30º	30º	30º	30º
Maximum span length ratio from span-to-span	3	2	2	1.5	1.5
Maximum bent/pier stiffness ratio from span-to-span excluding abutments)	—	4	4	3	2

The maximum subtended angle for the three span bridge may be determined by using the smallest bridge radius, 3000 ft. The chord length of the bridge and the radial length of the bridge may be considered approximately equal for the determination of the subtended angle, thus, based on the equation for angle from chord length, $A = 180^o(\text{arc length})/(\pi r)$. Based on a radius of 3000 ft., which will provide the largest angle, and an arc length of 241'-8" (241.67 ft.), the subtended angle is 4.6º. All other subtended angles will be smaller due to the larger radii.

To determine the maximum span length ratio from span to span, an end span, $L = 72.6$ ft. and the center span, $L = 96.7$ ft. of the three span bridge are considered. The span length ratio then becomes $96.7 \text{ ft.}/72.6 \text{ ft.} = 1.33$. All piers for the bridge are identical, thus, the bent/pier stiffness ratio is 1.33. D-17-DJ bridges meet all requirements for regular bridges, thus analysis Procedure 1 may be used, which involves Equivalent Static Analysis per section 5.4.3.

C4.1.5 **AASHTO GS Article 4.3.2 - Displacement Modification for Other than Five Percent Damped Bridges**

A list of criteria herein is provided for using alternative damping ratios.

AASHTO GS Article 4.3.3 - Displacement Magnification for Short-Period Bridges

$$R_d = \left(1 - \frac{1}{\mu_D}\right)\frac{T*}{T} + \frac{1}{\mu_D} \geq 1.0 \text{ for } \frac{T^*}{\mathrm{T}} > 1$$

$$R_d = 1.0\ for\ \frac{T^*}{\mathrm{T}} \leq 1.0$$

In which $T^* = 1.25T_s$

where:

μ_D= maximum local member displacement ductility demand

= 2 for SDC B

T_s = period determined from Article 3.4.1 (sec.)

$T_s = S_{D1}/S_{DS}$ (s) = 0.156/0.443 = 0.352

$T^* = 1.25T_s = 1.25*.352 = 0.44$

The fundamental period may be developed using analysis procedures in **AASHTO GS Article 5.4.3** (shown below) or developed from the model. Using the numerical model developed, the fundamental period is found to be T= 0.195

T*/T = 0.44/.195 = 2.26

$$R_d = \left(1 - \frac{1}{\mu_D}\right)\frac{T*}{T} + \frac{1}{\mu_D} \geq 1.0 \text{ for } \frac{T^*}{\mathrm{T}} > 1$$

$$R_d = \left(1 - \frac{1}{2}\right)2.2 + \frac{1}{2}$$

$$R_d = 1.6$$

C4.2 Seismic load analysis

AASHTO GS Article 5.4.3 – Procedure 1: Equivalent Static Analysis (ESA)

ESA should be considered to estimate displacement demands for structures where a more involved dynamic analyses will not provide additional information or insight on the performance of the bridge. Per the **AASHTO GS Commentary C5.4.2**, "Long bridges, or those with significant skew or horizontal curvature, have dynamic characteristics that should be assessed using multimode dynamic analyses."

Acceptable methods for ESA are the following:

A. Uniform Load Method – This method is based on calculating the longitudinal or transverse fundamental period of vibration, through a simplified representation of the bridge using a single spring and mass oscillator. The spring stiffness is found by applying an arbitrary uniform load and obtaining the corresponding maximum displacement. Per the commentary, the method is best suited for bridges that respond in their principally in their fundamental period of vibration. Displacements are estimated with reasonable accuracy, but can overstate transverse shear in the abutments by up to 100 percent. Consequently the columns may have inadequate lateral strength.

   Procedure: Found in AASHTO GS C5.4.2

B. Single-mode Spectral Analysis Method (Recommended) – This method is similarly based on longitudinal or transverse fundamental mode of vibration. The mode shape is developed by applying of a uniform horizontal load and calculating the resultant deformed shape. The natural period of vibration is subsequently obtained by equating maximum potential and kinetic energy. This method is recommended to avoid an improbable redistribution of seismic demand.

   Procedure: Found in AASHTO Bridge Spec. Article 4.7.4.3.2b

Examples of application AASHTO (1983) and ATC(1981)

C4.2.1 **AASHTO Article 4.7.4.3.2b Single Mode Spectral Method**

III. LONGITUDINAL RESPONSE

2. Calculate the static displacements $v_s(x)$ due to an assumed uniform loading p_o

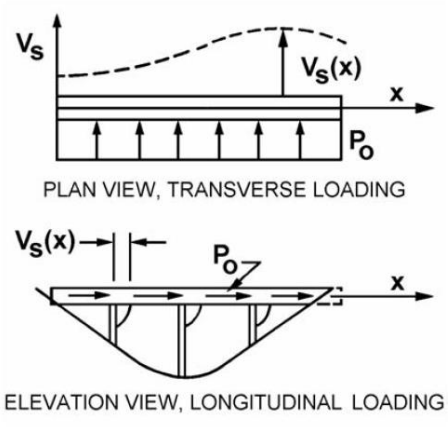

$$\alpha = \int v_s(x)dx \ (mm^2)$$

$$\beta = \int w(x)v_s(x)dx(N - mm)$$

$$\gamma = \int w(x)v_s^2(x)dx \ (N - mm^2)$$

where:

p_o = arbitrary uniform load equal to 1.0 kip/ft

$v_s(x)$ = deformation corresponding to p_o (ft)

$w(x)$ = nominal, unfactored dead load of the bridge superstructure and tributary substructure

Using the SAP2000 structural model, a 1 kip/ft load is applied in the longitudinal direction.

$v_s(x)$ =0 .0019 ft.

L = 241' 8"

w(x)= 16.26 kip/ft.

$$\alpha = \int_0^{241.667\ ft} 0.0019\ (ft)\ dx$$

$$\alpha = 0.45917\ ft^2$$

$$\beta = \int w(x) v_s(x) dx$$

$$\beta = \int_0^{241.667\ ft} 16.256\ kip/ft\ * 0.0019\ (ft) dx$$

$$\beta = 7.464\ (kip - ft)$$

$$\gamma = \int w(x) v_s^2(x) dx$$

$$\gamma = \int_0^{241.667\ ft} 16.256\ kip/ft * (0.0019)^2\ dx$$

$$\gamma = 0.01418(kip - ft^2)$$

$$T_m = 2\pi \sqrt{\frac{\gamma}{P_o g \alpha}}$$

$$T_m = 2\pi \sqrt{\frac{0.01418}{1 * 32.17 * 0.45917}}$$

$$T_m = \ 0.195\ seconds$$

This period matches the estimated period generated in SAP2000.

T_m = period of vibration of the mth mode (sec.)

Calculate C_{sm} using AASHTO equation 3.10.4.2-4 since

$T_m > T_0$ = 0.070 sec. and $T_m \le T_S = 0.352$ sec. (on linear portion of spectrum)

$$C_{sm} = S_{DS} = 0.443$$

C_{sm} = dimensionless elastic seismic resonance coefficient

T_m= period of vibration of mth modes (s) = 0.195 sec

T_0 = reference period used to defined spectral shape

$T_0 = 0.2\ T_s$ (s) = 0.070

T_s = corner period at which spectrum changes from being independent of period to being inversely proportional to period

$T_s = S_{D1}/S_{DS}$ (s) = 0.156/0.443 = 0.352

$$C_{sm} = 0.30$$

$$p_e(x) = \frac{\beta C_{sm}}{\gamma} w(x) v_s(x)$$

$$p_e(x) = \frac{7.464 * 0.443}{0.01418} * 16.256 * 0.0019$$

$$\boldsymbol{p_e(x) = 7.20\ (kips/ft)}$$

The resultant loading can be applied to the structural model and yield the seismic response.

IV. TRANSVERSE RESPONSE

Calculate the static displacements $v_s(x)$ due to an assumed uniform loading p_o

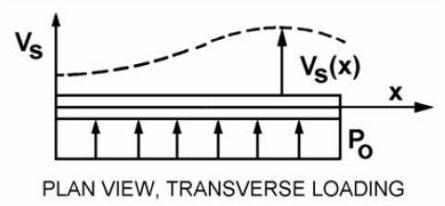

PLAN VIEW, TRANSVERSE LOADING

$$\alpha = \int v_s(x) dx\ (mm^2)$$

$$\beta = \int w(x) v_s(x) dx (N - mm)$$

$$\gamma = \int w(x) v_s^2(x) dx\ (N - mm^2)$$

$v_s(x)$ =0 .0015 ft

L = 241.667 ft

w(x)= 16.256 kip/ft

$$\alpha = \int_0^{241.667\ ft} 0.0015\ (ft)\ dx$$

$$\alpha = 0.363\ ft^2$$

$$\beta = \int w(x) v_s(x) dx$$

$$\beta = \int_0^{241.667\ ft} 16.256\ kip/ft\ * 0.0015\ (ft) dx$$

$$\beta = 5.893\ (kip - ft)$$

$$\gamma = \int w(x) v_s^2(x) dx$$

$$\gamma = \int_0^{241.667\ ft} 16.256\ kip/ft * (0.015)^2\ dx$$

$$\gamma = 0.00884(kip - ft^2)$$

$$T_m = 2\pi \sqrt{\frac{\gamma}{P_o g \alpha}}$$

$$T_m = 2\pi \sqrt{\frac{0.00884}{1 * 32.17 * 0.363}}$$

$$T_m = 0.173\ seconds$$

Actual modal period accounting for 60% transverse participation is 0.128 sec from SAP2000.

Calculate C_{sm} using the 3.10.4.2-4 since $T_m > T_0 = 0.070$ sec. and $T_m \leq T_S = 0.352$ sec. (on linear portion of spectrum)

$$C_{sm} = S_{DS} = 0.443$$

$$p_e(x) = \frac{\beta C_{sm}}{\gamma} w(x) v_s(x)$$

$$p_e(x) = \frac{5.893 \ * 0.443}{0.00884} * 16.256 * 0.0015$$

$$\boldsymbol{p_e(x) = 7.20(kips/ft)}$$

The resultant loading can be applied to the structural model and yield the structural response.

AASHTO Figure C4.7.4.3.2b-1 Bridge Deck Subjected to Assumed Transverse and Longitudinal Loading

C4.2.2 **Multimode Dynamic Analysis** (Recommended for large skew angles and high curvatures)

This method can be used to estimate displacement demands where ESA is considered inadequate. A multi modal spectral analysis can be performed on a numerical (FE) model using the demand obtained from an appropriate response spectrum (5 percent damping should be used). Further details on the procedure can be obtained in section 5.4.3 and the Commentary included. For development of the numerical model, specifications are provided in "5.5 - Mathematical Modeling Using EDA (Procedure 2)" and "5.6-Effective Section Properties". These guidelines include improvements to the structural model, as to assimilate a near as possible representation of the bridge response using a linear elastic analysis.

For development of a mathematical model: effective section properties can be found in Article 5.6, modeling provisions can be found on abutments in Articles 5.3 and foundations 6.8 (if liquefaction is present) and guidelines for the global model can be found in article 5.1.2.

C4.2.3 **AASHTO GS Article 4.4 - Combination of Orthogonal Seismic Displacement Demands**

Per the specifications two load cases are formulated including:

Load Case 1: 100 (%) of the absolute value of the seismic displacements resulting from the analysis of the longitudinal direction plus 30 (%) of the absolute value of the seismic displacements corresponding to analysis of the transverse direction

Load Case 2: 100 (%) of the absolute value of the seismic displacements resulting from the analysis of the transverse direction plus 30 (%) of the absolute value of the seismic displacements corresponding to analysis of the longitudinal direction

C.4.3 Displacement demand/capacity ratio and connection design

C.4.3.1 **AASHTO GS Article 4.8 - Structure Displacement Demand/Capacity for SDCS B, C, and D**

$$\Delta_D^L \leq \Delta_C^L$$

Δ_D^L = displacement demand taken along the local principal axis of the ductile member. The displacement demand may be conservatively taken as the bent displacement inclusive of flexibility contribution from the foundations, superstructure or both.

The displacement demand is obtained by imposing the demand from then ESA Single mode spectral method on the structural model. This estimate does not include any flex from the foundation.

Longitudinal Load: Δ^{L}_{DL} = 0.1068 in, Δ^{T}_{DL} = 0.037 in

Transverse Load: Δ^{L}_{DT} = 0.03 in, Δ^{T}_{DT} = 0.116 in

Combining load cases and using R_D = 1.6 for the longitudinal direction and R_D = 1.77 for the transverse direction.

Load Case 1: Δ^{L}_{D1} = 0. 185 in, Δ^{T}_{D1} = 0. 1152

Load Case 2: Δ^{L}_{D2} = 0.10 in, Δ^{T}_{D2}= 0. 203

Δ^{L}_{C} = displacement capacity taken along the local principal axis corresponding to Δ^{L}_{D} of the ductile member as determined in accordance with Article 4.8.1 for SDC's B and C."

AASHTO GS Article 4.8.1 – Local Displacement Capacity for SDCs B

For SDC B:

$$\Delta_C^L = 0.12H_0(-1.27\ln(x) - 0.32) \geq 0.12H_0$$

$$x = \frac{\Lambda B_0}{H_0}$$

where:

H_0 = clear height of the column (ft)

B_0 = column diameter or width measured parallel to the direction of displacement under consideration (ft)

Λ = factor for column end restraint condition

= 1 for fixed-free (pinned on one end)

= 2 for fixed top and bottom

LONGITUDINAL

$$x = \frac{1 * 2}{20.94} = 0.096$$

$$\Delta_C^L = 0.12 * 20.94(-1.27\ln(0.096) - 0.32) \geq 0.12 * 20.94$$

$$\Delta_C^L = 6.67 \geq 2.513(in.)$$

$$\Delta_D^L \leq \Delta_C^L$$

$$0.185\ in. \leq 6.67\ in.$$

TRANSVERSE

$$x = \frac{1 * 12}{20.94} = 0.573$$

$$\Delta_C^L = 0.12 * 20.94(-1.27 \ln(0.573) - 0.32) \geq 0.12 * 20.94$$

$$\Delta_C^L = 0.973 < 2.5127 \ \therefore \ \Delta_C^L = 2.5127$$

$$\Delta_D^L \leq \Delta_C^L$$

$$0.203\ in. \leq 2.513\ in.$$

C.4.3.2 **AASHTO GS Article 4.12 - Minimum Support Length Requirements**

Since integral sub-to-superstructure connections and integral abutments are used, there are no applicable support length requirements to meet.

C.4.3.3 **AASHTO GS Article 4.14 – Superstructure Shear Keys**

This bridge does employ shear keys in the longitudinal direction however, dowels are present between the pier cap concrete and the pier and between the pier and the pile cap, which will also act as shear keys, thus the requirements of this section apply. The overstrength shear capacity shall be taken as $V_{ok} = 1.5V_n$, where:

V_{ok} = overstrength shear key capacity
V_n = nominal interface shear capacity of shear key (AASHTO Spec. 5.8.4)

C.4.3.4**AASHTO GS Article 4.10 - Column Shear Requirements for SDCs B, C, and D**

For SDCs B, C, or D, shear demand requirements for reinforced concretes columns (V_u) shall satisfied to the requirements of AASHTO **GS Article 8.6**. For columns in SDC B, the force shall be determined on the basis of the lesser of:

- "The force obtained from a linear elastic seismic analysis, or
- The force V_{po} corresponding to plastic hinging of the column including an overstrength factor" (recommended whenever practical)

The maximum forces obtained from elastic analysis are shown in Figure C.7 - Resultant Factored Column Forces; these forces will be used for verification of the capacity of the dowels to adequately transfer the shear loads. The longitudinal shear load is 276 kips and the transverse shear load is 843 kips. Since the same dowels will be required to resist either the load at a time, the controlling (maximum) load of 843 kips should be used for verification.

C.4.4 Design Requirements

AASHTO GS Article 4.7 – Design Requirements for Seismic Design Categories B, C, and D

C.4.4.1 **AASHTO GS Article 4.7-1 Design methods for Lateral Seismic Displacement Demands**

"Dictates which displacement resisting system can be used. The most applicable is Limited-Ductility Response in which a plastic mechanism is activated in the pier-columns but the ductility demands are reduced ($\mu_D \leq 4.0$). Intended yielding should be restricted to locations that can be readily accessed for damage inspection following a design earthquake."

AASHTO GS Commentary 4.7.1

"A key element in the design procedure is the flexural capacity of the columns. Philosophically, the lower the flexural capacity of the column, the more economical will be the seismic design because the overstrength flexural capacity of a column drives the cost and capacity of both the foundations and connections to the superstructure. For SDC B, the capacity of the column design for non seismic loads is considered to be acceptable for this lower seismic hazard level."

C.4.4.2 **AASHTO GS Article 4.11 Capacity Design Requirement for SDCs B, C, and D**

"Capacity design principles require that those components not participating as part of the primary energy dissipating system, typically flexural hinging in columns above ground or in some cases flexural hinging of drilled shafts, solid wall encased pile bents, etc., below ground, shall be capacity protected. The components include the superstructure, joints and cap beams, spread footings, pile caps, and foundations. This is achieved by ensuring the maximum moment and shear from plastic hinges in the column, considering overstrength can be resisted elastically by adjoining elements."

"For SDC B, forces obtained from capacity design principles should be used when the plastic hinging forces are less than the forces obtained from an elastic analysis. In lieu of full capacity design using overstrength forces, capacity checks should be made to ensure that no weak links exist in the ERS. Joint shear checks are required."

AASHTO GS Commentary 4.11

"For SDC B, full capacity design is not required. However, it is good practice to ensure that no portions of load path are weaker than the elements that establish the plastic capacity of the

substructure (e.g., plastic hinging in the columns). Therefore checks of the load path are suggested, but full capacity design using plastic overstrength forces is not required. “

“The design of substructures using the elastic forces associated with the design ground motion is permitted in SDC B, although not encouraged, because potentially larger ground motions could produce undesirable performance, including collapse or partial collapse of the bridge.”

C.4.4.3 **AASHTO GS Article 6.2 - Foundation Investigation**

AASHTO GS Article 6.2.4 – “In addition to the normal site investigation, potential hazards and seismic design requirements related to (1) liquefaction potential, (2) seismic –induced settlement, (3) lateral spreading, (4) slope instability, and (5) increases in lateral earth pressure, all as a result of earthquake motions, should be evaluated. The seismic hazards evaluation shall also consider the potential for and influence of:

- Surface rupture due to faulting if an active fault has been identified within 1 mi of the bridge site (see Article 3.4 for the definition of an active fault),
- Differential ground displacement (lurching), and
- Cyclic loading on the deformation and strength characteristics of foundation soils.”

C.4.4.4 **AASHTO GS Article 6.8 - Liquefaction Assessment**

Given the local seismic hazard, site location and soil condition liquefaction was not considered in this study. Some basic information about liquefaction which applies to SDC B is cited below.

“Where loose to very saturated sands are within the subsurface profile such that liquefaction of these soils could impact the stability of the structure, the potential for liquefaction in SDC B should also be considered as discussed in the commentary.”